

**The Sequential Insertion of Carbon Monoxide and Imines into Nickel-  
Carbon  $\sigma$ -Bonds and Kinetic Analysis of Imine Insertion into  
Palladium-Acyl  $\sigma$ -Bonds**

A thesis submitted to McGill University  
in partial fulfillment of the requirements for the degree of  
Master of Science

by  
Carolynne Stafford

Department of Chemistry  
McGill University  
Montréal, Québec, Canada  
July 2007

© Carolynne Stafford 2007

*Je dédie ce mémoire à mon père et à ma mère et je les remercie  
Pour avoir éveillé une curiosité en moi,  
Pour avoir encouragé la confiance que « chu capade »,  
Pour tout simplement être mes parents!!!*

*“I want to stand as close to the edge as I can without going over. Out on the edge you  
see all the kinds of things you can't see from the center.”  
Kurt Vonnegut*

*“I work every day -- or at least I force myself into my office or room. I may get nothing  
done, but you don't earn bonuses without putting in time. Nothing may come for three  
months, but you don't earn the fourth without it.”  
Mordecai Richler*

## ❧ ABSTRACT ❧

### **The Sequential Insertion of Carbon Monoxide and Imines into Nickel-Carbon $\sigma$ -Bonds and Kinetic Analysis of Imine Insertion into Palladium-Acyl $\sigma$ -Bonds**

The coupling of imines and carbon monoxide mediated by late transition metals has been previously reported in the Arndtsen laboratory. The fundamental properties of 2,1-migratory insertion of imines into nickel- and palladium-acyl bonds are presented in this text.

This study investigates the use of neutral  $\kappa^2$ -*N,O*-salicylaldiminato nickel (II) systems (**Chapter 2**) as potential complexes to mediate the sequential insertion of carbon monoxide and imines. These complexes undergo rapid carbon monoxide insertion. Subsequent imine insertion is permitted when the imine substrate is sterically unencumbered. The coupling product disproportionates leading to the formation of 1,2-diamides.

In our laboratory, kinetic and thermodynamic studies on the coordination and 2,1-migratory insertion of imines into palladium-carbon  $\sigma$ -bonds were the focus of former student Rania Dghaym, Ph.D. **Chapter 3** completes these studies, and offers a mechanistic picture of the pathway by which 2,1-migratory insertion into palladium-acyl bonds proceeds. Our mechanistic data suggest that imine insertion is distinct from olefin insertion and involves the concerted migratory attack of the  $\sigma$ -coordinated imine to the electrophilic acyl ligand.

## ≈ RÉSUMÉ ≈

### **L'insertion séquentielle de monoxyde de carbone et d'imines dans des liens sigma nickel-carbone ainsi que l'analyse cinétique de l'insertion d'imines dans le lien palladium-acétyle**

Le couplage d'imines et de monoxyde de carbone médié par des métaux de transition a été récemment publié par le laboratoire du Professeur Arndtsen. Les propriétés fondamentales de l'insertion migratoire-2,1 d'imines dans les liens nickel- et palladium-acétyle sont présentées dans le texte ci-présent.

Les complexes neutres  $\kappa^2$ -*N,O*-salicylaldiminato de nickel (II) sont le sujet de recherche dans le **chapitre 2** pour leur potentiel de médier l'insertion séquentielle de monoxyde de carbone et d'imine. L'insertion de monoxyde de carbone dans le lien nickel-méthyle est rapide. Par contre, l'insertion d'imine subséquente est seulement observée dans les cas où l'encombrement stérique de celle-ci est minime. Le produit du couplage mène à la formation de 1,2-diamides.

Dans notre laboratoire, la cinétique et thermodynamique de l'insertion migratoire-2,1 dans les liens sigma palladium-carbone était le sujet d'étude de Rania Dghaym, Ph.D., une étudiante précédente du laboratoire. Au **chapitre 3** nous présentons la suite de ses études et offrons un portrait global du mécanisme par lequel l'insertion migratoire-2,1 dans les liens palladium-acétyle se produit. Nos résultats suggèrent que le mécanisme d'insertion d'imines est distinct de celui d'insertion d'oléfines et implique une attaque migratoire concertée de l'imine  $\sigma$ -coordonnée au ligand acétyle électrophilique.



## ❧ ACKNOWLEDGEMENTS ❧

The greatest gratitude I have is towards Professor Bruce Arndtsen, for the opportunity, for the learning experience, for the dynamic work environment. The knowledge I have gained over the past two and a half years, in retrospect, makes the entire experience invaluable! Thank you for the guidance, the discussions, the understanding.

Merci Mom! Sans toi je ne pense pas que j'aurais été aussi loin dans mes études! Tout se que j'ai accompli c'est grâce à toi et Dad! Merci Dad! Je pense à toi tous les jours. Tu es mon ange-gardien!

Thanks to all the people I've shared my days with in the lab: Dan Black, Daniel St-Cyr, Yingdong Lu, Ali Siamaki, Ramsay Beveridge, Weijuan Jia, Kraig Worrall, Marc Sakalaskaus and Sinziana Tugulea, in no specific order. You are all great people! I'll miss the reminiscing, the laughing, the glove shooting, listening to music while bustin' a move. The one thing I'll always keep is the extensive slang vocabulary I've gathered: you're so bad, y'all!

Thanks to all the great friends I've made in the department who make going to Otto Maass any day of the week enjoyable! The best part of graduate school is making new friends on a yearly basis, especially with awesome people like you guys!

Thanks to my fellow Kiss members!!! Erica, you're simply the best! Alison, babe, what would I have done without you?! Annie, merci pour toutes les jasettes dans le corridor!

Thank you to all the professors with whom I've interacted during my time at McGill: Dr. Li, Dr. Gleason, Dr. Sleiman, Dr. Dahma, Dr. Moitessier, Dr. Wiseman, Dr. Ronis.

Thanks to all the secretaries, the building would fall apart without you! Thanks Chantal for answering all my questions, for your guidance, for making all the paper work that much more easier!

Thanks to all the support staff without whom we could not survive. Thanks Fred Morin and Paul Xia for all the help with the NMRs. Thanks Rick Rossi, Fred Kluck,

Jean-Phillipe Guay and George Kopp for making gold out of the scraps we bring you!  
You have saved me and others out of binds so many times; a million thanks!

Also a great thank you to the man up the hill who measured impossible mass-specs for me Dr. Alain Lesimple at the Department of Medicine, Mass Spectrometry Unit.

And last but not least, thank you to NSERC, CFI and McGill University for funding.

## ❧ TABLE OF CONTENTS ❧

### ❧ CHAPTER 1 ❧

#### Introduction

<b>1.0 Perspective</b>	<b>1</b>
<b>1.1 Synthetic Routes to <math>\alpha</math>-Amino Acids and Peptides</b>	<b>3</b>
1.1.1 Traditional Synthesis of $\alpha$ -Amino Acids	3
1.1.2 Traditional Routes to Peptides	5
1.1.2.1 Solid-Phase Peptide Synthesis	5
1.1.2.2 Solution-Phase Peptide Synthesis	6
1.1.3 Transition Metal Complexes in $\alpha$ -Amino Acid Synthesis	6
1.1.4 Transition Metal Complexes in Peptide Synthesis	10
<b>1.2 Imines as Insertion Substrates</b>	<b>12</b>
1.2.1 Coordination of Imines to Transition Metals	12
1.2.2 1,2-Migratory Insertion of Imines in Metal-Carbon $\sigma$ -Bonds	13
<b>1.3 The Transition Metal Coupling of Imines and Carbon Monoxide in the Construction of Amide Bonds</b>	<b>19</b>
<b>1.4 Overview of Thesis</b>	<b>22</b>
<b>1.5 References</b>	<b>23</b>

### ❧ CHAPTER 2 ❧

#### Nickel (II) Mediated Sequential Insertion of Carbon Monoxide and Imine

<b>2.0 Introduction</b>	<b>30</b>
<b>2.1 Results and Discussion</b>	<b>33</b>
2.1.1 Synthesis and Stability of Imine $\kappa^2$ - <i>N,O</i> -Salicylaldiminato Ni (II)	33

Complexes	
2.1.2 Reaction of $\kappa^2$ - <i>N,O</i> -Salicylaldiminato Ni (II) Complexes with Carbon Monoxide	36
2.1.3 Reactivity of $\kappa^2$ - <i>N,O</i> -Salicylaldiminato Ni-acyl Complexes 2.13	38
2.1.4 Mechanism of <i>N,N'</i> -Diacyl-1,1',2,2',3,3',4,4'-octahydro-1,1'-biisoquinoline 2.17 Formation	40
<b>2.2 Conclusion</b>	43
<b>2.3 Experimental Section</b>	44
2.3.1 General Procedure for the Synthesis of the $\kappa^2$ - <i>N,O</i> -Salicylaldiminato Ni (II) Complexes	44
2.3.2 Decomposition Studies of the $\kappa^2$ - <i>N,O</i> -Salicylaldiminato Ni (II) Complexes	52
2.3.3 General Reaction Conditions for the Insertion Chemistry	52
<b>2.4 References</b>	57

## ❧ CHAPTER 3 ❧

### Mechanistic Studies on the Insertion of Imines into Palladium-Carbon $\sigma$ -Bonds: How Similar are Imines to Olefins as Insertion Monomers?

<b>3.0 Introduction</b>	61
<b>3.1 Results and Discussion</b>	64
3.1.1 Results Obtained From Previous Work by Rania Dghaym, Ph.D.	64
3.1.1.1 Characteristics of the Sequential Insertion of Carbon Monoxide and Imine with $[L_2Pd(CH_3)(R^1N=C(H)R^2)]^+X^-$	64
3.1.1.2 Mechanistic Investigation of Imine Insertion into the Palladium-Acyl Bond	65
3.1.2 My Results and Mechanistic Data Analysis	70

3.1.2.1 Base Additive Effect with Weakly Coordinating Imines	70
3.1.2.2 Effect of Carbon Monoxide Pressure on the Insertion Rate	71
3.1.3 Mechanistic Picture of Imine Insertion into Palladium-Acyl $\sigma$ -Bond	73
3.1.4 Comparison of Imine to Olefin Insertion Mechanisms into Pd-C Bonds	75
<b>3.2 Conclusion</b>	<b>79</b>
<b>3.3 Experimental Section</b>	<b>80</b>
3.3.1 Synthesis of $[(\text{bipy})\text{Pd}(\text{CH}_3)(\text{BnN}=\text{CH}_2)]^+\text{BAr}_4^{\text{f}-}$ ( <b>3.1i</b> )	80
3.3.2 Synthesis of $[(\text{bipy})\text{Pd}(\eta^2\text{-CH}_2\text{N}(\text{Bn})\text{COCH}_3)]^+\text{BAr}_4^{\text{f}-}$ ( <b>3.3i</b> )	81
3.3.3 Kinetic Experimental	81
3.3.4 Influence of CO Pressure on Imine Insertion	82
3.3.5 Influence of Base Additive on the Imine Insertion in <b>3.2c</b>	82
<b>3.4 References</b>	<b>83</b>

## ≈ APPENDIX A ≈

### <sup>1</sup>H and <sup>13</sup>C NMR spectra for Chapter 2 Compounds 2.11a-m,p, 2.12a-d, 2.15a-d and 2.17a-d

I

## ≈ APPENDIX B ≈

### <sup>1</sup>H and <sup>13</sup>C NMR spectra for Chapter 3 Compounds 3.1e and 3.3e

XXVII

## ❧ LIST OF FIGURES ❧

<b>Figure 1.1</b>	Auxiliaries employed for amino acid synthesis: Seebach's auxiliary <b>1.6</b> , oxazaborolidinone <b>1.7</b> , Evan's auxiliary <b>1.8</b> and <i>N</i> -acyl-oxazinone <b>1.9</b> and 3-bromo oxazinone <b>1.10</b> .	5
<b>Figure 1.2</b>	Solution-phase convergent synthesis in the construction of peptides.	6
<b>Figure 1.3</b>	The coordination of imines to transition metals.	12
<b>Figure 1.4</b>	Examples of $\eta^2$ -imine complexes.	13
<b>Figure 1.5</b>	Examples of $\mu$ -imines in bimetallic complexes.	13
<b>Figure 1.6</b>	The two resonance structures of coordinated iminium cations.	13
<b>Figure 2.1</b>	Neutral $\kappa^2$ - <i>N,O</i> -salicylaldiminato nickel (II) catalyst for the copolymerization of polar alkenes.	32
<b>Figure 3.1</b>	Plot of $k_{\text{obs}}$ vs. [CO] for the reaction of <b>3.2a</b> to form <b>3.3a</b> in the presence of 0.2 M ( $\square$ ) and 0.4 M ( $\blacklozenge$ ) of MeN=C(H)Tol.	71
<b>Figure 3.2</b>	Mechanism and kinetic barriers for ethylene, propene and imine insertion into cationic palladium-carbon bonds. Value of $\Delta G_{\text{C=N}}^\ddagger > 32$ kcal/mol for R = CH <sub>3</sub> estimated from decomposition of <b>3.2a</b> upon warming to 150 °C.	76

## ❧ LIST OF SCHEMES ❧

<b>Scheme 1.1</b>	Transition metal-mediated coupling of imine and carbon monoxide to form peptide bonds.	2
<b>Scheme 1.2</b>	Migratory insertion of carbon monoxide and imine in cationic palladium (II)- and nickel (II)-based systems.	2
<b>Scheme 1.3</b>	General Strecker reaction scheme towards $\alpha$ -amino acids.	3
<b>Scheme 1.4</b>	The mechanistic pathway of the Ugi reaction.	3
<b>Scheme 1.5</b>	The nucleophilic addition of nitrogen based nucleophiles to $\alpha$ -substituted carboxylic acids.	4
<b>Scheme 1.6</b>	Amino acid synthesis general scheme by adding the side-chain.	4
<b>Scheme 1.7</b>	$\alpha$ -Amino acid synthetic strategy utilizing Schöllkopf's <i>bis</i> -lactime ether <b>1.5</b> .	5
<b>Scheme 1.8</b>	Metal catalyzed amidocarbonylation.	7
<b>Scheme 1.9</b>	Proposed mechanism for the cobalt catalyzed aldehyde amidocarbonylation.	7
<b>Scheme 1.10</b>	<i>In-situ</i> generation of aldehydes in cobalt-catalyzed amidocarbonylation by substituting aldehydes with olefins <b>[A]</b> , acetals <b>[B]</b> , allylic alcohols <b>[C]</b> , and epoxides <b>[D]</b> .	8
<b>Scheme 1.11</b>	Proposed mechanism for the aldehyde amidocarbonylation catalyzed by palladium.	9
<b>Scheme 1.12</b>	Substituting ureas for amides in palladium-catalyzed amidocarbonylation.	9
<b>Scheme 1.13</b>	The (bipy)Ni(COD)-mediated polymerization of $\alpha$ -amino acid- <i>N</i> -carboxyanhydrides proceeding via amido-amidate nickelacycle species <b>1.17</b> .	10
<b>Scheme 1.14</b>	Postulated mechanism of aziridine and carbon monoxide copolymerization.	11
<b>Scheme 1.15</b>	The imine insertion into metal-carbon $\sigma$ -bonds of selected early transition metal complexes: <b>(A)</b> titanium complex <b>1.19</b> , <b>(B)</b> zirconium complex <b>1.20</b> and <b>(C)</b> samarium complex <b>1.21</b> .	14

<b>Scheme 1.16</b>	The catalytic cycle for imine allylation by <i>bis</i> - $\pi$ -allylpalladium.	15
<b>Scheme 1.17</b>	Rhodium catalyzed phenyl 1,2-addition to aldimines involving transmetalation chemistry.	16
<b>Scheme 1.18</b>	The catalytic cycle of aryl halides and aldimines in a Heck-type coupling.	17
<b>Scheme 1.19</b>	The 1,2-insertion of aldimines into rhodium-carbon bonds.	18
<b>Scheme 1.20</b>	The carbon monoxide and imine sequential 2,1-insertion mediated by group 10 transition metal complexes.	20
<b>Scheme 1.21</b>	The palladium catalyzed formation of Münchnones <b>1.37</b> .	20
<b>Scheme 1.22</b>	Lewis acid initiated imine insertion into a manganese-acyl complex.	21
<b>Scheme 2.1</b>	The sequential insertion of carbon monoxide and imine in palladium (II) <b>2.1</b> and nickel (II) <b>2.3</b> cationic species.	31
<b>Scheme 2.2</b>	The sequential insertion of carbon monoxide in Pd (II)-amide neutral species.	31
<b>Scheme 2.3</b>	The synthesis of the $\kappa^2$ - <i>N,O</i> -salicylaldiminato nickel (II) complex <b>2.11p</b> .	35
<b>Scheme 2.4</b>	The reactivity of 3,4-dihydroisoquinoline nickel complexes <b>2.11d,g</b> in the presence of 9,10-dihydroanthracene <b>2.18</b> .	41
<b>Scheme 3.1</b>	The sequential insertion of carbon monoxide and imines into palladium-methyl complexes towards $\alpha$ -amino acid derivatives.	61
<b>Scheme 3.2</b>	The postulated 1,2-insertion of imine into transition metal-hydride bonds.	62
<b>Scheme 3.3</b>	The sequential insertion of carbon monoxide and imine to generate an amide-palladacycle.	64
<b>Scheme 3.4</b>	The reaction of <i>N</i> -sulfonyl substituted imine palladium-methyl complex and carbon monoxide.	65
<b>Scheme 3.5</b>	The reaction of <i>N</i> -methyl tolualdimine and (bipy)Pd(CH <sub>3</sub> )Cl under 1 atm of CO.	65
<b>Scheme 3.6</b>	Four proposed mechanisms for the imine insertion into palladium-acyl complexes.	66

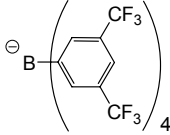
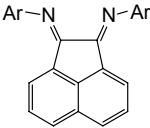
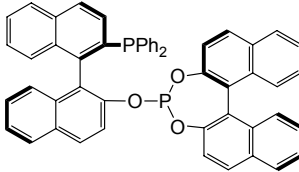
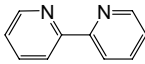
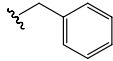
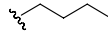
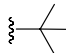
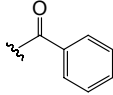
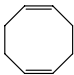

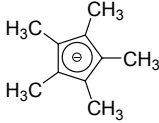


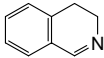

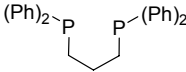
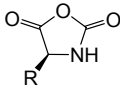
<b>Scheme 3.7</b>	The effect of amine base on the rate of insertion for <b>3.2c</b> .	70
<b>Scheme 3.8</b>	Mechanism of carbon monoxide insertion for Ni (II) complexes of 1,3- <i>bis</i> -(diphenylphosphino)propane (dppp) <b>3.14a</b> and 1,2- <i>bis</i> ( <i>bis</i> (2-methoxyphenyl)phosphino)ethane ( <i>o</i> -OMe-dppe) <b>3.14b</b> .	73
<b>Scheme 3.9</b>	Two proposed pathways involved in path B for the imine insertion palladium-acyl bond: concerted intramolecular nucleophilic attack of imine on acyl ligand.	75
<b>Scheme 3.10</b>	The 2,1-migratory insertion of formalimine H <sub>2</sub> C=NBn in complex <b>3.2i</b> .	77

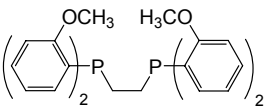
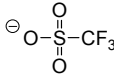
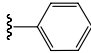
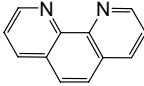
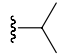
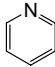

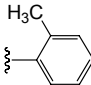
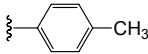
## ❧ LIST OF TABLES ❧

<b>Table 2.1</b>	The synthesis of $\kappa^2$ - <i>N,O</i> -salicylaldiminato nickel (II) complexes <b>2.11a-o</b> .	33
<b>Table 2.2</b>	Approximate decomposition times of selected nickel-imine complexes.	35
<b>Table 2.3</b>	The formation of nickel-acyl complexes <b>2.13b-m,p</b> and <b>2.14a-e</b> in the presence of 1 atm of carbon monoxide.	37
<b>Table 2.4</b>	Reaction products with <i>trans</i> -imine substrates in benzene under 1 atm CO.	38
<b>Table 2.5</b>	Reaction product distribution with 3,4-dihydroisoquinoline substrate.	39
<b>Table 3.1</b>	Rate expressions for the mechanisms of imine insertion.	67
<b>Table 3.2</b>	Insertion chemistry with poorly coordinative imines: the presence of iminum salt by-product formation.	68
<b>Table 3.3</b>	Influence of imine substituents on insertion rate.	69
<b>Table 3.4</b>	Insertion chemistry of <b>3.2c</b> with various ligands.	71

## ❧ LIST OF ABBREVIATIONS ❧

Ar	aryl	
atm	atmosphere	
$\text{BAr}_4^{\ominus}$	tetrakis(3,5-di-trifluoromethylphenyl)borate	
BIAN	N,N'-bis(aryl)-iminoacenaphtene	
BINAPHOS	2-(diphenylphosphino)-1,1'-binaphthalen-2'-yl 1,1'-binaphthalene-2,2'-diyl phosphite	
bipy	2,2'-bipyridyl	
Bn	benzyl	
Bu	butyl	
<sup>t</sup> Bu	<i>tert</i> -butyl	
Bz	benzoyl	
°C	degrees Celsius	
CO	carbon monoxide	$\text{C}\equiv\text{O}$
COD	1,5-cyclooctadiene	
Cp	cyclopentadienyl	
Cp'	pentamethyl-cyclopentadienyl	
d	doublet	
δ	chemical shift (NMR)	

dd	doublet of doublet	
3,4-DHQ	3,4-dihydroisoquinoline	
dppe	1,2- <i>bis</i> -(diphenylphosphino)ethane	
dppp	1,3- <i>bis</i> -(diphenylphosphino)propane	
dt	doublet of triplets	
ESI-HRMS	Electrospray Ionization-High Resolution Mass Spectrometry	
eq. or equiv.	equivalent	
g	gram	
h or hrs	hour(s)	
Hz	hertz	
<i>i</i>	iso	
<i>J</i>	coupling constant	
kcal	kilocalorie	
L	litre or ligand	
m	multiplet	
<i>m</i>	meta	
M	molar or metal	
Me	methyl	-CH <sub>3</sub>
MHz	megahertz	
min	minute(s)	
mg	milligram	
mL	millilitre	
mmol	millimole	
mol	mole	
n/a	non-applicable	
NCA	$\alpha$ -amino acid- <i>N</i> -carboxyanhydrides	
NMR	Nuclear Magnetic Resonance	
NOE	Nuclear Overhauser Effect	
<i>o</i>	ortho	

<i>o</i> -OMe-dppe	1,2- <i>bis</i> ( <i>bis</i> (2-methoxyphenyl)phosphino)ethane	
OTf <sup>-</sup>	trifluoromethanesulfonate	
<i>p</i>	para	
Ph	phenyl	
phen	1,10-phenanthroline	
ppm	parts per million	
<sup><i>i</i></sup> Pr	<i>iso</i> -propyl	
py	pyridine	
q	quartet	
r.t.	room temperature	
s	singlet	
S	solvent	
sept.	septet	
tmeda	<i>N, N, N', N'</i> -tetramethylethylenediamine	
<i>o</i> -tol	<i>ortho</i> -toluyl	
<i>p</i> -tol or Tol	<i>para</i> -toluyl	



## ❧ CHAPTER 1 ❧

### Introduction

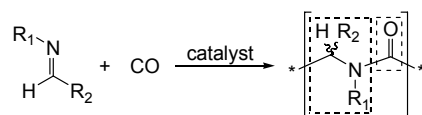
#### 1.0 Perspective

From drug design and enzymatic research to peptidomimetic materials, the peptide linkage is a focal point of research. This interest has stimulated the development of efficient new methods to construct peptides.

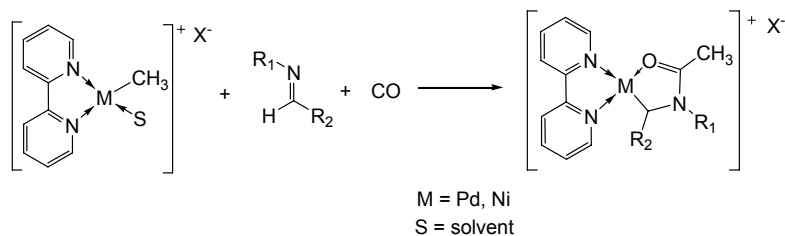
The classic approach to polypeptide synthesis involves condensing naturally or non-naturally occurring amino acids. However, because this route often requires initial synthesis of the  $\alpha$ -amino acids, and multiple protection and deprotection steps, the scope and scale upon which peptides can be prepared is limited. Alternative efficient and modular synthetic routes to form  $\alpha$ -amino acids and peptides will be indispensable synthetic tools for generating novel bio-molecules.

Transition metal complexes catalyze a wide range of synthetically useful transformations, with examples including hydrogenation,<sup>1</sup> cross-coupling,<sup>2</sup> oxidation/reduction,<sup>3</sup> cycloaddition,<sup>4</sup> polymerization,<sup>5</sup> and many others. This is due to their ability to coordinate multiple substrates and activate them for transformations that are difficult by organic synthetic methods. The elemental steps that transition metals mediate these transformations include ligand substitution, oxidative addition, reductive elimination, insertion, elimination, nucleophilic and electrophilic addition, abstraction, cycloaddition, and others.<sup>6</sup>

The reactivity of transition metal complexes led us to consider them in designing a new route towards peptides synthesis through sequential transition metal-mediated couplings of carbon monoxide (CO) and imines, as shown in **Scheme 1.1**. A critical step in this proposed synthesis is migratory insertion of imines into metal-carbon  $\sigma$ -bonds. We have previously developed cationic palladium (II)- and nickel (II)-systems which can undergo the sequential insertion of CO and imine to generate amide metal chelates [**Scheme 1.2**].<sup>7</sup> However, the strong chelation of the amide oxygen to the metal center prevents an empty coordination site from being formed to enable further insertion.



**Scheme 1.1:** Transition metal-mediated coupling of imine and carbon monoxide to form peptide bonds.



**Scheme 1.2:** Migratory insertion of carbon monoxide and imine in cationic palladium (II)- and nickel (II)-based systems.

To overcome this, we propose to weaken the amide chelation to the metal center by employing less Lewis acidic neutral nickel complexes for the sequential CO/imine insertion. The ability of such complexes to mediate the insertion of imine into a nickel-carbon  $\sigma$ -bond has not been reported. This is the subject of research in this thesis.

In order to provide some perspective to this research area, this introductory chapter will contain: (i) a brief overview of traditional and transition metal mediated amino acid and peptide syntheses; (ii) examples of imine migratory insertion into transition metal-carbon bonds; and (iii) a comparison between imine and alkene insertion mechanisms. Together, these discussions will highlight the focus of this thesis: the transition metal mediated migratory insertion of imines and its mechanism.

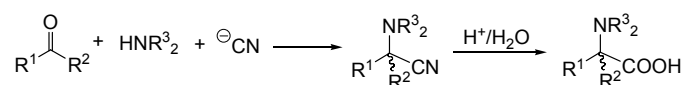


## 1.1 Synthetic Routes to $\alpha$ -Amino Acids and Peptides

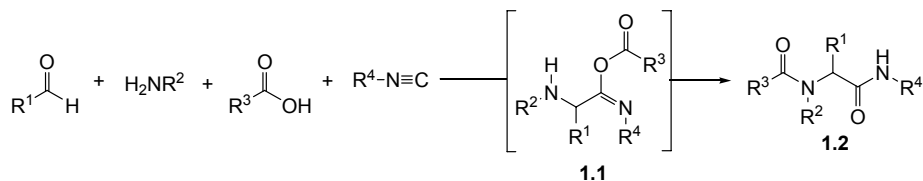
### 1.1.1 Traditional Synthesis of $\alpha$ -Amino Acids

As mentioned, traditional approaches to peptide syntheses rely upon  $\alpha$ -amino acid condensation. This therefore requires that non-natural  $\alpha$ -amino acids be synthesized prior for their incorporation into peptides. A wide range of methods exist for synthesizing  $\alpha$ -amino acids.<sup>8</sup> These include Strecker<sup>9</sup> and Ugi<sup>10</sup> reactions, amination of  $\alpha$ -halo acids (or esters),<sup>11</sup> and approaches through glycine anion or cation equivalents.<sup>12</sup> Enantioselectivity can be induced in these processes using chiral catalysts or auxiliaries.

The most common approaches for constructing amino acids involve the nucleophilic addition of a carboxylate synthon to a Schiff base (*e.g.* imine) that has been generated *in-situ* from an aldehyde and an amine. For example, the Strecker reaction involves the condensation of an aldehyde (or ketone), an amine and cyanide [**Scheme 1.3**].<sup>8</sup> Similarly, the multi-component Ugi reaction<sup>9</sup> combines four substrates to generate diamides: aldehyde (or ketone), amine, carboxylic acid and isonitrile [**Scheme 1.4**]. The latter reaction proceeds via formation of an activated imine, followed by sequential nucleophilic addition of isonitrile and carboxylate anion to generate intermediate **1.1**, which rearranges to the diamide **1.2**.

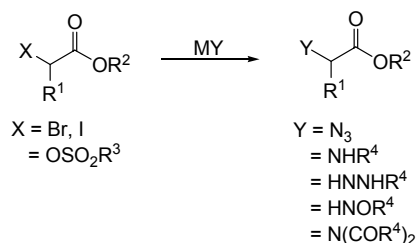


**Scheme 1.3:** General Strecker reaction scheme towards  $\alpha$ -amino acids.



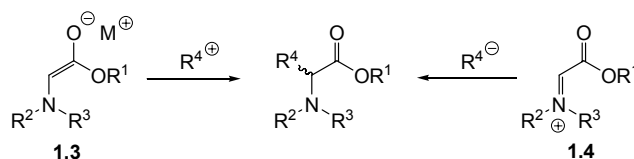
**Scheme 1.4:** The mechanistic pathway of the Ugi reaction.

Carboxylic acids can also be used as starting materials for synthesizing amino acids. The process involves nucleophilic displacement of an  $\alpha$ -halide or  $\alpha$ -pseudohalide with a range of *N*-nucleophiles [Scheme 1.5].<sup>13</sup>



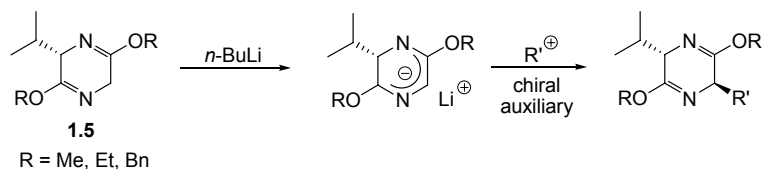
**Scheme 1.5:** The nucleophilic addition of nitrogen based nucleophiles to  $\alpha$ -substituted carboxylic acids.

An alternative approach to synthesizing  $\alpha$ -amino acids is to introduce the side-chain to a pre-existing amino acid scaffold. For example, an anion glycine synthon **1.3** can react with an electrophile, or a nucleophile can add to a glycoxylic-imine equivalent **1.4** [Scheme 1.6].

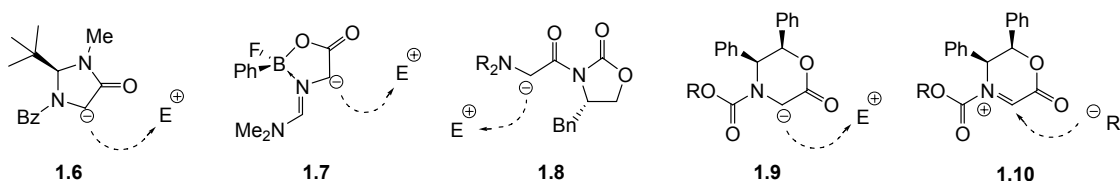


**Scheme 1.6:** Amino acid synthesis general scheme by adding the side-chain.

These approaches can be made stereoselective with the use of chiral auxiliaries. An example of using a chiral auxiliary to add an electrophile to an enolate is shown in **Scheme 1.7** with the Schöllkopf's *bis*-lactime ether<sup>14</sup> **1.5**. Other examples include Seebach's auxiliary<sup>15</sup> **1.6**, oxazaborolidinone<sup>16</sup> **1.7**, Evan's auxiliary<sup>17</sup> **1.8**, and *N*-acyl-oxazinone<sup>18</sup> **1.9** [Figure 1.1]. In nucleophilic addition, the electronics of the  $\alpha$ -carbon can be inversed by substituting one of the protons for a halide or other good leaving groups. One of the most comprehensive examples of this is 3-bromo-oxazinone **1.10** [Figure 1.1].<sup>19</sup>



**Scheme 1.7:**  $\alpha$ -Amino acid synthetic strategy utilizing Schöllkopf's *bis*-lactime ether **1.5**.



**Figure 1.1:** Auxiliaries employed for amino acid synthesis: Seebach's auxiliary **1.6**, oxazaborolidinone **1.7**, Evan's auxiliary **1.8** and *N*-acyl-oxazinone **1.9** and 3-bromo oxazinone **1.10**.

## 1.1.2 Traditional Routes to Peptides

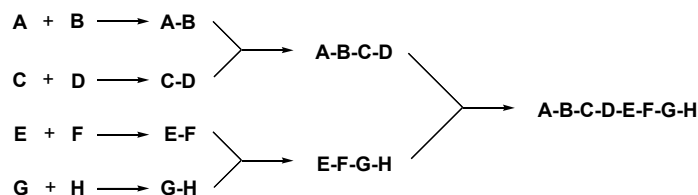
### 1.1.2.1 Solid-Phase Peptide Synthesis

The conventional process for synthesizing a peptide is to graft the growing chain on a solid support matrix and build the chain, monomer by monomer, in a linear fashion. The solid support is typically a crosslinked polystyrene resin with benzoyl alcohol monomers as grafting sites. A significant advantage to this heterogeneous method is that purifying the resulting peptide is simple since by-products can be washed away. Additionally, a heterogeneous synthesis medium permits the use of excess reagent, and therefore increases coupling yields.

There are disadvantages to this process, however. Every monomer addition to the chain requires a minimum of two steps: coupling and deprotection. Further, in order to construct large peptides, coupling must proceed in high yield, which can be difficult to achieve with heterogeneous reactions. Despite these issues, solid phase synthesis is by far the most common approach to peptide synthesis.

### 1.1.2.2 Solution-Phase Peptide Synthesis

In solution-phase synthesis, the standard strategy is a convergent synthesis, *i.e.*, selecting certain building blocks and fragments, which are prepared, isolated, purified, and coupled, to build the complete sequence [Figure 1.2]. Although a very laborious method, solution-phase synthesis is very economical; it is still used today as the method of choice to produce peptides in scales of 10-100 Kg.<sup>20</sup>

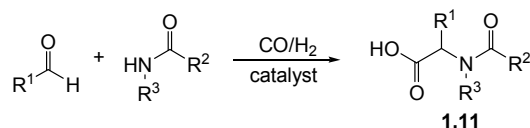


**Figure 1.2:** Solution-phase convergent synthesis in the construction of peptides.

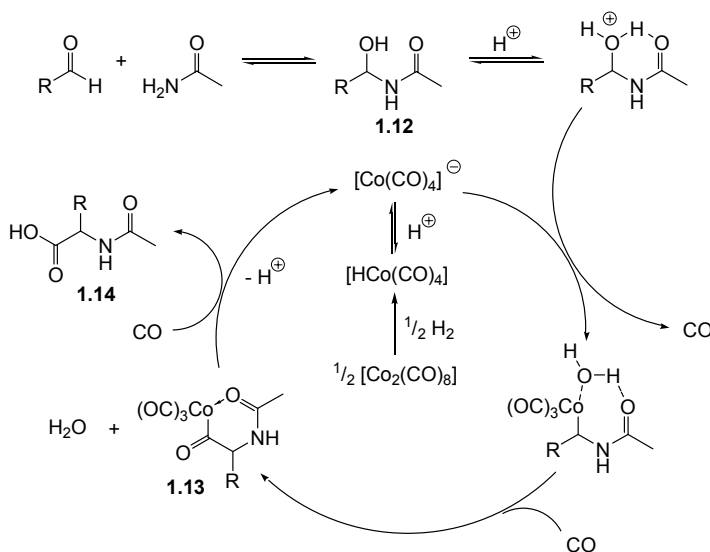
### 1.1.3 Transition Metal Complexes in $\alpha$ -Amino Acid Synthesis

Over the past several decades transition metal catalysis has become a very important tool in the development of new synthetic methodologies. Examples of  $\alpha$ -amino acids syntheses using this approach include catalytic versions of the reactions discussed in **section 1.1** (*e.g.* Strecker<sup>21</sup>), as well as a number of new methods, such as alcohol addition to chromium  $\alpha$ -aminocarbenes,<sup>22</sup> and the asymmetric hydrogenation of  $\alpha,\beta$ -dehydro-aminoacids.<sup>23</sup> Perhaps one of the most important transition metal catalyzed routes to  $\alpha$ -amino acids, which also relates to research in this thesis, is aldehyde amidocarbonylation [Scheme 1.8].<sup>24</sup>

The amidocarbonylation reaction involves a one step, multicomponent coupling of aldehydes, amides and carbon monoxide. This reaction is very atom economical (all the reagents are incorporated into the product), and all the starting materials are readily available. As such, this reaction is ideal for the industrial scale synthesis of a wide range of racemic *N*-acylamino acids **1.11**. The most common catalysts for amidocarbonylation are either cobalt carbonyl complexes (*e.g.*  $\text{Co}_2(\text{CO})_8$ ), or palladium complexes (*e.g.*  $\text{Pd}(\text{PPh}_3)_4$ ).



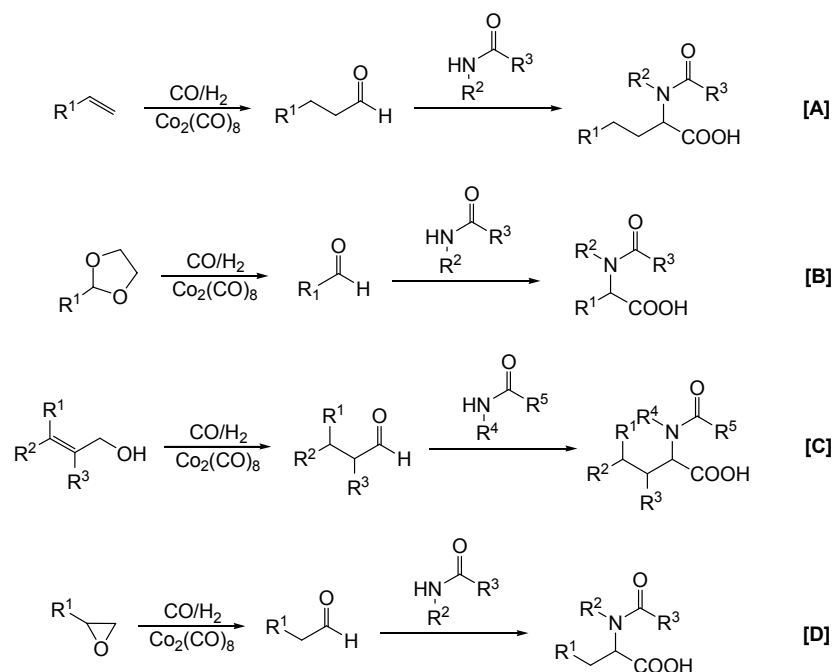
**Scheme 1.8:** Metal catalyzed amidocarbonylation.



**Scheme 1.9:** Proposed mechanism for the cobalt catalyzed aldehyde amidocarbonylation.

The first example of aldehyde amidocarbonylation was reported by Wakamatsu in 1971.<sup>25</sup> The reaction employed  $\text{Co}_2(\text{CO})_8$  as catalyst and proceeded at elevated temperature (110 °C) and CO (150 bar) and  $\text{H}_2$  (50 bar) pressures. Subsequent studies have led to a reasonable understanding of how the reaction proceeds. The active catalysts for this reaction are believed to be  $[\text{Co(CO)}_4]^-$  and/or  $\text{HCo(CO)}_4$ , formed via reaction of  $\text{Co}_2(\text{CO})_8$  with hydrogen gas. The postulated mechanism of the  $[\text{Co(CO)}_4]^-$  catalytic amidocarbonylation is shown in **Scheme 1.9**. The first step in the catalytic cycle is the formation of *N*- $\alpha$ -hydroxyalkyl amide **1.12**, formed from the nucleophilic addition of the amide to the aldehyde. In the presence of acid, the hydroxyl moiety in **1.12** is protonated, and the water molecule is displaced by a cobalt tetracarbonyl anion. This is followed by carbon monoxide insertion, to form the cobalt-acyl intermediate **1.13**. The resulting complex can then undergo either an intramolecular attack of the amide oxygen onto the acyl to release the oxazolonium salt<sup>26</sup> or the intermolecular attack of water on the acyl to

afford the carboxylic acid **1.14**. This reaction is not limited to aldehydes; olefins, acetals, epoxides, and allylic alcohols as well as alcohols and benzyl chloride can be used as precursors for *in-situ* generation of aldehydes [Scheme 1.10].<sup>27</sup>

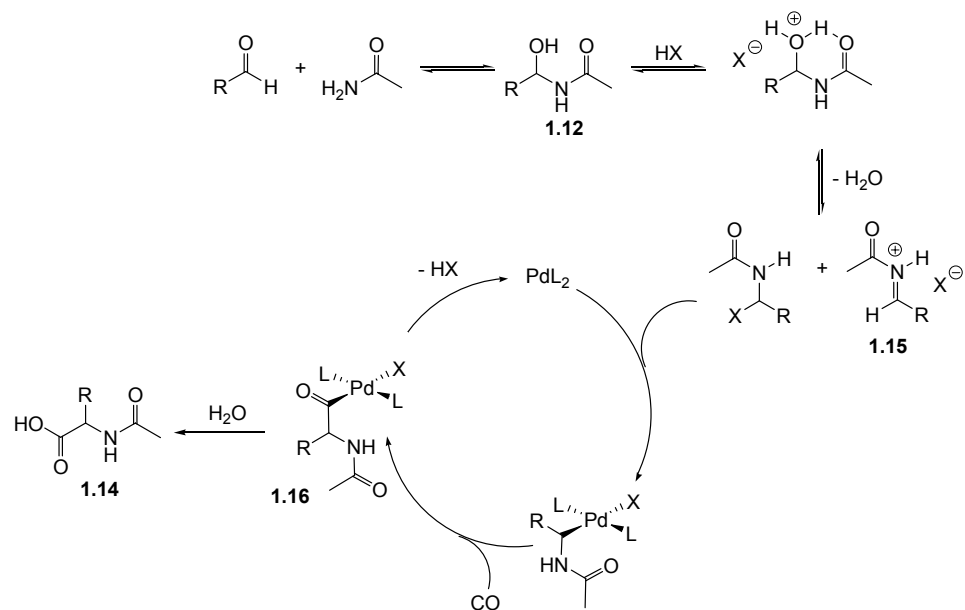


**Scheme 1.10:** *In-situ* generation of aldehydes in cobalt-catalyzed amidocarbonylation by substituting aldehydes with olefins [A], acetals [B], allylic alcohols [C], and epoxides [D].

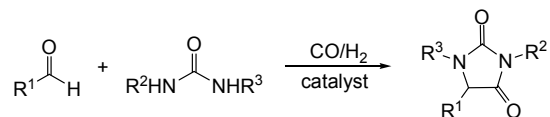
More recent research by Beller and co-workers has shown that palladium complexes can catalyze the amidocarbonylation reaction at lower temperatures and pressures.<sup>28</sup> The reaction is believed to proceed via a similar route to that with cobalt [Scheme 1.11], however mechanistically different, thus additives such as inorganic acids and salts are required in catalytic amounts to drive the reaction forward.<sup>29</sup> The latter are believed to activate the *N*- $\alpha$ -hydroxyalkyl amide **1.12** towards oxidative addition to palladium (0) by transforming **1.12** to an *N*-acyl iminium salt<sup>30</sup> **1.15**.

In general, the palladium catalysts for amidocarbonylation have greater activity under milder conditions (80 °C, 10 bar CO pressure) and superior functional-group tolerance compared to the cobalt catalysts. Alternatively, alcohols can be used in place of water as a trapping agent for **1.16** to provide esters.<sup>31</sup> In addition, a range of other

products can be synthesized via this chemistry, with a representative example shown in **Scheme 1.12**.<sup>24,32</sup> Today, standardized reactions with a heterogeneous palladium catalyst on activated carbon and a carbon monoxide pressure of 10 bar increases the methods applicability.<sup>33</sup>



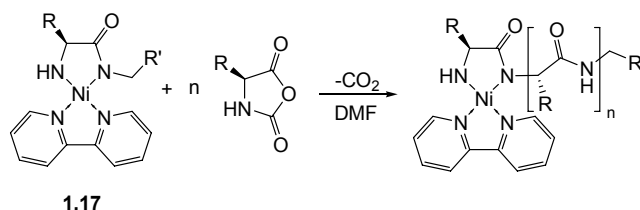
**Scheme 1.11:** Proposed mechanism for the aldehyde amidocarbonylation catalyzed by palladium.



**Scheme 1.12:** Substituting ureas for amides in palladium-catalyzed amidocarbonylation.

### 1.1.4 Transition Metal Complexes in Peptide Synthesis

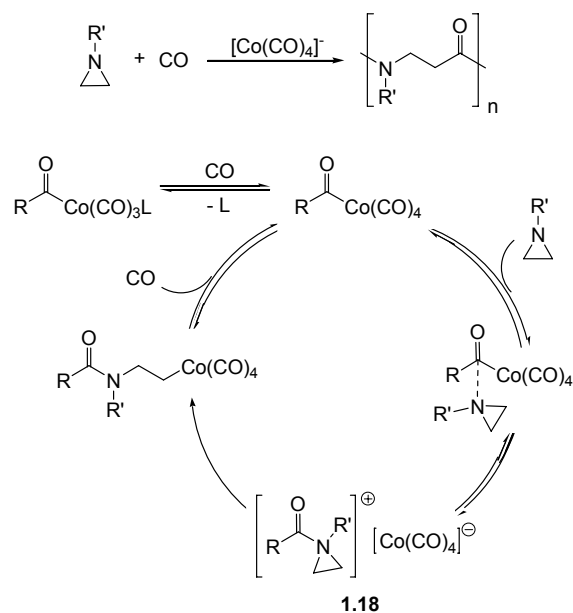
In contrast to synthesizing  $\alpha$ -amino acids, using transition metal catalysts to build peptides is less explored. Perhaps the most prominent example involves the catalyst reported by Deming.<sup>34</sup> In these studies, nickel complexes such as (bipy)Ni(COD) (bipy = 2,2'-bipyridyl, COD = 1,5-cyclooctadiene) or (Ph<sub>3</sub>P)<sub>2</sub>Ni(COD) reacted with two equivalents of  $\alpha$ -amino acid-*N*-carboxyanhydrides (NCA) to generate the active catalytic species amido-amidate nickelacycle **1.17**. Exposing the nickelacycle to an excess of NCA quickly affords a peptide-polymer formed by the ring-opening polymerization of NCA [Scheme 1.13]. Importantly, this polymer is living and has allowed the synthesis of a range of block copolymers (*e.g.* AB-diblock polymer where A = poly(methylacrylate) and B = poly( $\gamma$ -benzyl-L-glutamate)<sup>35</sup> and ABA-triblock polymer where A = poly( $\gamma$ -benzyl-L-glutamate) and B = poly(ethylene glycol)<sup>36</sup>).



**Scheme 1.13:** The (bipy)Ni(COD)-mediated polymerization of  $\alpha$ -amino acid-*N*-carboxyanhydrides proceeding via amido-amidate nickelacycle species **1.17**.

In addition to  $\alpha$ -peptides, transition metal catalysis has recently demonstrated utility in synthesizing  $\beta$ -peptides via catalytic copolymerization of aziridines and carbon monoxide.<sup>37</sup> To date, three catalysts have been successfully employed for this reaction: PhCH<sub>2</sub>C(O)Co(CO)<sub>4</sub>, CH<sub>3</sub>C(O)Co(CO)<sub>3</sub>(PPh<sub>3</sub>), and CH<sub>3</sub>C(O)Co(CO)<sub>3</sub>(P(*o*-tolyl)<sub>3</sub>). The hypothesized catalytic cycle of copolymerization is outlined in **Scheme 1.14**. The first step is aziridine insertion into the cobalt-acyl bond to generate *N*-acyl aziridinium species **1.18**. Subsequent nucleophilic addition of the cobaltate anion and migratory insertion of carbon monoxide complete the cycle. Reiteration of the aziridine/CO coupling reaction affords the poly- $\beta$ -peptoid product.





**Scheme 1.14:** Postulated mechanism of aziridine and carbon monoxide copolymerization.

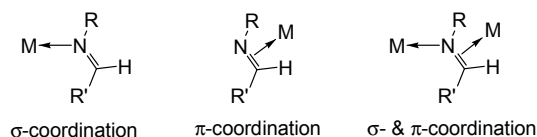
## 1.2 Imines as Insertion Substrates

Nucleophilic 1,2-addition to imines has become a powerful and relatively general approach to the synthesis of  $\alpha$ -substituted amines. This reaction typically involves relatively ionic organometallic reagents (*e.g.* organozinc, organomagnesium and organolithium reagents) and proceeds via nucleophilic attack of the organic group on the imine carbon, followed by nitrogen coordination to the metal center. In recent years, enantioselective processes were added to the repertoire of nucleophilic additions to imines.

In contrast, although transition metal processes involving imines as insertion substrates have been gaining focus in the last decade, they have received much less attention. In the following sections, we will elaborate on the coordination modes of imines to transition metal complexes, and look at examples of their insertion into transition metal carbon  $\sigma$ -bonds.

### 1.2.1 Coordination of Imines to Transition Metals

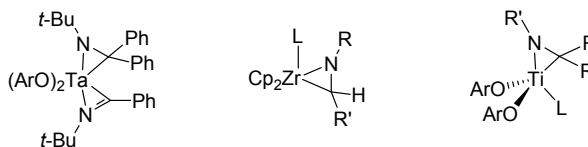
Although olefins and imines are isoelectronic species, there is significant difference in their insertion propensity, due to the difference in polarity of the unsaturation and the presence of the lone pair of electrons on the nitrogen. This lone pair provides a  $\sigma$ -coordination site in addition to the  $\pi$ -coordination which is believed to be crucial for insertion of olefins. Imines have been observed to coordinate to transition metals in three possible ways, depicted in **Figure 1.3**.



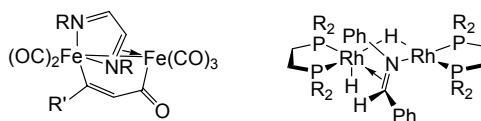
**Figure 1.3:** The coordination of imines to transition metals.

Most transition metals interact with imines to generate  $\eta^1$ -complexes. However, a few examples of  $\pi$ -coordinated imines have been reported<sup>38,42a</sup> that typically involve low

valent, strong back-bonding transition metal complexes [Figure 1.4]. The  $\eta^2$ -coordination in these imine complexes results from the strong  $\pi$ -donor character of the  $d^2$  early-transition metals. In addition, certain bimetallic complexes coordinate imines to both metal centers, one via its lone pair, and the other via its  $\pi$ -bond [Figure 1.5].<sup>39</sup>

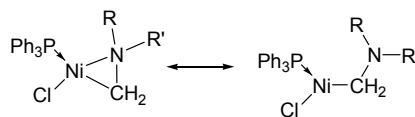


**Figure 1.4:** Examples of  $\eta^2$ -imine complexes.



**Figure 1.5:** Examples of  $\mu$ -imines in bimetallic complexes.

In contrast to imines, iminium cations ( $R_2N^+=CH_2$ ) favour coordination through the  $\pi$ -bond, since the quaternary nitrogen center is no longer capable of  $\sigma$ -coordination.<sup>40</sup> However, these cations have an alternative resonance structure involving  $\eta^1$ -coordination of the carbon [Figure 1.6]. Sepelak showed that in the case of low-valent nickel  $\eta^2$ -iminium complexes,  $\eta^1$ -coordination of the iminium carbon can be induced by introducing bulk and electron density on the Ni center.<sup>40e</sup>



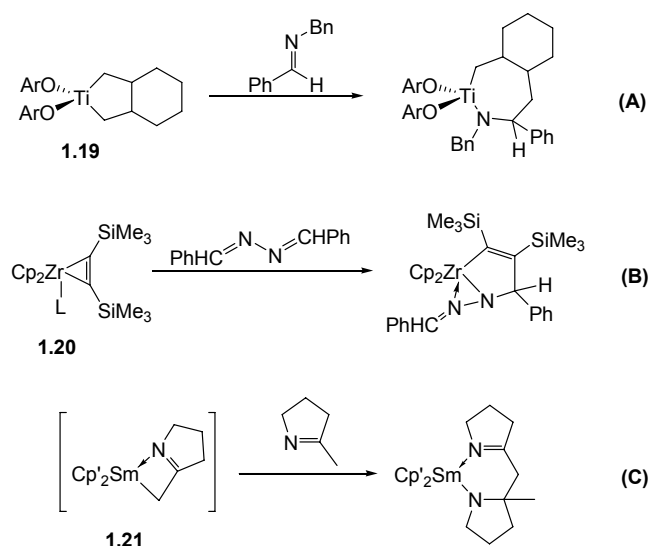
**Figure 1.6:** The two resonance structures of coordinated iminium cations.

### 1.2.2 1,2-Migratory Insertion of Imines in Metal-Carbon $\sigma$ -Bonds

The migratory insertion of substrates containing multiple bonds into metal-alkyl, -aryl, or -hydride bonds is a fundamental step in many catalytic cycles. Although

insertions of olefin C=C  $\pi$ -bonds into metal-alkyl, -acyl, -hydride, or -aryl bonds have substantial precedent,<sup>41</sup> well-defined examples of insertions involving C=O or C=N multiple bonds of imines, ketones, aldehydes, or related substrates into metal-carbon bonds are less common.<sup>42</sup>

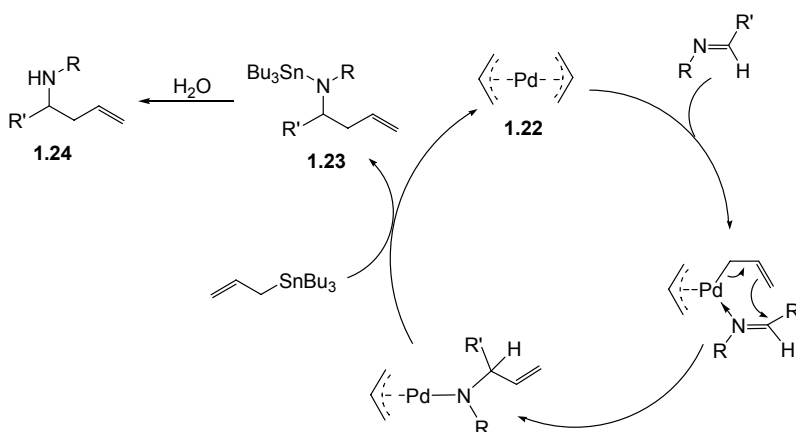
The first examples of this reaction involved early transition metals complexes, such as the titanium<sup>43</sup> complex **1.19** [Scheme 1.15 (A)], the zirconium<sup>44</sup> complex **1.20** [Scheme 1.15 (B)] and the samarium<sup>45</sup> complex **1.21** [Scheme 1.15 (C)]. All of these examples proceed via formal 1,2-insertion to generate the thermodynamically favoured metal-amide complexes. The mechanism of these reactions has yet to be examined, but it seems reasonable that metal-nitrogen bond formation drives the insertion.



**Scheme 1.15:** The imine insertion into metal-carbon  $\sigma$ -bonds of selected early transition metal complexes: (A) titanium complex **1.19**, (B) zirconium complex **1.20** and (C) samarium complex **1.21**.

Similarly, examples of imine insertions into late transition metal-carbon bonds are less common, and only recently observed. However, in contrast to early transition metal-amide complexes, these metal-amide complexes react further to liberate the free amines. This reactivity renders late metals attractive for use in catalytic systems involving imine insertion.

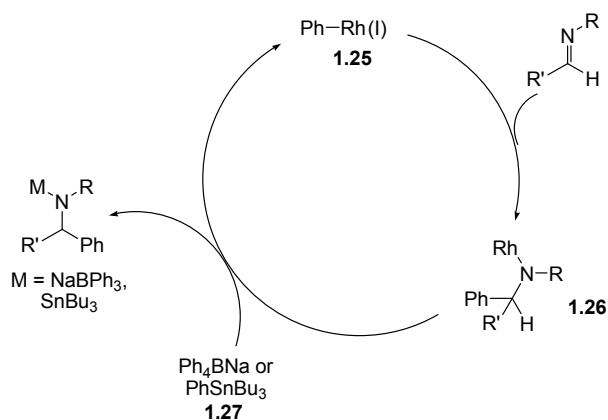
There have been a number of late transition metal mediated or catalyzed processes where imine insertion into a metal-carbon bond is postulated. For example, Yamamoto has recently reported a palladium-catalyzed coupling of imines with allylstannanes to afford homoallylic amines **1.24**.<sup>46</sup> The proposed active catalyst is a *bis- $\pi$ -allyl*palladium complex **1.22**. The postulated mechanism involves allylation of imine, followed by transmetalation of allyltributylstannane to palladium affording stannyl homoallylamide **1.23** [Scheme 1.16]. Allyl addition to the imine is thought to go through a six-membered ring transition state. Competitive studies between imines and aldehydes towards allylation reveal that the reaction is chemoselective towards imines. This observation is proposed to be a result of the stronger Lewis acid-base pairing between palladium and imines. Although palladium-amide species is a postulated reaction intermediate, it was not directly observed. The reaction worked equally well with ketones, aldehydes and  $\alpha,\beta$ -unsaturated substrates. Also, enantioselectivity can be induced in the allyl addition by employing an (1*S*)- $\beta$ -(-)-pinene derived  $\pi$ -allyl ligand.<sup>47</sup>



**Scheme 1.16:** The catalytic cycle for imine allylation by *bis- $\pi$ -allyl*palladium.

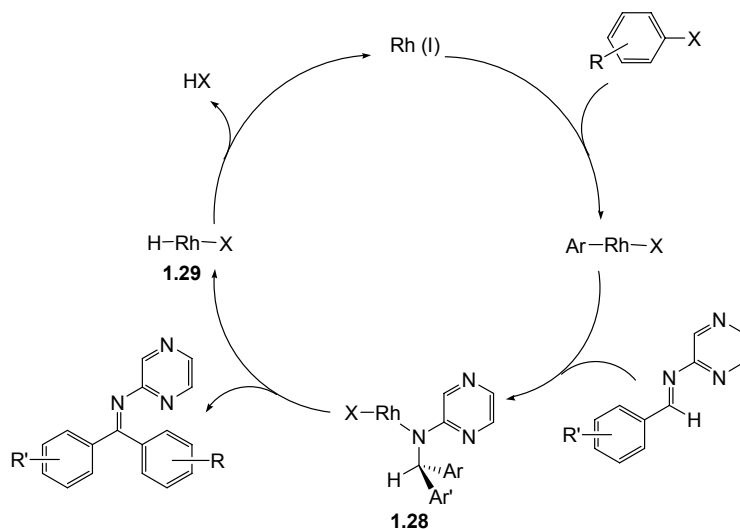
The rhodium mediated coupling reactions of aldimines with arylstannanes,<sup>48</sup> arylborates<sup>48b,49</sup> or arylboronic acids<sup>50</sup> to generate ketimines have also been explored, and have become useful method to construct  $\alpha$ -substituted amides. The general understanding of alkene cross-coupling processes with transmetalating agents leads to the following proposed cycle: (i) a rhodium-aryl (I) species **1.25** is formed *in-situ* from the

rhodium precursor and transmetalating agent, (ii) the formal 1,2-insertion of imine in the rhodium-carbon bond to afford a rhodium-amide (I) complex **1.26** and (iii) the transmetalation between **1.26** and **1.27** [Scheme 1.17].



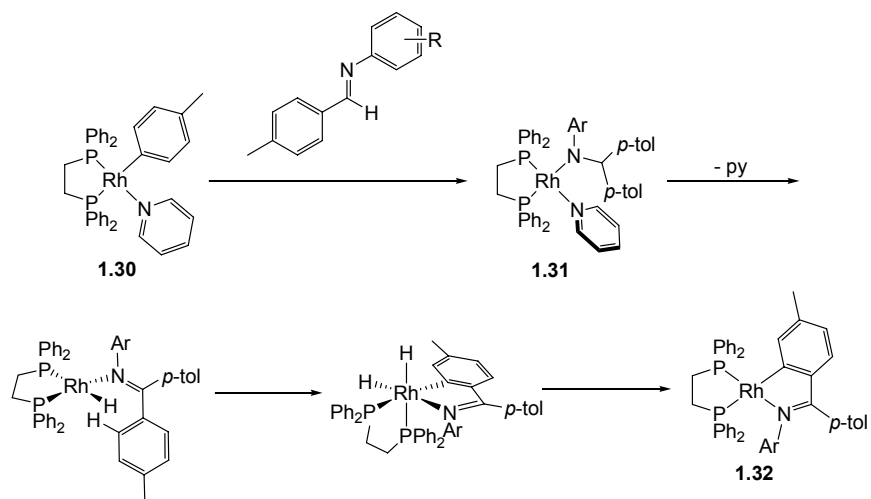
**Scheme 1.17:** Rhodium catalyzed phenyl 1,2-addition to aldimines involving transmetalation chemistry.

A Heck-type cross-coupling of imines with aryl halides was developed by Hartwig.<sup>51</sup> The proposed reaction pathway proceeds analogously to that of the Heck reaction involving alkenes, where the rhodium-aryl halide complex reacting with aldimine instead of olefin to afford ketimine product. To facilitate imine insertion it was demonstrated that an ancilliary donor is required on the aniline moiety of the aldimine substrate. The heteroatom of the pyrazyl moiety promotes coordination of the imine to the rhodium favouring insertion. The proposed catalytic cycle [Scheme 1.18] involves the oxidative addition of an aryl halide to rhodium (I), followed by aldimine 1,2-insertion in the rhodium-carbon bond of the generated rhodium (III) complex to yield a rhodium-amide complex **1.28**. Subsequently, the rhodium (III)-amide undergoes  $\beta$ -hydride elimination to afford ketimine and hydridorhodium complex **1.29**. Reductive elimination of HX from **1.29** regenerates the starting rhodium (I) complex.



**Scheme 1.18:** The catalytic cycle of aryl halides and aldimines in a Heck-type coupling.

Hartwig recently investigated the stoichiometric reaction of aldimines with rhodium-aryl complexes.<sup>52</sup> The formation of stable rhodium-amide products enabled mechanistic studies of the 1,2-insertion of imines. The studies provide evidence to distinguish between a 1,2-insertion versus 1,2-addition mechanism [Scheme 1.19]. The kinetic data demonstrated first-order dependence in both rhodium-aryl **1.30** and imine, with reverse first-order in pyridine. The data confirms substitution of pyridine by imine prior to insertion; however, it does not confirm the coordination mode of imine. Insertion of *N*-aryl benzaldimines into the rhodium-carbon bond affords two isolable products: a rhodium-amide **1.31** or a metallacycle **1.32**. The latter results from  $\beta$ -hydride elimination of the rhodium-amide followed by *ortho*-metalation. Reactivity investigations of the rhodium-aryl complex **1.30** show that the rhodium-carbon bond is polarized; the aryl has greater nucleophilicity and thus is more nucleophilic towards insertion.



**Scheme 1.19:** The 1,2-insertion of aldimines into rhodium-carbon bonds.

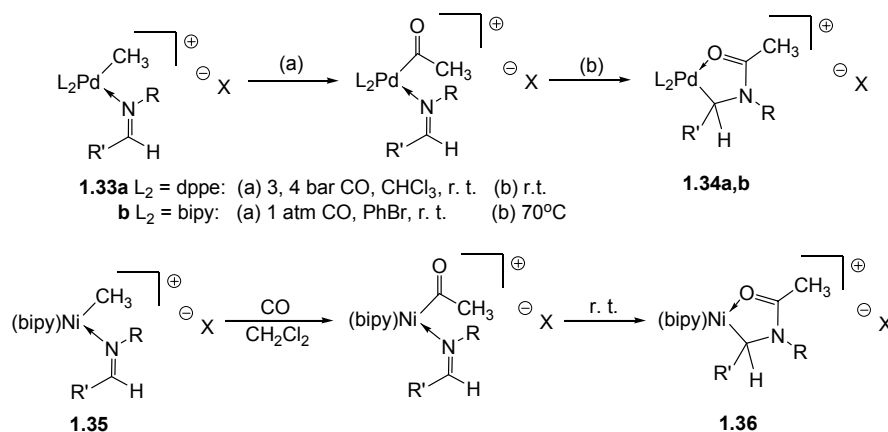


### 1.3 The Transition Metal Coupling of Imines and Carbon Monoxide in the Construction of Amide Bonds

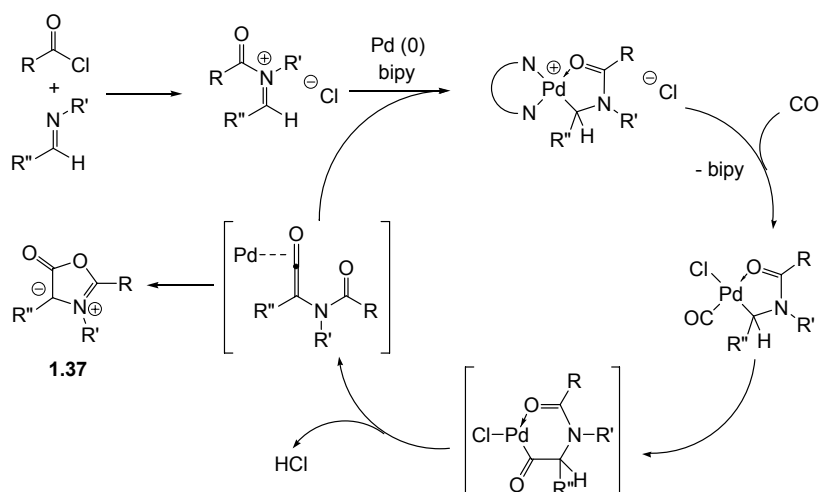
Until 1998, there were no examples of imine insertion into late transition metal-carbon bonds to form stable complexes, though the reaction had been postulated in several systems.<sup>39b,53,54</sup>

The compatibility of the Pd(II) olefin/CO copolymerization catalysts toward heteroatoms<sup>55</sup> has stimulated studies in our research group to determine if these systems would allow similar insertion reactions with imines. This showed that cationic palladium<sup>7a,56</sup> **1.33** and nickel<sup>7b</sup> **1.35** complexes can undergo the sequential insertion of carbon monoxide and imines into a metal-methyl bond, and represent the first well-defined examples of imine insertions into late transition metal-carbon bonds [**Scheme 1.20**]. In contrast to olefins, which insert rapidly into metal-alkyl  $\sigma$ -bonds, these complexes show no evidence of imine insertion into Pd-CH<sub>3</sub> bond, even with prolonged heating. It is reasoned that the thermodynamic and kinetic barriers are too high to observe the imine insertion product.

However, the insertion of carbon monoxide into the metal-alkyl bond to afford a metal-acyl complex facilitates the insertion of imine. The main difference is the thermodynamic stability of the amide-metallacycle generated. Initial attempts to insert carbon monoxide into the metal-carbon of **1.34b** and **1.36** failed due to the intrinsic strength of the chelate, which prevents a free coordination site from being generated. It was when a neutral palladium (II) species was employed that a subsequent insertion of CO was achieved. However, this success lead to the  $\beta$ -hydride elimination product: Münchnones **1.37** [**Scheme 1.21**]. While these small molecules are interesting synthons for a variety of heterocycles, they put us on a tangent from our goal.

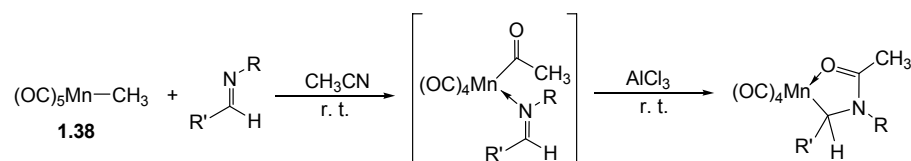


**Scheme 1.20:** The carbon monoxide and imine sequential 2,1-insertion mediated by group 10 transition metal complexes.



**Scheme 1.21:** The palladium catalyzed formation of Münchnones **1.37**.

Neutral manganese complex **1.38** displayed similar reactivity; however, due to the lower electropositive nature of the complex, a Lewis acid was required to aid the imine insertion [Scheme 1.22].<sup>57</sup> The electrophilicity of the acyl group is believed to allow the direct nucleophilic attack by the imine nitrogen at the acyl carbon.



**Scheme 1.22:** Lewis acid initiated imine insertion into a manganese-acyl complex.

The cationic palladium complexes **1.33** were the subject of a Density Functional Theory study carried out by Cavallo.<sup>58</sup> The results obtained provided insight into the characteristics of the imine insertion transition state. Comparison of the 2,1-migratory insertion of imines into both Pd-methyl and -acyl species show that the barrier of insertion into Pd-CH<sub>3</sub> is approximately 20 kcal/mol higher in energy than into Pd-COCH<sub>3</sub>. These results reflect the stability of [(bipy)Pd(CH<sub>3</sub>)(imine)]<sup>+</sup> observed experimentally.<sup>7a</sup> Comparing this data with the analogous insertion of olefins into Pd-methyl and -acyl bonds reveals that olefins<sup>59</sup> have a lower barrier to insertion than imines ( $\Delta H^\ddagger = 16.6$  kcal/mol for CH<sub>2</sub>=CH<sub>2</sub> vs.  $\Delta H^\ddagger = 22.2$  kcal/mol for CH<sub>2</sub>=NH into Pd-COCH<sub>3</sub>). The reaction energy profile drawn by these calculations shows the imine adopts a  $\pi$ -bond geometry only as it approaches the transition state for insertion. Furthermore, analysis of the bond lengths is consistent with an early transition state.

## 1.4 Overview of Thesis

Cationic Pd (II)- and Ni (II)-complexes have demonstrated to allow the migratory insertion of imine into metal-acyl bonds, leading to the coupling of carbon monoxide and imines to form products with the amide scaffold. However, a stable metallacycle is formed and inhibits the use of this system for further insertion chemistry. This can be postulated to result from the Lewis acidic nature of the cationic metal centers, which promote strong coordination of the acyl oxygen and prevent desired empty coordination sites from being generated for further insertions. Consequently, to achieve multi-insertions a novel catalyst is required. The recent successful use of neutral nickel catalysts to copolymerize ethylene with substrates containing heteroatoms suggest such lower Lewis acidic neutral complexes may be a good candidate for the sequential insertion of CO and imines.<sup>60</sup> The synthesis of imine coordinated nickel (II)-salicylaldiminato complexes and the reactivity of these complexes towards insertion is described in **Chapter 2**.

In addition, the mechanistic understanding of how imine 2,1-migratory insertion occurs could prove important for the proper design of transition metal mediated coupling of imines and carbon monoxide. The mechanism of this process with the cationic palladium (II) system has been a subject of numerous kinetic studies in our laboratory. This investigation will be elaborated in **Chapter 3** and a fitting mechanistic picture will be proposed. Correspondingly, the palladium complex also mediates the analogous alkene insertion; hence both mechanisms of insertion will be compared.

## 1.5 References

- (1) (a) Zassinovich, G.; Mestron, G. *Chem. Rev.* **1992**, 92, 1051. (b) Naota, T.; Takaya, H.; Murahashi, S.I. *Chem. Rev.* **1998**, 98, 2599. (c) Wheatley, N.; Kalck, P. *Chem. Rev.* **1999**, 99, 3379. (d) Rossen, K. *Angew. Chem. Int. Ed.* **2001**, 40, 4611. (e) Adolfsson, H. *Angew. Chem. Int. Ed.* **2005**, 44, 3340.
- (2) (a) Holt, M.S.; Wilson, W.L.; Nelson, J.H. *Chem. Rev.* **1989**, 89, 11. (b) Hegedus, L.S. *J. Organomet. Chem.*, **1993**, 457, 167. (c) Luh, T.Y.; Leung, M.K.; Wong, K.T. *Chem. Rev.* **2000**, 100, 3187.
- (3) (a) Ungváry, F. *J. Organomet. Chem.*, **1993**, 457, 273. (b) Alonso, F.; Beletskaya, I.P.; Yus, M. *Chem. Rev.* **2002**, 102, 4009. (c) Punniyamurthy, T.; Velusamy, S.; Iqbal, J. *Chem. Rev.* **2005**, 105, 2329.
- (4) (a) Schore, N.E. *Chem. Rev.* **1988**, 88, 1081. (b) Welker, M.E. *Chem. Rev.* **1992**, 92, 97. (c) Lautens, M.; Klute, W.; Tam, W. *Chem. Rev.* **1996**, 96, 49. (d) Frühauf, H.W. *Chem. Rev.* **1997**, 97, 523.
- (5) (a) Ittel, S.D.; Johnson, L.K. *Chem. Rev.* **2000**, 100, 1169. (b) Boffa, L.S.; Novak, B.M. *Chem. Rev.* **2000**, 100, 1479. (c) Kamigaito, M.; Ando, T.; Sawamoto, M. *Chem. Rev.* **2001**, 101, 3689. (d) Mecking, S. *Angew. Chem., Int. Ed.* **2001**, 40, 534. (e) Poli, R. *Angew. Chem. Int. Ed.* **2006**, 45, 5058.
- (6) (a) Crabtree, R.H. *The Organometallic Chemistry of Transition Metals*, Wiley-Interscience: Hoboken, N.J., **2005**. (b) Collman, J.P.; Hegedus, L.S.; Norton, J.R.; Finke, R.G. *Principles and Application of Organotransition Metal Chemistry*, University Science Books: Sausalito, **1987**.
- (7) (a) Dghaym, R.D.; Yaccato, K.J.; Arndtsen, B.A. *Organometallics* **1998**, 17, 4. (b) Davis, J.L.; Arndtsen, B.A. *Organometallics* **2000**, 19, 4657.
- (8) (a) Williams, R. M. *Synthesis of Optically Active  $\alpha$ -Amino Acids*, Pergamon Press, Oxford, **1989**. (b) Durhaler, R. *Tetrahedron* **1994**, 50, 1539.
- (9) (a) Strecker, A. *Ann. Chem. Pharm.* **1850**, 75, 27. (b) Strecker, A. *Ann. Chem. Pharm.* **1854**, 91, 349.

- (10) Ugi, I.; Offermann, K. *Chemische Berichte* **1964**, 97, 2996. (b) Gokel, G.; Luedke, G.; Ugi, I. *Isonitrile Chem.* **1971**, 145.
- (11) (a) Saito, S.; Yokoyama, H.; Ishikawa, T.; Niwa, N.; Moriwake, T. *Tetrahedron Lett.* **1991**, 32, 663. (b) Evans, D.A.; Ellman, J.A.; Dorow, R.L. *Tetrahedron Lett.* **1987**, 28, 1123. (c) Evans, D.A.; Britton, T.C.; Ellmann, J.A.; Dorow, R.L. *J. Am. Chem. Soc.* **1990**, 112, 4011. (d) Calmes, M.; Daunis, J. *Amino Acids* **1999**, 16, 215. (e) Erdik, E. *Tetrahedron* **2004**, 60, 8747. (f) Greck, C.; Drouillat, B.; Thomassigny, C. *Eur. J. Org. Chem.* **2004**, 1377.
- (12) (a) Schöllkopf, U. *Topics in Current Chemistry*; Boschke, F.L.: Springer, Berlin **1983**. (b) Belokon', Y.N. *Pure Appl. Chem.* **1992**, 64, 1917. (c) Williams, R.M. *Aldrichimica Acta* **1992**, 25, 11.
- (13) With tetramethylguanidinium azide (TMGA): (a) Hoffmann, R.V.; Kim, H.-O. *Tetrahedron* **1992**, 48, 3007. (b) Hansson, T.G.; Kihlberg, J.O. *J. Org. Chem.* **1986**, 51, 4490. (c) Barrett, A.G.M.; Lebold, S.A. *J. Org. Chem.* **1990**, 55, 3853. With amines: (d) Kogan, T.P.; Somers, T.C.; Vemuti, M.C. *Tetrahedron* **1990**, 46, 6623. (e) D'Angeli, F.; Marchetti, P.; Cavicchioni, G.; Catelani, G.; Nejad, F.M.K. *Tetrahedron: Asymmetry* **1990**, 1, 155. With hydrazines: (f) Hoffmann, R.V.; Kim, H.-O. *Tetrahedron Lett.* **1990**, 31, 2953. With hydroxylamines: (g) Feenstra, R.W.; Stokkingreef, E.H.M.; Nivard, R.J.F.; Ottenheijm, H.C.J. *Tetrahedron* **1988**, 44, 5583. With imides: (h) Degerbeck, F.; Fransson, B.; Grehn, L.; Ragnarsson, U. *J. Chem. Soc., Perkin Trans. I* **1992**, 245. (i) Degerbeck, F.; Fransson, B.; Grehn, L.; Ragnarsson, U. *J. Chem. Soc., Perkin Trans. I* **1993**, 11.
- (14) (a) Schöllkopf, U. *Pure Appl. Chem.* **1983**, 55, 1799. (b) Schöllkopf, U.; Busse, U.; Kilger, R.; Lehr, P. *Synthesis* **1984**, 271. (c) Schöllkopf, U.; Westphalen, K.O.; Schröder, J.; Horn, K. *Liebigs Ann. Chem.* **1988**, 781.
- (15) Studer, A.; Seehach, D. *Liebigs Ann.* **1995**, 217.
- (16) (a) Vedejs, E.; Fields, S.C.; Schrimpf, M.R. *J. Am. Chem. Soc.* **1993**, 115, 11612. (b) Vedejs, E.; Chapman, R.W.; Fields, S.C.; Lin, S.; Schrimpf, M.R. *J. Org. Chem.* **1995**, 60, 3020. (c) Vedejs, E.; Fields, S.C.; Lin, S.; Schrimpf, M.R. *J. Org. Chem.* **1995**, 60, 3028.

- (17) (a) Evans, D.A.; Weber, A.E. *J. Am. Chem. Soc.* **1986**, *108*, 6757. (b) Evans, D.A.; Weber, A.E. *J. Am. Chem. Soc.* **1987**, *109*, 7151. (c) Evans, D.A.; Ellman, J.A.; Dorow, R.L. *Tetrahedron Lett.* **1987**, *28*, 1123. (d) Evans, D.A.; Britton, T.C.; Ellmann, J.A.; Dorow, R.L. *J. Am. Chem. Soc.* **1990**, *112*, 4011.
- (18) (a) Williams, R.M.; Im, M.N. *J. Am. Chem. Soc.* **1991**, *113*, 9276. (b) Baldwin, J.E.; Lee, V.; Schofield, C.J. *Synlett* **1992**, 249.
- (19) (a) Sinclair, P.J.; Zhai, D.; Reibenspies, J.; Williams, R.M. *J. Am. Chem. Soc.* **1986**, *108*, 1103. (b) Williams, R.M.; Sinclair, P.J.; Zhai, D.; Chen, D. *J. Am. Chem. Soc.* **1988**, *110*, 1547. (c) Williams, R.M.; Zhai, W. *Tetrahedron* **1988**, *44*, 5425. (d) Williams, R.M.; Hendrix, J.A. *J. Org. Chem.* **1990**, *55*, 3723.
- (20) (a) Eggen, I.F.; Bakelaar, F.T.; Petersen, A.; Ten Kortenaar, P.B.W.; Ankone, N.H.S.; Bijsterveld, H.E.J.M.; Bours, G.H.L.; El Bellaj, F.; Hartsuiker, M.J.; Jan Kuiper, G.; Ter Voert, E.J.M. *J. Peptide Sci.* **2005**, *11*, 633. (b) Bruckdorfer, T.; Marder, O.; Albericio, F. *Curr. Pharm. Biotech.* **2004**, *5*, 29. (c) Andersson, L.; Blomberg, L.; Flegel, M.; Lepsa, L.; Nilsson, B.; Verlander, M. *Biopolymer* **2000**, *55*, 227.
- (21) Gröger, Harald *Chem. Rev.* **2003**, *103*, 2795.
- (22) (a) Hegedus, L.S.; de Week, G.; D'Andrea, S. *J. Am. Chem. Soc.* **1988**, *110*, 2122. (b) Schwindt, M.A.; Miller, J.R.; Hegedus, L.S. *J. Organomet. Chem.* **1991**, *413*, 143. (c) Vernier, J.-M.; Hegedus, L.S.; Miller, D.B. *J. Org. Chem.* **1992**, *57*, 6914. (d) Hegedus, L.S.; Lastra, E.; Narukawa, Y.; Snustad, D.C. *J. Am. Chem. Soc.* **1992**, *114*, 2991. (e) Hegedus, L.S.; Schwindt, M.A.; De Lombaert, S.; Imwinkelried, R. *J. Am. Chem. Soc.* **1990**, *112*, 2264. (f) Lastra, E.; Hegedus, L.S. *J. Am. Chem. Soc.* **1993**, *115*, 87.
- (23) (a) Scott, J.W. in *Topics in Stereochemistry*, Eliel, E.L.; Wilen, S.H.; J. Wiley & Sons, New York, **1989**. (b) Sakuraba, S.; Morimoto, T.; Achiwa, K. *Tetrahedron: Asymmetry* **1991**, *2*, 597. (c) Giovannetti, J.S.; Kelly, C.M.; Landis, C.R. *J. Am. Chem. Soc.* **1993**, *115*, 4040. (d) Kagan, H.B.; Sasaki, M. *Optically Active Phosphines: Preparation, Uses, and Chiroptical Properties in the Chemistry of*

- Organophosphorus Compounds, Vol. 1* Hartley, F.R.; J. Wiley & Sons, New York, **1990**. (e) Markó, L.; Ungvári, F. *J. Organomet. Chem.* **1992**, 432, 1.
- (24) Beller, M.; Eckert, M. *Angew. Chem. Int. Ed.* **2000**, 39, 1010.
- (25) (a) Wakamatsu, H.; Uda, J.; Yamakami, N. *J. Chem. Soc. Chem. Commun.* **1971**, 1540.
- (26) (a) Izawa, K. *Yuki Gosei Kagaku Kyokaishi* **1988**, 46, 218. (b) Ojima, I.; Zhang, Z. *Organometallics* **1990**, 9, 3122.
- (27) Knifton, J.F. *Applied Homogeneous Catalysis with Organometallic Compounds* Wiley-VCH Verlag GmbH: Weinheim, Germany, **2002**.
- (28) (a) Beller, M.; Eckert, M.; Vollmüller, F.; Geissler, H.; Bogdanovic, S.; (Hoechst AG), DEB 196 27 717, **1996**. (b) Beller, M.; Eckert, M.; Vollmüller, F.; Bogdanovic, S.; Geissler, H. *Angew. Chem. Int. Ed.* **1997**, 36, 1494. (c) Dyker, G. *Angew. Chem. Int. Ed. Engl.* **1997**, 36, 1700.
- (29) Enzmann, A.; Eckert, M.; Ponikwar, W.; Polborn, K.; Schneiderbauer, S.; Beller, M.; Beck, W. *Eur. J. Inorg. Chem.* **2004**, 1330.
- (30) (a) Gabriel, S. *S. Ber. Dtsch. Chem. Ges.* **1908**, 41, 242. (b) Böhme, H.; Broese, R.; Dick, A.; Eiden, F.; Schünemann, D. *Chem. Ber.* **1959**, 92, 1599. (c) Böhme, H.; Ellenberg, H.; Herboth, O.E.; Lehnert, W. *Chem. Ber.* **1959**, 92, 1608. (d) Böhme, H.; Dick, A.; Driesen, G. *Chem. Ber.* **1961**, 94, 1879. (e) Couture, A.; Deniau, E.; Grandclaude, P.; Moreira, R.; Mendes, E.; Calheiros, T.; Bacelo, M.J.; Iley, J. *Tetrahedron Lett.* **1994**, 35, 7107. (f) Couture, A.; Deniau, E.; Grandclaude, P. *Synthesis* **1994**, 953. (g) Couture, A.; Deniau, E.; Grandclaude, P. *Synth. Commun.* **1992**, 22, 2381. (h) Weygand, F.; Steglich, W.; Lengyel, I.; Fraunberger, F.; Maierhofer, A.; Oettmeier, W. *Chem. Ber.* **1966**, 99, 1944. (i) Venkov, A.P.; Mollov, N.M. *Synthesis* **1982**, 216. (j) Kasper, F.; Böttger, H. *Z. Chem.* **1987**, 27, 70.
- (31) (a) Klaus, S.; Neumann, H.; Jiao, H.; Jacobi von Wangelin, A.; Gördes, D.; Strübing, D.; Hübner, S.; Hateley, M.; Weckbecker, C.; Huthmacher, K.; Riermeier, T.; Beller, M. *J. Organomet. Chem.* **2004**, 689, 3685.



- (32) (a) Ware, E. *Chem. Rev.* **1950**, 46, 403. (b) Lopez, C.A.; Trigo, G.G. *Adv. Heterocycl. Chem.* **1985**, 38, 177. (c) Bucherer, H.T.; Steiner, W. *J. Prakt. Chem.* **1934**, 140, 291. (d) Bucherer, H.T.; Lieb, V.A. *J. Prakt. Chem.* **1934**, 141, 5.
- (33) Beller, M.; Moradi, W.A.; Eckert, M.; Neumann, H. *Tetrahedron Lett.* **1999**, 40, 4523.
- (34) (a) Deming, T. *Nature*, **1997**, 390, 386. (b) Deming, T. *J. Am. Chem. Soc.* **1998**, 120, 4240. (c) Curtin, S.A.; Deming, T. *J. Am. Chem. Soc.* **1999**, 121, 7427. (d) Deming, T.; Curtin, S.A. *J. Am. Chem. Soc.* **2000**, 122, 5710.
- (35) Brzezinska, K.R.; Deming, T.J. *Macromol. Biosci.* **2004**, 4, 566.
- (36) Brzezinska, K.R.; Deming, T.J. *Macromolecules* **2001**, 34, 4348.
- (37) (a) Jia, L.; Ding, E.; Anderson, W.R. *Chem. Commun.* **2001**, 1436. (b) Xu, H.; LeGall, N.; Jia, L.; Brennessel, W.W.; Kucera, B.E., *J. Organomet. Chem.* **2005**, 690, 5150. (c) Darensbourg, D.J.; Phelps, A.L.; LeGall, N.; Jia, L. *J. Am. Chem. Soc.* **2004**, 126, 13808.
- (38) (a) Chamberlain, L.R.; Steffey, B.D.; Rothwell, I.P.; Huffman, J.C. *Polyhedron* **1989**, 8, 341. (b) Durfee, L.D.; Hill, J.E.; Fanwick, P.E.; Rothwell, I.P. *Organometallics* **1990**, 9, 75.
- (39) (a) Fryzuk, M.D.; Piers, W.E. *Organometallics* **1990**, 9, 986. (b) Muller, F.; van Koten, G.; Vrieze, K. *Organometallics* **1989**, 8, 33.
- (40) (a) Abel, E.W.; Rowley, R.J. *J. Chem. Soc., Dalton Trans.* **1975**, 1096. (b) Fong, C.W.; Wilkinson, G. *J. Chem. Soc., Dalton Trans.* **1975**, 1100. (c) Matsumoto, M.; Nakatsu, K.; Tani, K.; Nakamura, A.; Otsuka, S. *J. Am. Chem. Soc.* **1974**, 96, 6777. (d) Crawford, S.S.; Firestein, G.; Kaesz, H.D. *J. Organomet. Chem.* **1975**, 91, C57. (e) Sepelak, D.J.; Pierpont, C.G.; Barefield, E.K.; Budz, J.T.; Poffenberger, C.A. *J. Am. Chem. Soc.* **1976**, 98, 6178.
- (41) Crabtree, R. H. *The Organometallic Chemistry of the Transition Metals*, 2nd ed., John Wiley and Sons, New York, 1994.
- (42) For C=N multiple bond insertions: (a) Buchwald, S.L.; Watson, B.T.; Wannamaker, M.W.; Dewad, J.C. *J. Am. Chem. Soc.* **1989**, 111, 4486. (b) Willoughby, C.A.; Buchwald, S.L. *J. Am. Chem. Soc.* **1994**, 116, 11703. (c) Debad, J.D.; Legzdins, P.;

- Lumb, S.A.; Batchelor, R.J.; Einstein, F.W.B. *Organometallics* **1995**, *14*, 2543. (d) Obora, Y.; Ohta, T.; Stern, C.L.; Marks, T.J. *J. Am. Chem. Soc.* **1997**, *119*, 3745.
- (43) Thorn, M.G.; Hill, J.E.; Waratuke, S.A.; Johnson, E.S.; Fanwick, P.E.; Rothwell, I.P. *J. Am. Chem. Soc.* **1997**, *119*, 8630.
- (44) Zippel, T.; Arndt, P.; Ohff, A.; Spannenberg, A.; Kempe, R.; Rosenthal, U. *Organometallics* **1998**, *17*, 4429.
- (45) Obora, Y.; Ohta, T.; Stern, C.L.; Marks, T.J. *J. Am. Chem. Soc.* **1997**, *119*, 3745.
- (46) (a) Nakamura, H.; Iwama, H.; Yamamoto, Y. *J. Am. Chem. Soc.* **1996**, *118*, 6641. (b) Nakamura, H.; Aoyagi, K.; Shim, J.G.; Yamamoto, Y. *J. Am. Chem. Soc.* **2001**, *123*, 372.
- (47) (a) Nakamura, H.; Nakamura, K.; Yamamoto, Y. *J. Am. Chem. Soc.* **1998**, *120*, 4242. (b) Fernandes, R.A.; Stimac, A.; Yamamoto, Y. *J. Am. Chem. Soc.* **2003**, *125*, 14133.
- (48) (a) Oi, S.; Moro, M.; Fukuhara, H.; Kawanishi, T.; Inoue, Y. *Tetrahedron Lett.* **1999**, *40*, 9259. (b) Ueda, M.; Miyaura, N. *J. Organomet. Chem.* **2000**, *595*, 31. (c) Hayashi, T.; Ishigedani, M. *J. Am. Chem. Soc.* **2000**, *122*, 976.
- (49) Ueura, K.; Miyamura, S.; Satoh, T.; Miura, M. *J. Organomet. Chem.* **2006**, *691*, 2821.
- (50) Ueda, M.; Saito, A.; Miyaura, N. *Synlett* **2000**, 1637.
- (51) Ishiyama, T.; Hartwig, J. *J. Am. Chem. Soc.* **2000**, *122*, 12043.
- (52) (a) Krug, C.; Hartwig, J.F. *J. Am. Chem. Soc.* **2004**, *126*, 2694. (b) Krug, C.; Hartwig, J.F. *Organometallics* **2004**, *23*, 4594.
- (53) (a) Gladysz, J.A.; Williams, G.M.; Tam, W.; Johnson, D.L.; Parker, D.W.; Selover, J. C. *Inorg. Chem.* **1979**, *18*, 553. (b) Alper, H.; Amaratunga, S. *Tetrahedron Lett.* **1981**, *22*, 3811. (c) Alper, H.; Amaratunga, S. *J. Org. Chem.* **1982**, *47*, 3593.
- (54) Reduto dos Reis, A.C.; Hegedus, L.S. *Organometallics* **1996**, *14*, 1586.
- (55) (a) Drent, E.; Budzelaar, P. H. M. *Chem. Rev.* **1996**, *96*, 663. (b) Sen, A. *Acc. Chem. Res.* **1993**, *26*, 303. (c) Rix, F. C.; Brookhart, M.; White, P. S. *J. Am. Chem. Soc.* **1996**, *118*, 4746 and references therein.

- (56) (a) Kacker, S.; Kim, J. S.; Sen, A. *Angew. Chem., Int. Ed.* **1998**, *37*, 1251. (b) Kang, M.; Sen, A. *Organometallics* **2005**, *24*, 3508.
- (57) Lafrance, D.; Davis, J.L.; Dhawan, R.; Arndtsen, B.A. *Organometallics* **2001**, *20*, 1128.
- (58) Cavallo, L. *J. Am. Chem. Soc.* **1999**, *121*, 4238.
- (59) (a) Johnson, L.K.; Killian, C.M.; Brookhart, M. *J. Am. Chem. Soc.* **1995**, *117*, 6414.  
(b) Riz, F. C.; Brookhart, M.; White, P. C. *J. Am. Chem. Soc.* **1996**, *118*, 4746.
- (60) (a) Wang, C.; Friedrich, S.; Younkin, T.R.; Li, R.T.; Grubbs, R.H.; Bansleben, D.A.; Day, M.W. *Organometallics* **1998**, *17*, 3149. (b) Younkin, T.R.; Connor, E.F.; Henderson, J.I.; Friedrich, S.K.; Grubbs, R.H.; Bansleben, D.A. *Science* **2000**, *287*, 460.

## ❧ CHAPTER 2 ❧

### Nickel (II) Mediated Sequential Insertion of Carbon Monoxide and Imine

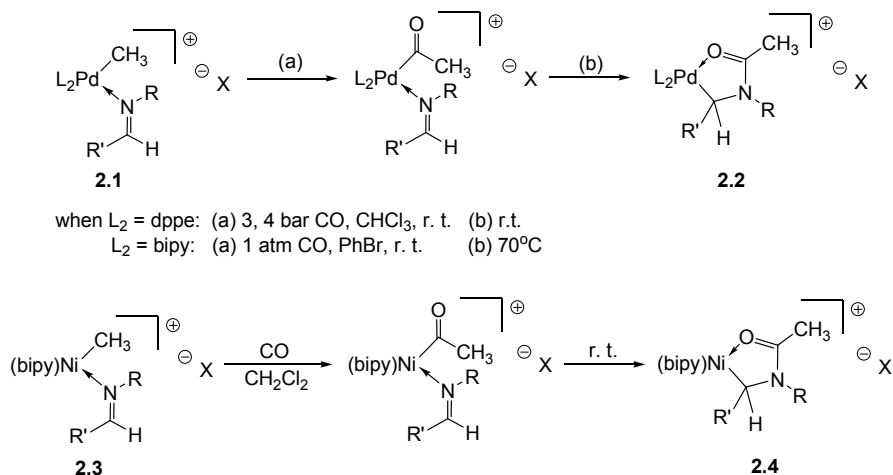
#### 2.0 Introduction

The migratory insertion of unsaturated substrates into transition metal-carbon bonds has significant utility in synthetic chemistry. This has been perhaps most thoroughly explored with carbon-carbon multiple bonds. The polymerization of olefins or alkynes is indispensable for the preparation of a wide-range of polymeric materials.<sup>1</sup> Additionally, the migratory insertion of alkenes is a critical step in many organic synthetic transformations (*e.g.* Heck reaction,<sup>2</sup> alkene-alkyne coupling reactions,<sup>3</sup> reductions,<sup>4</sup> and many others<sup>5</sup>).

In contrast to olefins, the use of C=N bonds<sup>6</sup> in migratory insertion into late transition metal-carbon bonds is much more limited. This difference may result from both thermodynamic and kinetic factors. The insertion of imines entails the cleavage of a strong C=N  $\pi$ -bond, and formation of a C-N single bond, which can be less favoured. In addition, stable aldimines bear substituents at N and C that render them more hindered than  $\alpha$ -olefins. Finally, imines typically coordinate to transition metals in a  $\sigma$ -fashion through the nitrogen lone pair, instead of via  $\pi$ -coordination, the postulated requirement for insertion.<sup>7</sup> Despite these features, examples of both catalytic and stoichiometric processes involving imine insertion into late transition metal-carbon bonds have been recently reported.<sup>8</sup> These processes typically involve the 1,2-insertion of imine and lead to the formation of metal-nitrogen bonded intermediates or products.

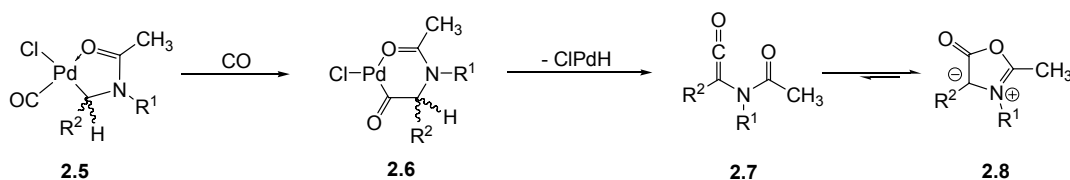
Both we<sup>9</sup> and Sen<sup>10</sup> have recently demonstrated that cationic Pd (II) complexes mediate the sequential insertion of carbon monoxide (CO) and imines to generate metal-amide chelates [**Scheme 2.1**]. A similar reaction can also occur with Ni (II) complexes.<sup>11</sup> Notably, imine insertion proceeds in a 2,1-fashion leading to the formation of a new metal-carbon bond, and thus represent the fundamental steps in a potential CO/imine copolymerization. However, the strong coordination of the acyl-oxygen to these metal

centers in **2.2** and **2.4** inhibits the creation of an empty coordination site and blocks further insertion steps.



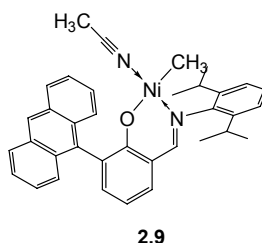
**Scheme 2.1:** The sequential insertion of carbon monoxide and imine in palladium (II) **2.1** and nickel (II) **2.3** cationic species.

While the cationic metal-amine complexes **2.2** and **2.4** are stable, we have recently observed that the less Lewis acidic neutral Pd (II) complexes **2.5** [Scheme 2.2], generated via oxidative addition of *N*-acyl iminium salts to palladium (0), can undergo further insertion of carbon monoxide to afford a transient six-membered palladacycle. This intermediate lacks any stabilizing ligand on **2.6**, however, and undergoes rapid  $\beta$ -hydride elimination to generate an  $\alpha$ -amide substituted ketene **2.7** which is in equilibrium with its closed heterocyclic form (1,3-oxazolium-5-oxide or Münchnone **2.8**).<sup>12</sup>



**Scheme 2.2:** The sequential insertion of carbon monoxide in Pd (II)-amide neutral species.

The lack of further insertion chemistry with cationic complexes **2.2** and **2.4** is analogous to the well known inhibition in the polymerization of functionalized alkenes. The chelation of strongly coordinating functional groups on the alkene can slow or block polymerization with cationic late transition metal catalysts.<sup>13</sup> However, recent results have shown that neutral, less Lewis acidic nickel and palladium catalysts can, under certain conditions, more easily polymerize functionalized alkenes. For example, neutral  $\kappa^2$ -*N,O*-salicylaldiminato nickel (II) complexes [**Figure 2.1**] are known to catalyze the copolymerization of polar alkenes with substituted norbornenes, carbon monoxide, and  $\alpha$ - $\omega$  functional olefins.<sup>14</sup> The lower Lewis acidity in complex **2.9** has been postulated to inhibit chelation of polar functional groups, thereby allowing further alkene insertions. In addition, the sterically bulky groups of the salicylaldiminato ligand prevent  $\beta$ -hydride elimination. In light of these features, we became interested in the potential of these neutral nickel complexes to mediate the sequential insertion of carbon monoxide and imines. The synthesis and reactivity of the imine coordinated nickel (II)-salicylaldiminato complexes ( $N^{\wedge}O$ )Ni(R)( $R^1N=C(H)R^2$ ) ( $N^{\wedge}O$  = salicylaldiminato; R = CH<sub>3</sub>, Ph; R<sup>1</sup> = alkyl; R<sup>2</sup> = aryl) are presented below. We have found that these nickel complexes undergo rapid insertion of carbon monoxide. For certain coordinated imines, these complexes undergo imine insertion, followed by disproportionation to generate 1,2-diamides.



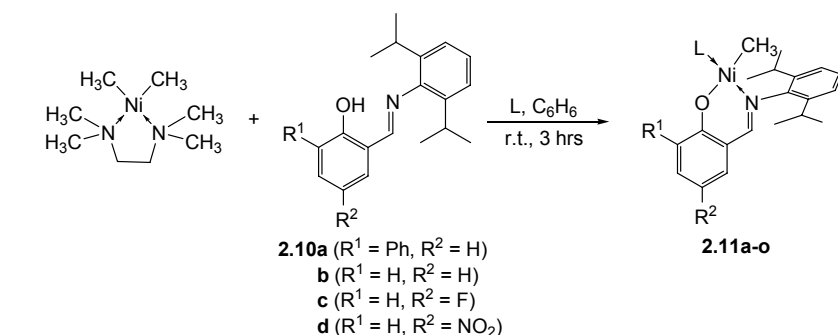
**Figure 2.1:** Neutral  $\kappa^2$ -*N,O*-salicylaldiminato nickel (II) catalyst for the copolymerization of polar alkenes.

## 2.1 Results and Discussion

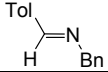
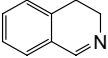
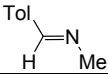
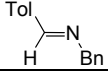
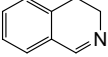
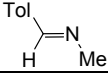
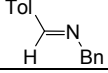
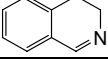
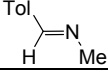
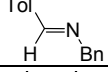
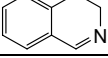
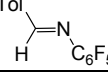
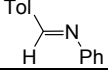
### 2.1.1 Synthesis and Stability of Imine $\kappa^2$ -*N,O*-Salicylaldiminato Ni (II) Complexes

Nickel-imine complexes **2.11a-o** of the form  $(N^{\wedge}O)Ni(R)(R^1N=C(H)R^2)$  ( $N^{\wedge}O$  = salicylaldiminato;  $R = CH_3$ ;  $R^1$  = alkyl;  $R^2$  = aryl) can be synthesized via the reaction of  $(tmeda)NiMe_2$  ( $tmeda = N, N, N', N'$ -tetramethylethylenediamine), free phenolic ligand **2.10** and imine in benzene. This procedure is analogous to the synthesis of **2.9** reported by Grubbs.<sup>15</sup> Removal of solvents and washing with pentane yielded complexes **2.11a-m** as orange powders. The  $^1H$  and  $^{13}C$  NMR spectra for **2.11a-o** display a downfield shift in the imine resonances upon coordination, consistent with  $\eta^1$ -binding of the imine through the nitrogen (*e.g.* **2.11g**  $^1H$  NMR:  $\delta$  8.43 (s,  $CH=N$ ),  $^{13}C$  NMR:  $\delta$  166.1 ( $CH=N$ ), versus free imine  $^1H$  NMR: 8.26 ppm (s,  $CH=N$ ),  $^{13}C$  NMR:  $\delta$  159.3 ( $CH=N$ )).<sup>9,11</sup> All other spectroscopic data are consistent with the structure shown and are in agreement with the literature.<sup>14-16</sup> The regiochemistry of **2.11g**, with the imine coordinated *cis* to the Ni-O bond, was assigned based on  $^1H$ -NOE NMR studies. These studies revealed the nickel-methyl ligand (**2.11g**  $^1H$  NMR:  $\delta$  -0.73 (s, 3H)) in close proximity to both the aldimine hydrogen, and the methine (**2.11g**  $^1H$  NMR:  $\delta$  4.16 (sept., 2H)) and methyl (**2.11g**  $^1H$  NMR:  $\delta$  1.51 (d, 6H), 1.04 (d, 6H)) protons of the isopropyl group.

**Table 2.1:** The synthesis of  $\kappa^2$ -*N,O*-salicylaldiminato nickel (II) complexes **2.11a-o**.



Compound	$R^1$	$R^2$	L	Yield <b>2.11</b> <sup>a</sup>
<b>2.11a</b>	Ph	H		60%
<b>2.11b</b>	Ph	H		91%

<b>2.11c</b>	Ph	H		88%
<b>2.11d</b>	Ph	H		89%
<b>2.11e</b>	H	H		81%
<b>2.11f</b>	H	H		76%
<b>2.11g</b>	H	H		81%
<b>2.11h</b>	H	F		73%
<b>2.11i</b>	H	F		74%
<b>2.11j</b>	H	F		78%
<b>2.11k</b>	H	NO <sub>2</sub>		83%
<b>2.11l</b>	H	NO <sub>2</sub>		87%
<b>2.11m</b>	H	NO <sub>2</sub>		92%
<b>2.11n</b>	Ph	H		0% (20%) <sup>b,c</sup>
<b>2.11o</b>	Ph	H		0% (44%) <sup>b,c</sup>

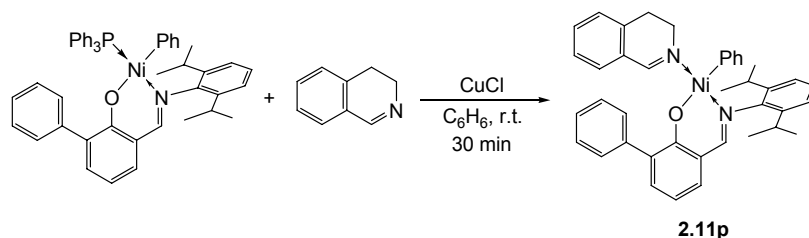
**a** Isolated yields; **b** Determined by <sup>1</sup>H NMR analysis for the formation of **2.11**; **c** Not isolable, thermally unstable.

While nickel complexes **2.11a-m** were generally isolated in good yields, complexes of poorly coordinating imines, *N*-pentafluoro tolualdimine **2.11n** and *N*-phenyl tolualdimine **2.11o**, were not isolable, despite being observed *in-situ* by <sup>1</sup>H NMR spectroscopy.<sup>17</sup> The lower stability of these complexes is likely the result of a weaker nickel-imine bond, results from the low basicity of these imines and the poor Lewis acidity of the neutral nickel complex.

The phenyl substituted nickel complex **2.11p** can also be prepared via reaction of (N<sup>^</sup>O)Ni(Ph)(PPh<sub>3</sub>)<sup>18</sup> (N<sup>^</sup>O = salicylaldiminato) and 3,4-dihydroisoquinoline, with CuCl as a phosphine scavenger [Scheme 2.3]. Precipitation of the complex with pentane afforded a yellow powder. The spectroscopic data observed for **2.11p** are analogous to



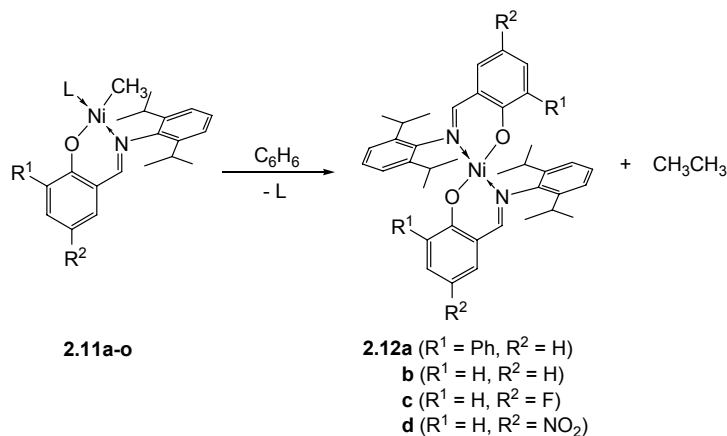
those for the nickel-methyl complexes, and  $^1\text{H}$ -NOE NMR analysis confirms the regiochemistry depicted in **2.11p**.



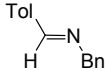
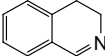
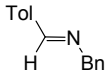
**Scheme 2.3:** The synthesis of the  $\kappa^2$ -*N,O*-salicylaldiminato nickel (II) complex **2.11p**.

As it was previously noted for the analogous nickel-acetonitrile complex **2.9**,<sup>15</sup> these imine complexes decompose in benzene at ambient temperature to generate uncoordinated imine and *bis*-salicylaldiminato nickel (II) complexes **2.12**.<sup>19</sup> As shown in **Table 2.2**, this decomposition is accelerated by steric bulk and electron withdrawing groups on the salicylaldiminato ligand **2.10**, as well as by polar solvents. Notably, imine insertion into the Ni-methyl bond was not observed under any conditions.

**Table 2.2:** Approximate decomposition times of selected nickel-imine complexes.



Compound	$R^1$	$R^2$	L	Time <sup>a</sup>	Yield <b>2.12</b> <sup>b</sup>
<b>2.11f</b>	H	H		61 hrs	96 %
<b>2.11i</b>	H	F		39 hrs	91 %
<b>2.11l</b>	H	NO <sub>2</sub>		10 hrs	95 %

<b>2.11c</b>	Ph	H		6 hrs	84 % <sup>c</sup>
<b>2.11g</b>	H	H		11 hrs	89 %
<b>2.11f<sup>d</sup></b>	H	H		5 hrs	88 % <sup>c</sup>

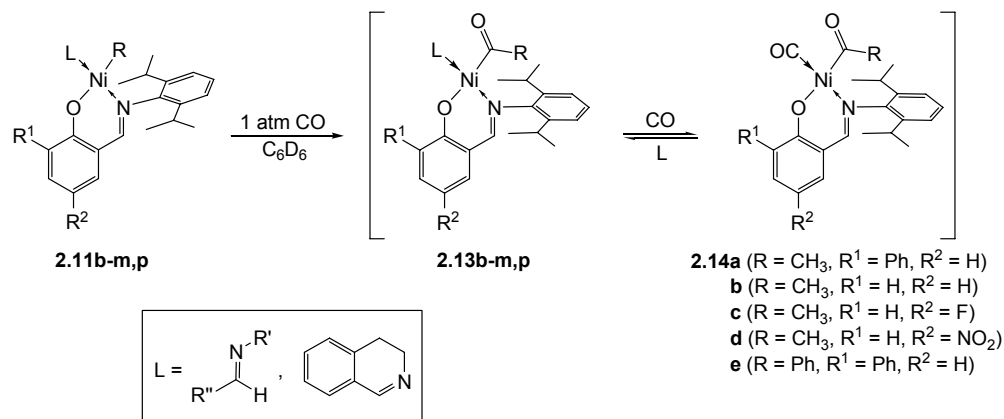
**a** General conditions: 0.02 M of **2.11** in *d*<sub>6</sub>-benzene at 25°C, monitored *in-situ* by <sup>1</sup>H NMR; **b** <sup>1</sup>H NMR yields with ligand as the limiting reagent; **c** isolated yield; **d** in *d*<sub>3</sub>-acetonitrile.

### 2.1.2 Reaction of $\kappa^2$ -*N,O*-Salicylaldiminato Ni (II) Complexes With Carbon Monoxide

Exposing complexes **2.11b-m** to 1 atm of carbon monoxide (CO) in the presence of 3 equivalents of imine at ambient temperature results in the rapid insertion of CO to afford what has been preliminarily assigned as Ni-acyl complexes **2.13b-m**. These complexes are formed in equilibrium with CO-coordinated complexes **2.14a-d** [Scheme 2.4]. For examples, monitoring the reaction of **2.11g** by <sup>1</sup>H NMR spectroscopy reveals the disappearance of the Ni-CH<sub>3</sub> singlet after 15 minutes at ambient temperature, along with the appearance of two new Ni-COCH<sub>3</sub> singlets at  $\delta$  1.92 ppm (**2.13g**) and  $\delta$  2.49 ppm (**2.14b**) in a 7 to 1 ratio. <sup>1</sup>H-NOE NMR studies confirm *cis*-coordination of these two ligands in **2.13g**. Although <sup>1</sup>H NMR spectra of **2.14** show a similar Ni-acyl ligand, no corresponding coordinated imine is detected. As expected, this same CO-coordinated complex is observed regardless of the imine in **2.11**.

The ratio of **2.13** and **2.14** varies with the coordination ability of the imine, and the bulk and electronic properties of the ligand [Table 2.3]. As predicted, increasing the steric bulk around the nickel center favours the generation of **2.14** (*e.g.* **2.14a** vs. **2.14b**). However, having electron withdrawing substituents on the ligand framework, which presumably increases the Lewis acidity of the metal center, favours imine coordination. The ratio of imine coordinated complex **2.13** increased with the addition of excess imine.

**Table 2.3:** The formation of nickel-acyl complexes **2.13b-m,p** and **2.14a-e** in the presence of 1 atm of carbon monoxide.



Complex <sup>a</sup>	R	R <sup>1</sup>	R <sup>2</sup>	R'	R''	[Imine]	Ratio <sup>b</sup> 2.13:2.14
<b>2.11b</b>	CH <sub>3</sub>	Ph	H	Me	Tol	0.15 M	1.2 : 1
<b>2.11c</b>	CH <sub>3</sub>	Ph	H	Bn	Tol	0.15 M	1.2 : 1
<b>2.11d</b>	CH <sub>3</sub>	Ph	H	3,4-DHQ	Tol	0.15 M	5.4 : 1
<b>2.11e</b>	CH <sub>3</sub>	H	H	Me	Tol	0.15 M	1.9 : 1
<b>2.11e</b>	CH <sub>3</sub>	H	H	Me	Tol	2.5 M	> 20 : 1
<b>2.11f</b>	CH <sub>3</sub>	H	H	Bn	Tol	0.15 M	2.0 : 1
<b>2.11f</b>	CH <sub>3</sub>	H	H	Bn	Tol	2.5 M	> 20 : 1
<b>2.11g</b>	CH <sub>3</sub>	H	H	3,4-DHQ	Tol	0.15 M	7.3 : 1
<b>2.11g</b>	CH <sub>3</sub>	H	H	3,4-DHQ	Tol	2.5 M	> 20 : 1
<b>2.11h</b>	CH <sub>3</sub>	H	F	Me	Tol	0.15 M	7.8 : 1
<b>2.11i</b>	CH <sub>3</sub>	H	F	Bn	Tol	0.15 M	3.1 : 1
<b>2.11j</b>	CH <sub>3</sub>	H	F	3,4-DHQ	Tol	0.15 M	11.5 : 1
<b>2.11k</b>	CH <sub>3</sub>	H	NO <sub>2</sub>	Me	Tol	0.15 M	5.5 : 1
<b>2.11l</b>	CH <sub>3</sub>	H	NO <sub>2</sub>	Bn	Tol	0.15 M	3.2 : 1
<b>2.11m</b>	CH <sub>3</sub>	H	NO <sub>2</sub>	3,4-DHQ	Tol	0.15 M	6.9 : 1
<b>2.11p</b>	Ph	Ph	H	3,4-DHQ	Tol	0.15 M	3.2 : 1

**a** General conditions: 1 atm of CO at 25°C in *d*<sub>6</sub>-benzene with 0.05 M of **2.11**; **b** measured at 15 mins following the addition of CO to the reaction. (3,4-dihydroisoquinoline (3,4-DHQ))

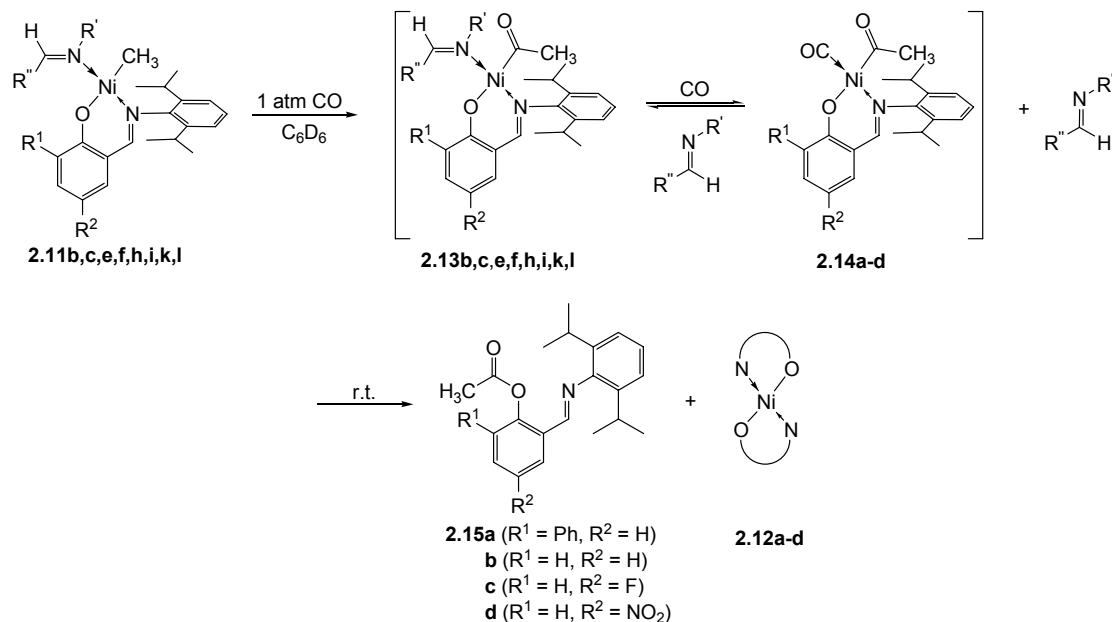
Under 1 atm of CO, Ni-phenyl complex **2.11p** undergoes CO insertion at a similar rate to **2.11b-m**.<sup>20</sup> The Ni-benzoyl complex **2.13p** generated is preliminarily assigned by <sup>1</sup>H NMR and NOE spectroscopy. As with the Ni-acyl complexes, **2.13p** exist in dynamic

equilibrium with the CO-coordinated complex **2.14e**, with the larger steric bulk surrounding the nickel center pushed the equilibrium towards **2.14**.

### 2.1.3 Reactivity of $\kappa^2$ -*N,O*-Salicylaldiminato Ni-acyl Complexes **2.13**

The synthesis of nickel-acyl imine complexes **2.13** allows us to probe the imine insertion propensity of these neutral complexes. In contrast to what is observed with the cationic nickel complexes, where imine insertion occurs rapidly to form amide palladacycle **2.4**, the *N*-methyl and *N*-benzyl substituted imine complexes **2.13** do not undergo insertion into the Ni-acyl bond. Rather, after 5 hours at ambient temperature, the acyl and the phenolic moieties of the salicylaldiminato ligand reductively eliminate to generate the respective acetyl esters **2.14a-d** along with uncoordinated imine and **2.12** [Table 2.4].<sup>21</sup> Although higher concentrations of imine increase the presence of **2.13** relative to **2.14**, reductive elimination remains the favoured reaction pathway.

**Table 2.4:** Reaction products with *trans*-imine substrates in benzene under 1 atm CO.



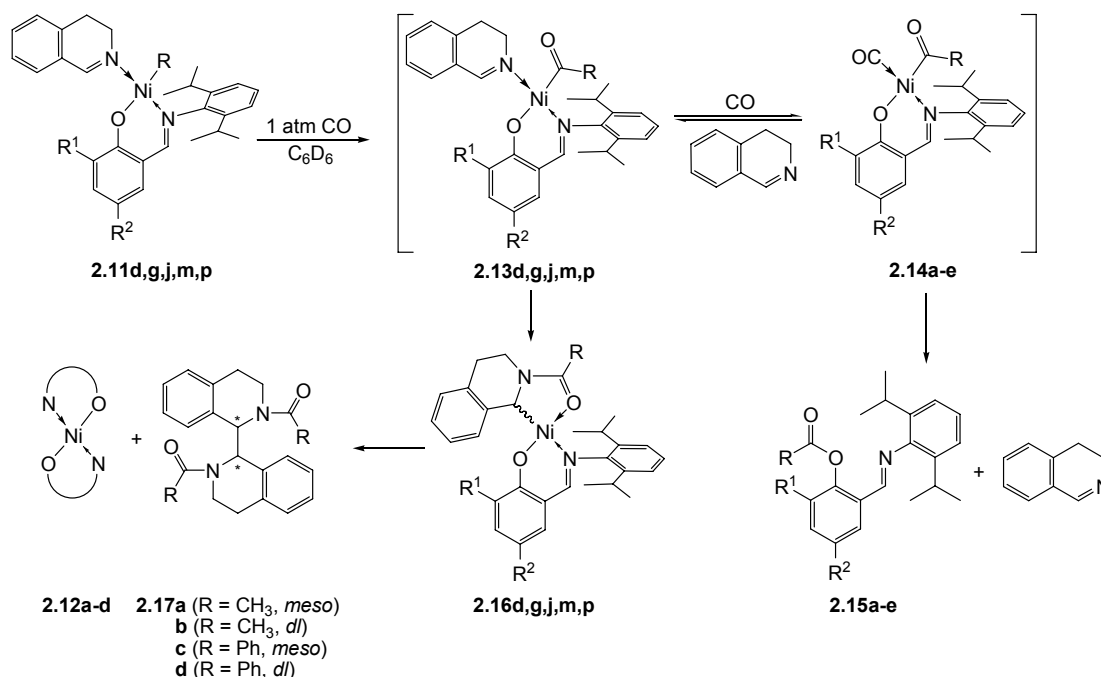
Complex <sup>a</sup>	R <sup>1</sup>	R <sup>2</sup>	R'	R''	[Imine]	Yield <b>2.15</b> <sup>b</sup>	Yield <b>2.12</b> <sup>c</sup>
<b>2.11b</b>	Ph	H	Me	Tol	0.15 M	89 %	n/a <sup>d</sup>
<b>2.11c</b>	Ph	H	Bn	Tol	0.15 M	90 %	n/a <sup>d</sup>
<b>2.11e</b>	H	H	Me	Tol	0.15 M	86 %	13 %

<b>2.11e</b>	H	H	Me	Tol	2.5 M	33 %	62 %
<b>2.11f</b>	H	H	Bn	Tol	0.15 M	87 %	11 %
<b>2.11f</b>	H	H	Bn	Tol	2.5 M	40 %	56 %
<b>2.11h</b>	H	F	Me	Tol	0.15 M	84 %	13 %
<b>2.11i</b>	H	F	Bn	Tol	0.15 M	78 %	21 %
<b>2.11k</b>	H	NO <sub>2</sub>	Me	Tol	0.15 M	41 %	42 %
<b>2.11l</b>	H	NO <sub>2</sub>	Bn	Tol	0.15 M	76 %	23 %

**a** General conditions: 1 atm of CO at 25°C in *d*<sub>6</sub>-benzene with 0.05 M of **2.11**; **b** <sup>1</sup>H NMR yields; **c** <sup>1</sup>H NMR yields with ligand as the limiting reagent; **d** Paramagnetic in nature.

This data suggests that reductive elimination from **2.13** or **2.14** has a lower activation energy barrier than imine insertion into the Ni-acyl bond. To address the issue of faster reductive elimination than imine insertion, we hypothesized that less sterically encumbered *cis*-tethered imines, such as 3,4-dihydroisoquinoline, might coordinate more tightly to **2.11** and undergo faster insertion. Indeed, nickel complex **2.13d** reacted in the presence of 3 equivalents of imine for 5 hours at ambient temperature to form 1,2-diamides **2.17a,b** as the major products, along with an approximate 15 % yield of ester **2.15a**. Similar results are obtained with other 3,4-dihydroisoquinoline complexes, **2.13g,j,m**, each forming 1,2-diamides as major products.

**Table 2.5:** Reaction product distribution with 3,4-dihydroisoquinoline substrate.



Entry	Complex <sup>a</sup>	R <sup>1</sup>	R <sup>2</sup>	[3,4-dihydro-isoquinoline]	[CO]	Yield 2.17 <sup>b</sup>	Yield 2.15 <sup>c</sup>	Yield 2.12 <sup>d</sup>
1	2.11d	Ph	H	0.15 M	1 atm	74 %	15 %	n/a <sup>e</sup>
2	2.11d	Ph	H	0.50 M	1 atm	94 %	5 %	n/a <sup>e</sup>
3	2.11d	Ph	H	0.15M	3 atm	64 %	26 %	n/a <sup>e</sup>
4 <sup>f</sup>	2.11d	Ph	H	0.15 M	1 atm	25 %	75 %	n/a <sup>e,g</sup>
5 <sup>h</sup>	2.11d	Ph	H	0.15 M	1 atm	75 %	24 %	n/a <sup>e</sup>
6	2.11g	H	H	0.15 M	1 atm	77 %	14 %	80 %
7	2.11g	H	H	0.50 M	1 atm	97 %	3 %	95 %
8	2.11g	H	H	0.15 M	3 atm	63 %	28 %	72 %
9 <sup>f</sup>	2.11g	H	H	0.15 M	1 atm	40 %	53 %	n/a <sup>g</sup>
10 <sup>h</sup>	2.11g	H	H	0.15 M	1 atm	79 %	20 %	75 %
11	2.11j	H	F	0.15 M	1 atm	75 %	15 %	85 %
12	2.11m	H	NO <sub>2</sub>	0.15 M	1 atm	82 %	15 %	84 %
13	2.11p	Ph	H	0.15 M	1 atm	5 %	40 %	51 %
14	2.11p	Ph	H	0.50M	1 atm	25 %	14 %	78 %

**a** General conditions: 1 atm of CO at 25°C in *d*<sub>6</sub>-benzene with 0.05 M of **2.11**; **b** <sup>1</sup>H NMR yields of both diastereomers; **c** <sup>1</sup>H NMR yields; **d** <sup>1</sup>H NMR yields with ligand as the limiting reagent; **e** Paramagnetic in nature; **f** *d*<sub>3</sub>-Acetonitrile; **g** Precipitates out of acetonitrile; **h** With 1 equivalent of 9,10-dihydroanthracene **2.18**.

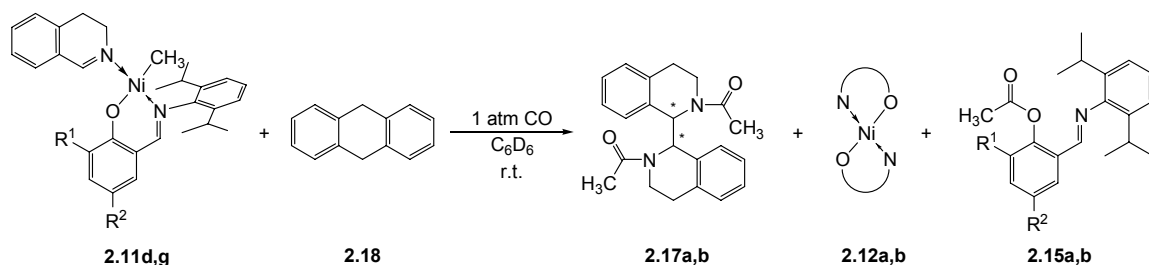
In the case of the Ni-benzoyl complexes, higher concentrations of imine are required in order to increase the concentration of **2.13p** and favour imine insertion [Table 2.5, entry 14]. Thus for similar reaction conditions, the yields of 1,2-diamides **2.17c,d** are lower with complex **2.11p**. The reactivity and products afforded are otherwise analogous to those of the Ni-acyl complexes.

#### 2.1.4: Mechanism of *N,N'*-Diacyl-1,1',2,2',3,3',4,4'-octahydro-1,1'-biisoquinoline 2.17 Formation

The generation of 1,2-diamides in the reaction mixture supports the presence of a transient amide-nickelacycle, the result of imine insertion into the nickel-acyl σ-bond. This would provide a reasonable mechanism for the coupling of imine and acyl ligand in **2.13**, which subsequently decompose to form the 1,2-diamide **2.17**. As shown in Table 2.5, the addition of excess imine increases the yield of **2.17**, while increased CO pressure favours **2.15**. Similarly, performing this reaction in coordinating solvents also favours

ester **2.15** formation as these are also competitors to imine coordination. Considering the dynamic equilibrium between **2.13** and **2.14**, this data suggests that the 1,2-diamide **2.17** product forms via imine coordinated complexes **2.13**.

In order to further probe the intermediacy of the imine insertion product **2.17** in this chemistry, the reaction of **2.11g** was monitored by  $^1\text{H}$  NMR spectroscopy in  $d_6$ -benzene. This reveals the formation of a transient species preliminarily assigned as **2.16g**. This complex builds up to a maximum of *ca.* 30% yield over the course of 5 hours at ambient temperature. **2.16g** shows a new acyl resonance at  $\delta$  0.65 (s, 3H,  $\text{NiC(H)NCOCH}_3$ ), and an up shift in the formal imine hydrogen resonance from  $\delta$  8.63 (s,  $\text{CH=N}$ ) in **2.13g** to  $\delta$  5.42 (s, 1H,  $\text{NiC(H)NCOCH}_3$ ) in **2.16g**.<sup>22</sup> The latter is consistent with the reduction of the  $\text{C=N}$   $\pi$ -bond in **2.16**, and is similar to related imine insertion products with cationic nickel complexes.<sup>11</sup> Analogous behaviour is also observed with the other 3,4-dihydroisoquinoline products. The formation of these imine insertion products is rapid relative to that with cationic palladium complexes (70  $^\circ\text{C}$ , 6 hrs) and similar in rate to what has been observed with cationic nickel complexes (70  $^\circ\text{C}$ , 30 min). This suggests that, provided the imine is sufficiently nucleophilic to compete with ester reductive elimination, sequential CO/imine insertion is viable with neutral complexes.



**Scheme 2.4:** The reactivity of 3,4-dihydroisoquinoline nickel complexes **2.11d,g** in the presence of 9,10-dihydroanthracene **2.18**.

Further, monitoring the reaction by  $^1\text{H}$  NMR spectroscopy shows the disappearance of **2.16** coincides with the growth of **2.17**, consistent with its intermediacy in 1,2-diamide formation. The bimolecular coupling of nickel-alkyl ligands to form alkenes is an established transformation.<sup>23</sup> These processes could proceed via a number of pathways, including radical, ionic or bimetallic mechanisms. While at present we have

no conclusive data on the mechanism of 1,2-diamide formation, it is notable that the addition of radical traps<sup>24</sup> [**Table 2.5, entries 5 and 10, and Scheme 2.4**] does not alter product distribution, arguing against a radical pathway.



## 2.2 Conclusion

The sequential insertion of carbon monoxide and imine in  $(\text{N}^{\wedge}\text{O})\text{Ni}(\text{R})(\text{R}^2(\text{H})\text{C}=\text{NR}^1)$  **2.11** complexes was investigated. The insertion of carbon monoxide leads to the rapid and general formation of nickel-acyl imine complexes  $(\text{N}^{\wedge}\text{O})\text{Ni}(\text{COCH}_3)(\text{R}^1\text{N}=\text{C}(\text{H})\text{R}^2)$  **2.13**, which are in dynamic equilibrium with the CO-coordinated  $(\text{N}^{\wedge}\text{O})\text{Ni}(\text{COCH}_3)(\text{CO})$  **2.14** complexes. The reductive elimination of the nickel-acyl and the phenolic ligands to form esters is the dominant reaction with bulky *trans*-imines. However, with the *cis*-substituted 3,4-dihydroisoquinoline imine insertion is quite rapid (ambient temperature, 5 hrs) leading to the formation of **2.16** intermediate, which ultimately disproportionates to form 1,2-diamides **2.17**. Overall, this suggests that imine insertion into neutral nickel-acyl bonds is a viable process, and that inhibition of subsequent disproportionation could allow these products to be used in subsequent chemistry. Efforts towards the latter are currently underway.

## 2.3 Experimental Section

All manipulations were carried out in dried glassware under a dry, dioxygen-free ( $O_2$ ), dinitrogen ( $N_2$ ) atmosphere, using standard Schlenk or glovebox techniques and a Vacuum Atmosphere 553-2 drybox. Unless otherwise noted, all reagents were purchased from commercial sources and used without purification: carbon monoxide (Matheson, 99.98%), 9,10-dihydroanthracene (Aldrich, 97%), benzyl benzoate (Aldrich, 99+%). All solvents were freshly distilled and de-gassed before use and stored under nitrogen over activated molecular sieves. Diethyl ether was distilled using sodium benzophenone. Pentane, benzene and toluene were distilled using  $CaH_2$ . Acetonitrile was distilled using  $P_4O_{10}$ . Deuterated solvents were dried as their protonated analogs, but vacuum transferred from the drying agent. Tolualdimines,<sup>25</sup> 3,4-dihydroisoquinoline,<sup>26</sup> (tmeda)Ni(CH<sub>3</sub>)<sub>2</sub>,<sup>27</sup> and (6-phenyl-2-((2,6-diisopropylphenyl)iminomethyl)phenoxy)Ni(Ph)(PPh<sub>3</sub>)<sup>18</sup> were prepared via literature procedures. Salicylaldimines<sup>15,28</sup> and their salicylaldehyde precursors were also prepared as described in the literature.

Nuclear magnetic resonance (NMR) characterization was obtained on JEOL 270MHz, Varian Mercury 200MHz, 300MHz, 400MHz and Varian Unity 500MHz spectrometers. <sup>1</sup>H and <sup>13</sup>C NMR chemical shifts were referenced to residual solvent. Electrospray ionization-high resolution mass spectrometry (ESI-HRMS) analyses were performed by Alain Lesimple, Ph.D. at the Department of Medicine, Mass Spectrometry Unit, McGill University, Montréal, Canada. **2.12b**<sup>15</sup> and **2.17a-d**<sup>29</sup> are previously reported compounds.

### 2.3.1 General Procedure for the Synthesis of the $\kappa^2$ -*N,O*-Salicylaldiminato Ni (II) Complexes

Standard procedure for the synthesis of complexes **2.11a-o** is as follows. (tmeda)Ni(CH<sub>3</sub>)<sub>2</sub> (50.0 mg, 0.244 mmol) was dissolved in a 20 mL scintillation vial in benzene (*ca.* 5 mL) to give a yellow brown solution. In a separate vessel, imine (0.732 mmol) and salicylaldimine **2.10** (0.244 mmol) were dissolved in benzene (*ca.* 10 mL) and

the mixture was added to the nickel solution, dropwise, while stirring. The resulting dark reddish brown mixture was left to stir at ambient temperature for 3 hrs. The solution was then filtered through a Celite plug. The filtrate was concentrated under vacuo and triturated with pentane (*ca.* 5 mL). Orange solids were then collected by filtration and washed with pentane thrice (3 x 2 mL) to afford orange powder product.

**(6-phenyl-2-((2,6-diisopropylphenyl)iminomethyl)phenoxy)Ni(CH<sub>3</sub>)(pyridine)**

**(2.11a)**

No modifications to the procedure were made.

**Yield:** 60%

**<sup>1</sup>H NMR (400 MHz, C<sub>6</sub>D<sub>6</sub>):** δ 8.43 (d, 2H, *J*<sub>HH</sub> = 8.2 Hz), 7.57 (s, 1H), 7.40-7.38 (m, 3H), 7.31-6.88 (m, 5H), 6.54 (dt, 2H, <sup>1</sup>*J*<sub>HH</sub> = 29.6 Hz, <sup>2</sup>*J*<sub>HH</sub> = 7.3 Hz), 6.13 (s, 2H), 4.20 (sept., 2H, *J*<sub>HH</sub> = 6.6 Hz), 1.49 (d, 6H, *J*<sub>HH</sub> = 6.6 Hz), 1.06 (d, 6H, *J*<sub>HH</sub> = 6.6 Hz), -0.71 (s, 3H).

**<sup>13</sup>C NMR (500 MHz, C<sub>6</sub>D<sub>6</sub>):** δ 166.4, 165.2, 151.8, 150.1, 141.1, 140.6, 135.4, 134.5, 133.8, 133.3, 131.8, 129.8, 127.4, 126.4, 125.6, 123.5, 122.9, 120.6, 114.0, 28.5, 24.8, 23.1, -7.5.

**(6-phenyl-2-((2,6-diisopropylphenyl)iminomethyl)phenoxy)Ni(CH<sub>3</sub>)(*N*-methyl**

**tolualdimine) (2.11b)**

No modifications to the procedure were made.

**Yield:** 91%

**<sup>1</sup>H NMR (300 MHz, C<sub>6</sub>D<sub>6</sub>):** δ 9.47 (d, 2H, *J*<sub>HH</sub> = 8.2 Hz), 7.61 (s, 1H), 7.55-7.52 (m, 2H), 7.35 (d, 1H, *J*<sub>HH</sub> = 5.5 Hz), 7.10-6.89 (m, 6H), 6.86 (d, 1H, *J*<sub>HH</sub> = 1.7 Hz), 6.45 (t, 1H, *J*<sub>HH</sub> = 7.7 Hz), 4.22 (sept., 1H, *J*<sub>HH</sub> = 6.9 Hz), 4.02 (sept., 1H, *J*<sub>HH</sub> = 6.9 Hz), 3.35 (s, 3H), 2.03 (s, 3H), 1.51 (d, 3H, *J*<sub>HH</sub> = 6.9 Hz), 1.35 (d, 3H, *J*<sub>HH</sub> = 6.9 Hz), 1.19 (d, 3H, *J*<sub>HH</sub> = 6.9 Hz), 1.04 (d, 3H, *J*<sub>HH</sub> = 6.9 Hz), -1.09 (s, 3H).

**<sup>13</sup>C NMR (300 MHz, C<sub>6</sub>D<sub>6</sub>):** δ 166.2, 165.4, 165.2, 149.9, 142.0, 141.2, 141.0, 140.7, 134.5, 133.9, 133.4, 131.8, 130.8, 129.8, 129.3, 127.3, 126.4, 126.0, 123.6, 123.4, 120.6, 114.0, 50.1, 28.5, 28.4, 25.3, 24.9, 23.4, 23.1, 21.5, -11.6.

**ESI-HRMS:** calculated for C<sub>35</sub>H<sub>41</sub>N<sub>2</sub>ONi<sup>+</sup> (M + H<sup>+</sup>) 563.25614; found 563.25585.

**(6-phenyl-2-((2,6-diisopropylphenyl)iminomethyl)phenoxy)Ni(CH<sub>3</sub>)(N-benzyltolualdimine) (2.11c)**

No modifications to the procedure were made.

**Yield:** 88%

**<sup>1</sup>H NMR (500 MHz, C<sub>6</sub>D<sub>6</sub>):** δ 9.57 (d, 2H,  $J_{\text{HH}} = 7.3$  Hz), 7.57 (s, 1H), 7.51 (s, 2H), 7.33 (d, 1H,  $J_{\text{HH}} = 7.3$  Hz), 7.10-7.02 (m, 9H), 6.93 (d, 2H,  $J_{\text{HH}} = 6.4$  Hz), 6.85 (d, 2H,  $J_{\text{HH}} = 6.9$  Hz), 6.43 (t, 1H,  $J_{\text{HH}} = 7.3$  Hz), 4.93 (dd, 2H,  $^1J_{\text{HH}} = 135.9$  Hz,  $^2J_{\text{HH}} = 15.1$  Hz), 4.03 (sept., 2H,  $J_{\text{HH}} = 6.4$  Hz), 2.03 (s, 3H), 1.41 (dd, 6H,  $^1J_{\text{HH}} = 17.8$  Hz,  $^2J_{\text{HH}} = 6.9$  Hz), 1.19 (d, 3H,  $J_{\text{HH}} = 6.9$  Hz), 1.06 (d, 3H,  $J_{\text{HH}} = 6.9$  Hz), -1.10 (s, 3H).

**<sup>13</sup>C NMR (500 MHz, C<sub>6</sub>D<sub>6</sub>):** δ 166.1, 165.0, 164.8, 161.1, 149.8, 142.0, 141.1, 140.9, 135.7, 134.3, 133.7, 133.6, 132.0, 130.9, 130.6, 129.9, 129.4, 129.2, 128.6, 127.9, 127.4, 126.9, 126.3, 125.8, 123.4, 123.3, 120.3, 113.7, 65.7, 65.1, 28.3, 25.2, 24.9, 23.3, 23.1, 22.6, 21.4, 21.2, -11.1.

**ESI-HRMS:** calculated for C<sub>41</sub>H<sub>45</sub>N<sub>2</sub>ONi<sup>+</sup> (M + H<sup>+</sup>) 639.28774; found 639.28799.

**(6-phenyl-2-((2,6-diisopropylphenyl)iminomethyl)phenoxy)Ni(CH<sub>3</sub>)(3,4-dihydroisoquinoline) (2.11d)**

No modifications to the procedure were made.

**Yield:** 89%

**<sup>1</sup>H NMR (400 MHz, C<sub>6</sub>D<sub>6</sub>):** δ 8.27 (s, 1H), 7.59-7.57 (m, 3H), 7.41 (dd, 2H,  $^1J_{\text{HH}} = 4.9$  Hz,  $^2J_{\text{HH}} = 2.2$  Hz), 7.14-7.05 (m, 3H), 6.92-6.72 (m, 6H), 6.52-6.47 (m, 3H), 4.18 (sept., 2H,  $J_{\text{HH}} = 6.9$  Hz), 3.58 (t, 2H,  $J_{\text{HH}} = 6.3$  Hz), 1.91 (t, 2H,  $J_{\text{HH}} = 8.0$  Hz), 1.52 (d, 6H,  $J_{\text{HH}} = 6.9$  Hz), 1.07 (d, 6H,  $J_{\text{HH}} = 6.9$  Hz), -0.74 (s, 3H).

**<sup>13</sup>C NMR (300 MHz, C<sub>6</sub>D<sub>6</sub>):** δ 166.4, 165.3, 164.5, 150.2, 141.1, 141.0, 135.8, 134.5, 133.9, 133.5, 131.7, 129.9, 128.2, 127.9, 127.5, 127.2, 126.9, 126.5, 125.8, 123.6, 120.8, 113.9, 49.8, 28.5, 25.3, 24.9, 23.2, -9.8.

**ESI-HRMS:** calculated for C<sub>35</sub>H<sub>39</sub>N<sub>2</sub>ONi<sup>+</sup> (M + H<sup>+</sup>) 560.23376; found 560.23391.

**(2-((2,6-diisopropylphenyl)iminomethyl)phenoxide)Ni(CH<sub>3</sub>)(N-methyl tolualdimine)**  
**(2.11e)**

No modifications to the procedure were made.

**Yield:** 81%

**<sup>1</sup>H NMR (300 MHz, C<sub>6</sub>D<sub>6</sub>):** δ 9.41 (d, 2H,  $J_{\text{HH}} = 8.0$  Hz), 7.58 (s, 1H), 7.09-6.99 (m, 7H), 6.92 (d, 1H,  $J_{\text{HH}} = 7.0$  Hz), 6.40 (t, 1H,  $J_{\text{HH}} = 7.0$  Hz), 4.22 (sept., 1H,  $J_{\text{HH}} = 7.0$  Hz), 4.04 (sept., 1H,  $J_{\text{HH}} = 7.0$  Hz), 3.61 (s, 3H), 2.05 (s, 3H), 1.53 (d, 3H,  $J_{\text{HH}} = 6.6$  Hz), 1.31 (d, 3H,  $J_{\text{HH}} = 7.0$  Hz), 1.17 (d, 3H,  $J_{\text{HH}} = 7.0$  Hz), 1.03 (d, 3H,  $J_{\text{HH}} = 6.6$  Hz), -1.09 (s, 3H).

**<sup>13</sup>C NMR (300 MHz, C<sub>6</sub>D<sub>6</sub>):** δ 168.4, 166.1, 165.8, 150.1, 141.8, 141.2, 141.0, 134.3, 134.1, 131.9, 131.0, 129.3, 126.4, 123.6, 123.4, 122.9, 119.9, 113.7, 50.3, 28.5, 28.4, 25.2, 24.8, 23.3, 23.1, 21.4, -11.2.

**ESI-HRMS:** calculated for C<sub>29</sub>H<sub>36</sub>N<sub>2</sub>ONi<sup>+</sup> (M + H<sup>+</sup>) 487.22518; found 487.22539.

**(2-((2,6-diisopropylphenyl)iminomethyl)phenoxide)Ni(CH<sub>3</sub>)(N-benzyl tolualdimine)**  
**(2.11f)**

No modifications to the procedure were made.

**Yield:** 76 %

**<sup>1</sup>H NMR (500 MHz, C<sub>6</sub>D<sub>6</sub>):** δ 9.39 (d, 2H,  $J_{\text{HH}} = 7.8$  Hz), 7.55 (s, 1H), 7.37 (d, 1H,  $J_{\text{HH}} = 6.9$  Hz), 7.13-6.96 (m, 11H), 6.92 (d, 2H,  $J_{\text{HH}} = 6.4$  Hz), 6.42 (t, 1H,  $J_{\text{HH}} = 6.9$  Hz), 5.17 (dd, 2H,  $^1J_{\text{HH}} = 215.5$  Hz,  $^2J_{\text{HH}} = 14.2$  Hz), 3.97 (d of sept., 2H,  $^1J_{\text{HH}} = 33.8$  Hz,  $^2J_{\text{HH}} = 6.9$  Hz), 2.03 (s, 3H), 1.32 (dd, 6H,  $^1J_{\text{HH}} = 23.8$  Hz,  $^2J_{\text{HH}} = 6.9$  Hz), 1.13 (d, 3H,  $J_{\text{HH}} = 6.9$  Hz), 1.05 (d, 3H,  $J_{\text{HH}} = 6.9$  Hz), -1.27 (s, 3H).

**<sup>13</sup>C NMR (500 MHz, C<sub>6</sub>D<sub>6</sub>):** δ 168.1, 166.1, 165.4, 149.8, 141.8, 141.1, 140.9, 136.6, 134.2, 134.0, 132.1, 131.0, 130.4, 129.4, 129.1, 128.7, 126.9, 126.2, 123.4, 123.2, 122.8, 119.8, 113.6, 66.4, 28.2, 25.2, 25.0, 23.3, 23.2, 21.4, -9.9.

**ESI-HRMS:** calculated for C<sub>35</sub>H<sub>41</sub>N<sub>2</sub>ONi<sup>+</sup> (M + H<sup>+</sup>) 563.25689; found 563.25669.

**(2-((2,6-diisopropylphenyl)iminomethyl)phenoxy)Ni(CH<sub>3</sub>)(3,4-dihydroisoquinoline) (2.11g)**

No modifications to the procedure were made.

**Yield:** 81 %

**<sup>1</sup>H NMR (300 MHz, C<sub>6</sub>D<sub>6</sub>):** δ 8.43 (s, 1H), 7.53 (s, 1H), 7.18 (dt, 1H, <sup>1</sup>J<sub>HH</sub> = 5.2 Hz, <sup>2</sup>J<sub>HH</sub> = 1.6 Hz), 7.09-7.06 (m, 3H), 7.00 (d, 1H, J<sub>HH</sub> = 8.5 Hz), 6.91 (dd, 1H, <sup>1</sup>J<sub>HH</sub> = 7.3 Hz, <sup>2</sup>J<sub>HH</sub> = 1.6 Hz), 6.84 (t, 1H, J<sub>HH</sub> = 7.1 Hz), 6.72 (t, 1H, J<sub>HH</sub> = 7.1 Hz), 6.53-6.42 (m, 3H), 4.16 (sept., 2H, J<sub>HH</sub> = 6.9 Hz), 3.78 (t, 2H, J<sub>HH</sub> = 7.4 Hz), 2.10 (t, 2H, J<sub>HH</sub> = 7.7 Hz), 1.51 (d, 6H, J<sub>HH</sub> = 6.9 Hz), 1.04 (d, 6H, J<sub>HH</sub> = 6.9 Hz), -0.73 (s, 3H).

**<sup>13</sup>C NMR (300 MHz, C<sub>6</sub>D<sub>6</sub>):** δ 168.1, 166.1, 164.3, 150.3, 141.2, 135.7, 134.3, 134.1, 131.8, 127.3, 127.1, 126.4, 123.6, 122.9, 120.1, 113.7, 49.8, 28.5, 25.7, 24.9, 23.2, -9.1.

**ESI-HRMS:** calculated for C<sub>29</sub>H<sub>35</sub>N<sub>2</sub>ONi<sup>+</sup> (M + H<sup>+</sup>) 484.20246; found 484.20286.

**(4-fluoro-2-((2,6-diisopropylphenyl)iminomethyl)phenoxy)Ni(CH<sub>3</sub>)(N-methyltolualdimine) (2.11h)**

No modifications to the procedure were made.

**Yield:** 73 %

**<sup>1</sup>H NMR (300 MHz, C<sub>6</sub>D<sub>6</sub>):** δ 9.41 (d, 2H, J<sub>HH</sub> = 8.2 Hz), 7.37 (s, 1H), 7.07-6.98 (m, 6H), 6.80-6.72 (m, 2H), 6.57 (dd, 1H, J<sub>HH</sub> = 9.2 Hz, J<sub>HF</sub> = 3.0 Hz), 4.16 (sept., 1H, J<sub>HH</sub> = 6.9 Hz), 3.97 (sept., 1H, J<sub>HH</sub> = 6.9 Hz), 3.56 (s, 3H), 2.04 (s, 3H), 1.51 (d, 3H, J<sub>HH</sub> = 6.9 Hz), 1.30 (d, 3H, J<sub>HH</sub> = 6.9 Hz), 1.14 (d, 3H, J<sub>HH</sub> = 6.9 Hz), 1.02 (d, 3H, J<sub>HH</sub> = 6.9 Hz), -1.09 (s, 3H).

**<sup>13</sup>C NMR (300 MHz, C<sub>6</sub>D<sub>6</sub>):** δ 165.9, 165.1, 165.0, 154.2, 151.2, 149.8, 142.0, 140.9 (d, J<sub>CF</sub> = 13.4 Hz), 131.7, 131.0, 129.3, 126.5, 123.8 (d, J<sub>CF</sub> = 6.9 Hz), 123.5 (d, J<sub>CF</sub> = 12.0 Hz), 123.1, 122.8, 117.9 (d, J<sub>CF</sub> = 7.8 Hz), 116.2 (d, J<sub>CF</sub> = 21.2 Hz), 50.3, 28.5, 28.4, 25.1, 24.8, 23.3, 23.1, 21.4, -10.9.

**<sup>19</sup>F NMR (400 MHz, C<sub>6</sub>D<sub>6</sub>):** δ -137.9.

**ESI-HRMS:** calculated for C<sub>29</sub>H<sub>36</sub>N<sub>2</sub>ONiF<sup>+</sup> (M + H<sup>+</sup>) 505.21554; found 505.21597.

**(4-fluoro-2-((2,6-diisopropylphenyl)iminomethyl)phenoxy)Ni(CH<sub>3</sub>)(N-benzyltolualdimine) (2.11i)**

No modifications to the procedure were made.

**Yield:** 74%

**<sup>1</sup>H NMR (200 MHz, C<sub>6</sub>D<sub>6</sub>):** δ 9.38 (d, 2H,  $J_{\text{HH}} = 7.3$  Hz), 7.34 (s, 1H), 7.06-7.00 (m, 6H), 6.80-6.72 (m, 2H), 6.57 (d, 1H,  $J_{\text{HH}} = 7.3$  Hz), 5.11 (dd, 2H,  $^1J_{\text{HH}} = 80.8$  Hz,  $^2J_{\text{HH}} = 14.3$  Hz), 3.91 (sept., 2H,  $J_{\text{HH}} = 7.3$  Hz), 2.03 (s, 3H), 1.31 (t, 6H,  $J_{\text{HH}} = 7.7$  Hz), 1.07 (dd, 6H,  $^1J_{\text{HH}} = 14.1$  Hz,  $^2J_{\text{HH}} = 6.6$  Hz), -1.26 (s, 3H).

**<sup>13</sup>C NMR (300 MHz, C<sub>6</sub>D<sub>6</sub>):** δ 165.5, 165.1, 164.7, 153.5, 151.7, 149.6, 141.9, 140.8 (d,  $J_{\text{CF}} = 28.7$  Hz), 136.5, 132.0, 131.0, 130.4, 129.1, 128.7, 128.4, 126.3, 123.7, 123.3 (d,  $J_{\text{CF}} = 17.7$  Hz), 122.8 (d,  $J_{\text{CF}} = 24.4$  Hz), 117.7, 116.2 (d,  $J_{\text{CF}} = 21.1$  Hz), 66.4, 28.2, 25.1, 24.9, 23.3, 23.2, 21.4, -9.8.

**<sup>19</sup>F NMR (400 MHz, C<sub>6</sub>D<sub>6</sub>):** δ -132.9.

**ESI-HRMS:** calculated for C<sub>35</sub>H<sub>40</sub>N<sub>2</sub>ONiF<sup>+</sup> (M + H<sup>+</sup>) 581.24635; found 581.24727.

**(4-fluoro-2-((2,6-diisopropylphenyl)iminomethyl)phenoxy)Ni(CH<sub>3</sub>)(3,4-dihydroisoquinoline) (2.11j)**

No modifications to the procedure were made.

**Yield:** 78%

**<sup>1</sup>H NMR (500 MHz, C<sub>6</sub>D<sub>6</sub>):** δ 8.39 (s, 1H), 7.33 (s, 1H), 7.10-7.05 (m, 3H), 6.90 (dt, 1H,  $^1J_{\text{HH}} = 4.6$  Hz,  $^2J_{\text{HF}} = 1.4$  Hz), 6.83 (dt, 1H,  $^1J_{\text{HH}} = 8.7$  Hz,  $^2J_{\text{HF}} = 1.4$  Hz), 6.76-6.70 (m, 2H), 6.57 (dd, 1H,  $^1J_{\text{HH}} = 8.9$  Hz,  $^2J_{\text{HF}} = 3.2$  Hz), 6.51 (d, 1H,  $J_{\text{HH}} = 6.9$  Hz), 6.46 (d, 1H,  $J_{\text{HH}} = 7.3$  Hz), 4.10 (sept., 2H,  $J_{\text{HH}} = 6.9$  Hz), 3.73 (t, 2H,  $J_{\text{HH}} = 7.8$  Hz), 2.08 (t, 2H,  $J_{\text{HH}} = 7.8$  Hz), 1.50 (d, 6H,  $J_{\text{HH}} = 6.9$  Hz), 1.03 (d, 6H,  $J_{\text{HH}} = 6.9$  Hz), -0.73 (s, 3H).

**<sup>13</sup>C NMR (500 MHz, C<sub>6</sub>D<sub>6</sub>):** δ 165.1, 164.6, 164.3, 153.5, 151.7, 150.0, 140.8, 135.6, 131.7, 127.1 (d,  $J_{\text{CF}} = 24.5$  Hz), 126.4, 123.7, 123.6, 123.5, 123.0, 122.8 (d,  $J_{\text{CF}} = 24.0$  Hz), 118.0 (d,  $J_{\text{CF}} = 8.2$  Hz), 116.3 (d,  $J_{\text{CF}} = 21.6$  Hz), 49.7, 29.1, 28.4, 25.5, 24.7, 24.3, 23.6, 23.1, -9.0.

**<sup>19</sup>F NMR (400 MHz, C<sub>6</sub>D<sub>6</sub>):** δ -132.6.

**ESI-HRMS:** calculated for C<sub>29</sub>H<sub>34</sub>FN<sub>2</sub>ONi<sup>+</sup> (M + H<sup>+</sup>) 502.19304; found 502.19362.

**(4-nitro-2-((2,6-diisopropylphenyl)iminomethyl)phenoxy)Ni(CH<sub>3</sub>)(N-methyl tolualdimine) (2.11k)**

No modifications to the procedure were made.

**Yield:** 83%

**<sup>1</sup>H NMR (500 MHz, C<sub>6</sub>D<sub>6</sub>):** δ 9.29 (d, 2H,  $J_{\text{HH}} = 7.8$  Hz), 7.96 (s, 1H), 7.88 (dd, 1H,  $^1J_{\text{HH}} = 9.6$  Hz,  $^2J_{\text{HH}} = 2.7$  Hz), 7.22 (s, 1H), 7.09-6.92 (m, 6H), 6.46 (d, 1H,  $J_{\text{HH}} = 9.1$  Hz), 4.02 (sept, 1H,  $J_{\text{HH}} = 6.9$  Hz), 3.79 (sept, 1H,  $J_{\text{HH}} = 6.9$  Hz), 3.42 (s, 3H), 2.03 (s, 3H), 1.48 (d, 3H,  $J_{\text{HH}} = 6.9$  Hz), 1.27 (d, 3H,  $J_{\text{HH}} = 6.9$  Hz), 1.08 (d, 3H,  $J_{\text{HH}} = 6.9$  Hz), 0.99 (d, 3H,  $J_{\text{HH}} = 6.9$  Hz), -1.05 (s, 3H).

**<sup>13</sup>C NMR (500 MHz, C<sub>6</sub>D<sub>6</sub>):** δ 171.7, 166.6, 166.1, 161.5, 148.9, 142.4, 140.4, 140.3, 136.2, 131.9, 131.3, 130.7, 129.3, 129.2, 128.7, 128.4, 128.2, 128.0, 127.8, 126.7, 123.6, 123.5, 122.5, 118.4, 49.8, 48.0, 28.5, 28.4, 25.0, 24.6, 23.2, 22.9, 21.3, 21.2 -10.2.

**ESI-HRMS:** calculated for C<sub>29</sub>H<sub>36</sub>N<sub>3</sub>O<sub>3</sub>Ni<sup>+</sup> (M + H<sup>+</sup>) 532.21090; found 532.21047.

**(4-nitro-2-((2,6-diisopropylphenyl)iminomethyl)phenoxy)Ni(CH<sub>3</sub>)(N-benzyl tolualdimine) (2.11l)**

No modifications to the procedure were made.

**Yield:** 87 %

**<sup>1</sup>H NMR (300 MHz, C<sub>6</sub>D<sub>6</sub>):** δ 9.31 (d, 2H,  $J_{\text{HH}} = 8.2$  Hz), 7.95-7.90 (m, 2H), 7.32-7.30 (m, 3H), 7.14-6.94 (m, 9H), 6.40 (d, 1H,  $J_{\text{HH}} = 10.4$  Hz), 4.84 (dd, 2H,  $^1J_{\text{HH}} = 62.4$  Hz,  $^2J_{\text{HH}} = 14.0$  Hz), 3.78 (sept., 1H,  $J_{\text{HH}} = 6.9$  Hz), 3.69 (sept., 1H,  $J_{\text{HH}} = 6.9$  Hz), 2.01 (s, 3H), 1.32-1.26 (m, 6H), 1.03 (d, 3H,  $J_{\text{HH}} = 6.9$  Hz), 0.99 (d, 3H,  $J_{\text{HH}} = 6.9$  Hz), -1.19 (s, 3H).

**<sup>13</sup>C NMR (300 MHz, C<sub>6</sub>D<sub>6</sub>):** δ 171.6, 166.2, 148.9, 142.6, 140.6, 140.3, 136.2, 131.9, 131.7, 131.0, 130.4, 129.3, 128.8, 128.7, 127.9, 126.7, 123.6, 123.5, 122.6, 118.4, 66.7, 28.4, 25.1, 24.9, 23.4, 23.3, 21.5, -9.2.

**ESI-HRMS:** calculated for C<sub>35</sub>H<sub>40</sub>N<sub>3</sub>O<sub>3</sub>Ni<sup>+</sup> (M + H<sup>+</sup>) 608.24184; found 608.24177.



**(4-nitro-2-((2,6-diisopropylphenyl)iminomethyl)phenoxy)Ni(CH<sub>3</sub>)(3,4-dihydroisoquinoline) (2.11m)**

No modifications to the procedure were made.

**Yield:** 92%

**<sup>1</sup>H NMR (500 MHz, C<sub>6</sub>D<sub>6</sub>):** δ 8.21 (s, 1H), 8.04 (d, 1H, *J*<sub>HH</sub> = 9.2 Hz), 7.98 (s, 1H), 7.18-7.02 (m, 4H), 6.84 (t, 1H, *J*<sub>HH</sub> = 6.9 Hz), 6.71 (t, 1H, *J*<sub>HH</sub> = 7.3 Hz), 6.50-6.45 (m, 3H), 3.96 (sept., 2H, *J*<sub>HH</sub> = 6.4 Hz), 3.59 (t, 2H, *J*<sub>HH</sub> = 7.8 Hz), 2.03 (t, 2H, *J*<sub>HH</sub> = 8.2 Hz), 1.47 (d, 6H, *J*<sub>HH</sub> = 6.4 Hz), 1.00 (d, 6H, *J*<sub>HH</sub> = 6.4 Hz), -0.70 (s, 3H).

**<sup>13</sup>C NMR (500 MHz, C<sub>6</sub>D<sub>6</sub>):** δ 171.5, 166.1, 164.8, 149.2, 140.4, 136.2, 135.5, 132.1, 131.9, 128.7, 127.7, 127.2, 127.1, 126.8, 123.6, 122.5, 118.5, 49.6, 28.5, 25.4, 24.6, 23.1, -8.2.

**ESI-HRMS:** calculated for C<sub>29</sub>H<sub>24</sub>N<sub>3</sub>NiO<sub>3</sub><sup>+</sup> (M + H<sup>+</sup>) 529.18754; found 529.18743.

**(6-phenyl-2-((2,6-diisopropylphenyl)iminomethyl)phenoxy)Ni(Ph)(3,4-dihydroisoquinoline) (2.11p)**

(6-phenyl-2-((2,6-diisopropylphenyl)iminomethyl)phenoxy)Ni(Ph)(PPh<sub>3</sub>) (150.0 mg, 0.199 mmol) and 3,4-dihydroisoquinoline (31.4 mg, 0.239 mmol) were dissolved in benzene (*ca.* 10 mL). In a second vessel, a slurry of CuCl (29.6 mg, 0.239 mmol) in benzene (*ca.* 2 mL) was added to the mixture with stirring. After 30 min at room temperature, the solution was filtered through a Celite plug. The filtrate was concentrated under vacuo and redissolved in minimal pentane for crystallization at -40°C. Yellow crystals were then collected by filtration and washed with cold pentane thrice (3 x 2 mL) (104.2 mg, 84 % yield).

**<sup>1</sup>H NMR (400 MHz, C<sub>6</sub>D<sub>6</sub>):** δ 8.35 (s, 1H), 7.67-7.59 (m, 5H), 7.42 (d, 2H, *J*<sub>HH</sub> = 4.9 Hz), 6.93-6.39 (m, 13H), 4.13 (sept., 2H, *J*<sub>HH</sub> = 6.9 Hz), 3.42 (t, 2H, *J*<sub>HH</sub> = 6.3 Hz), 1.81 (t, 2H, *J*<sub>HH</sub> = 6.6 Hz), 1.39 (d, 6H, *J*<sub>HH</sub> = 6.9 Hz), 1.01 (d, 6H, *J*<sub>HH</sub> = 6.9 Hz).

**<sup>13</sup>C NMR (300 MHz, C<sub>6</sub>D<sub>6</sub>):** δ 167.5, 165.1, 164.8, 150.9, 150.8, 140.7, 140.6, 136.7, 135.8, 134.8, 134.7, 134.5, 134.1, 133.8, 133.7, 133.5, 131.9, 129.9, 129.7, 128.8, 128.7,

128.2, 127.5, 127.1, 126.8, 126.4, 125.0, 124.9, 123.0, 122.2, 120.7, 114.4, 49.8, 28.8, 25.6, 25.2, 22.8.

**ESI-HRMS:** calculated for  $C_{40}H_{41}N_2NiO^+$  ( $M + H^+$ ) 622.24941; found 622.24933.

### 2.3.2 Decomposition Studies of the $\kappa^2$ -*N,O*-Salicylaldiminato Ni (II) Complexes

A J-Young tube was charged with a 0.02 M solution of nickel complex **2.11f** (6.4 mg, 0.01 mmol) in  $C_6D_6$  (0.50 mL). Benzyl benzoate was added as the internal standard. The formation of *bis*-salicylaldiminato nickel (II) complexes **2.12** was monitored by  $^1H$  NMR spectroscopy at 25 °C. The decomposition time was determined by measuring both the disappearance of the complex and the appearance of uncoordinated imine.

(6-phenyl-2-((2,6-diisopropylphenyl)iminomethyl)phenoxide)Ni(CH<sub>3</sub>)(*N*-benzyl tolualdimine) (**2.11c**): ~ 6 hrs;

(2-((2,6-diisopropylphenyl)iminomethyl)phenoxide)Ni(CH<sub>3</sub>)(*N*-benzyl tolualdimine) (**2.11f**): ~ 61 hrs;

(2-((2,6-diisopropylphenyl)iminomethyl)phenoxide)Ni(CH<sub>3</sub>)(3,4-dihydroisoquinoline) (**2.11g**): ~ 11 hrs;

(4-fluoro-2-((2,6-diisopropylphenyl)iminomethyl)phenoxide)Ni(CH<sub>3</sub>)(*N*-benzyl tolualdimine) (**2.11i**): ~ 39 hrs;

(4-nitro-2-((2,6-diisopropylphenyl)iminomethyl)phenoxide)Ni(CH<sub>3</sub>)(*N*-benzyl tolualdimine) (**2.11l**):  $t_{1/2} \approx 10$  hrs.

### 2.3.3 General Reaction Conditions for the Insertion Chemistry

A 25 mL reaction bomb was charged with the appropriate amount of Ni complex **2.11** (0.0618 mmol) and imine (0.185 mmol) dissolved in benzene (*ca.* 10 mL). The solution was placed under 1 atm (14.70 psi) of carbon monoxide and stirred at ambient temperature for 5 hrs. Carbon monoxide atmosphere was removed by a freeze-pump-thaw process. The resulting solution was concentrated under vacuo and then stirred in acetonitrile, causing the *bis*-salicylaldiminato nickel (II) complex **2.12** to precipitate. The

solids were removed by filtration and the filtrate was concentrated under vacuo. Purification was achieved via silica gel chromatography using a 60% hexanes and 40% dichloromethane mixture as the eluent. Note: When 3,4-dihydroisoquinoline is the reaction substrate a gradient mixture was used starting with 60 hexanes: 40 dichloromethane and incorporating 3 % triethyl amine and 3 % methanol.

**Acetic acid 3-((2,6-diisopropylphenyl)iminomethyl)-biphenyl-2-yl ester (2.15a)**

**<sup>1</sup>H NMR (300 MHz, CDCl<sub>3</sub>):** δ 8.28 (s, 1H), 8.18 (dd, 1H, <sup>1</sup>J<sub>HH</sub> = 8.2 Hz, <sup>2</sup>J<sub>HH</sub> = 1.6 Hz), 7.55-7.36 (m, 7H), 7.18-7.10 (m, 4H), 2.96 (sept., 2H, J<sub>HH</sub> = 6.9 Hz), 1.98 (s, 3H), 1.16 (d, 12H, J<sub>HH</sub> = 6.9 Hz).

**<sup>13</sup>C NMR (300 MHz, CDCl<sub>3</sub>):** δ 169.0, 157.5, 149.3, 148.0, 137.6, 137.1, 136.2, 133.7, 128.9, 128.4, 127.9, 127.8, 126.7, 124.3, 123.1, 27.9, 23.5, 20.5.

**ESI-HRMS:** calculated for C<sub>27</sub>H<sub>30</sub>NO<sub>2</sub><sup>+</sup> (M + H<sup>+</sup>) 400.22686; found 400.22711

**Acetic acid 2-((2,6-diisopropylphenyl)iminomethyl)-phenyl ester (2.15b)**

**<sup>1</sup>H NMR (300 MHz, CDCl<sub>3</sub>):** δ 8.29 (s, 1H), 8.17 (dd, 1H, <sup>1</sup>J<sub>HH</sub> = 7.9 Hz, <sup>2</sup>J<sub>HH</sub> = 1.5 Hz), 7.53 (dt, 1H, <sup>1</sup>J<sub>HH</sub> = 7.3 Hz, <sup>2</sup>J<sub>HH</sub> = 1.8 Hz), 7.39 (t, 1H, J<sub>HH</sub> = 6.2 Hz), 7.19-7.12 (m, 4H), 2.95 (sept., 2H, J<sub>HH</sub> = 7.0 Hz), 2.27 (s, 3H), 1.16 (d, 12H, J<sub>HH</sub> = 7.0 Hz).

**<sup>13</sup>C NMR (300 MHz, CDCl<sub>3</sub>):** δ 169.0, 157.2, 150.6, 149.3, 137.6, 132.1, 128.7, 128.0, 126.4, 124.3, 123.1, 123.0, 27.8, 23.4, 20.7.

**ESI-HRMS:** calculated for C<sub>21</sub>H<sub>26</sub>NO<sub>2</sub><sup>+</sup> (M + H<sup>+</sup>) 324.19577; found 324.19581

**Acetic acid 2-((2,6-diisopropylphenyl)iminomethyl)-4-fluoro-phenyl ester (2.15c)**

**<sup>1</sup>H NMR (300 MHz, CDCl<sub>3</sub>):** δ 8.24 (d, 1H, J<sub>HF</sub> = 2.2 Hz), 7.90 (dd, 1H, <sup>1</sup>J<sub>HH</sub> = 8.9 Hz, <sup>2</sup>J<sub>HH</sub> = 3.0 Hz), 7.26-7.13 (m, 5H), 2.92 (sept., 2H, J<sub>HH</sub> = 6.9 Hz), 2.28 (s, 3H), 1.17 (d, 12H, J<sub>HH</sub> = 6.9 Hz).

**<sup>13</sup>C NMR (300 MHz, CDCl<sub>3</sub>):** δ 169.2, 162.1, 158.9, 156.1, 148.9, 146.5, 137.5, 129.6 (d, J<sub>CF</sub> = 7.8 Hz), 124.6 (d, J<sub>CF</sub> = 5.1 Hz), 124.5, 123.1, 119.0 (d, J<sub>CF</sub> = 23.5 Hz), 114.4 (d, J<sub>CF</sub> = 24.4 Hz), 27.9, 23.5, 20.7.

**<sup>19</sup>F NMR (400 MHz, CDCl<sub>3</sub>):** δ -115.3 (s).

**ESI-HRMS:** calculated for  $C_{21}H_{25}NO_2F^+$  ( $M + H^+$ ) 342.18631; found 342.18638.

**Acetic acid 2-((2,6-diisopropylphenyl)iminomethyl)-4-nitro-phenyl ester (2.15d)**

**$^1H$  NMR (300 MHz,  $CDCl_3$ ):**  $\delta$  9.05 (d, 1H,  $J_{HH} = 2.9$  Hz), 8.37 (dd, 1H,  $^1J_{HH} = 9.0$  Hz,  $^2J_{HH} = 2.9$  Hz), 8.32 (s, 1H), 7.40 (d, 1H,  $J_{HH} = 8.8$  Hz), 7.17 (s, 3H), 2.90 (sept., 2H,  $J_{HH} = 7.0$  Hz), 2.32 (s, 3H), 1.17 (d, 12H,  $J_{HH} = 7.0$  Hz).

**$^{13}C$  NMR (300 MHz,  $CDCl_3$ ):**  $\delta$  168.2, 155.2, 154.6, 148.6, 146.1, 137.5, 129.2, 126.7, 124.9, 124.3, 124.2, 123.2, 28.0, 23.5, 20.8.

**ESI-HRMS:** calculated for  $C_{21}H_{25}N_2O_4^+$  ( $M + H^+$ ) 369.18077; found 369.18088.

**Benzoic acid 3-((2,6-diisopropylphenyl)iminomethyl)-biphenyl-2-yl ester (2.15e)**

**$^1H$  NMR (400 MHz,  $C_6D_6$ ):**  $\delta$  8.58 (s, 1H), 8.40 (d, 1H,  $J_{HH} = 8.1$  Hz), 7.89 (d, 2H,  $J_{HH} = 7.0$  Hz), 7.39 (d, 2H,  $J_{HH} = 7.0$  Hz), 7.26 (d, 1H,  $J_{HH} = 7.7$  Hz), 7.09-6.89 (m, 8H), 6.83 (t, 2H,  $J_{HH} = 7.7$  Hz), 3.23 (sept., 2H,  $J_{HH} = 7.0$  Hz), 1.13 (d, 12H,  $J_{HH} = 7.0$  Hz).

**$^{13}C$  NMR (300 MHz,  $CDCl_3$ ):**  $\delta$  164.8, 157.2, 149.2, 137.6, 136.9, 136.3, 133.8, 133.6, 130.0, 129.2, 128.9, 128.5, 128.4, 128.3, 127.7, 127.6, 124.2, 123.0, 27.8, 23.5.

**ESI-HRMS:** calculated for  $C_{32}H_{32}NO_2^+$  ( $M + H^+$ ) 462.24245; found 462.24276.

**bis(6-phenyl-2-((2,6-diisopropylphenyl)iminomethyl)phenoxide)Ni (2.12a)**

Due to the paramagnetic nature of this complex, NMR characterization could not be achieved.<sup>15</sup>

**ESI-HRMS:** calculated for  $C_{50}H_{53}N_2O_2Ni^+$  ( $M + H^+$ ) 771.34593; found 771.34550.

**bis(2-((2,6-diisopropylphenyl)iminomethyl)phenoxide)Ni (2.12b)**

**$^1H$  NMR (300 MHz,  $C_6D_6$ ):**  $\delta$  7.19 (t, 2H,  $J_{HH} = 2.1$  Hz), 7.06 (m, 4H), 6.75 (t, 2H,  $J_{HH} = 4.9$  Hz), 6.65 (d, 2H,  $J_{HH} = 6.4$  Hz), 6.22 (t, 2H,  $J_{HH} = 6.7$  Hz), 5.92 (d, 2H,  $J_{HH} = 8.5$  Hz), 4.38 (sept., 4H,  $J_{HH} = 6.7$  Hz), 1.46 (d, 12H,  $J_{HH} = 7.0$  Hz), 1.11 (d, 12H,  $J_{HH} = 7.0$  Hz).

**$^{13}C$  NMR (300 MHz,  $C_6D_6$ ):**  $\delta$  164.6, 164.2, 146.4, 142.3, 134.4, 132.8, 126.3, 123.1, 121.5, 119.7, 115.2, 29.3, 24.4, 23.7.

**ESI-HRMS:** calculated for  $C_{38}H_{45}N_2O_2Ni^+$  ( $M + H^+$ ) 619.28288; found 619.28290

**bis(4-fluoro-2-((2,6-diisopropylphenyl)iminomethyl)phenoxy)Ni (2.12c)**

**<sup>1</sup>H NMR (300 MHz, C<sub>6</sub>D<sub>6</sub>):** δ 7.16 (t, 2H,  $J_{\text{HH}} = 7.7$  Hz), 7.00 (d, 4H,  $J_{\text{HH}} = 7.7$  Hz), 6.82 (s, 2H), 6.47 (dt, 2H,  $J_{\text{HH}} = 8.7$  Hz,  $J_{\text{HF}} = 3.0$  Hz), 6.28 (dd, 2H,  $J_{\text{HH}} = 8.7$  Hz,  $J_{\text{HF}} = 3.0$  Hz), 5.69 (dd, 2H,  $J_{\text{HH}} = 9.2$  Hz,  $J_{\text{HF}} = 4.4$  Hz), 4.28 (sept., 4H,  $J_{\text{HH}} = 6.7$  Hz), 1.43 (d, 12H,  $J_{\text{HH}} = 6.9$  Hz), 1.09 (d, 12H,  $J_{\text{HH}} = 6.9$  Hz).

**<sup>13</sup>C NMR (300 MHz, C<sub>6</sub>D<sub>6</sub>):** δ 163.9, 160.6, 155.0, 151.9, 146.0, 142.0, 126.5, 123.2, 123.1, 122.9, 122.3 (d,  $J_{\text{CF}} = 7.4$  Hz), 118.1 (d,  $J_{\text{CF}} = 8.3$  Hz), 115.5 (d,  $J_{\text{CF}} = 22.1$  Hz), 29.3, 24.3, 23.7.

**<sup>19</sup>F NMR (400 MHz, C<sub>6</sub>D<sub>6</sub>):** δ -130.4.

**ESI-HRMS:** calculated for C<sub>38</sub>H<sub>43</sub>N<sub>2</sub>O<sub>2</sub>NiF<sub>2</sub><sup>+</sup> (M + H<sup>+</sup>) 655.26400; found 655.26406.

**bis(4-nitro-2-((2,6-diisopropylphenyl)iminomethyl)phenoxy)Ni (2.12d)**

**<sup>1</sup>H NMR (300 MHz, C<sub>6</sub>D<sub>6</sub>):** δ 7.57 (d, 2H,  $J_{\text{HH}} = 2.7$  Hz), 7.45 (dd, 2H,  $J_{\text{HH}}^1 = 9.2$  Hz,  $J_{\text{HH}}^2 = 2.7$  Hz), 7.14 (m, 2H), 6.95 (m, 4H), 6.56 (s, 2H), 4.00 (sept., 4H,  $J_{\text{HH}} = 7.0$  Hz), 1.35 (d, 12H,  $J_{\text{HH}} = 7.0$  Hz), 1.06 (d, 12H,  $J_{\text{HH}} = 7.0$  Hz).

**<sup>13</sup>C NMR (300 MHz, C<sub>6</sub>D<sub>6</sub>):** δ 167.4, 165.0, 144.7, 141.6, 137.8, 130.5, 129.0, 127.1, 118.0, 29.3, 24.1, 23.5.

**ESI-HRMS:** calculated for C<sub>38</sub>H<sub>42</sub>N<sub>4</sub>O<sub>6</sub>NiNa<sup>+</sup> (M + Na<sup>+</sup>) 731.23506; found 731.23501.

**meso N,N'-diacyl-1,1',2,2',3,3',4,4'-octahydro-1,1'-biisoquinoline (2.17a)**<sup>29</sup>

**<sup>1</sup>H NMR (300 MHz, 25 °C, CDCl<sub>3</sub>):** (two conformers: A *ca.* 67%, and B *ca.* 33%) δ 7.56 (d, 2H,  $J_{\text{HH}} = 7.1$  Hz, A), 7.30-7.07 (m, 10H), 7.01-6.94 (m, 2H), 6.47 (d, 2H,  $J_{\text{HH}} = 7.7$  Hz, A), 6.03 (s, 2H, B), 5.86 (d, 2H,  $J_{\text{HH}} = 5.2$  Hz, A), 5.36 (d, 2H,  $J_{\text{HH}} = 5.0$  Hz, B), 4.89 (s, 2H, B), 4.62-4.53 (dt,  $J_{\text{HH}}^1 = 11.8$  Hz,  $J_{\text{HH}}^2 = 5.2$  Hz, B), 4.41-4.36 (m, 2H, A), 3.94-3.87 (m, 2H), 3.66-3.51 (m, 4H), 3.36-3.28 (m, 2H), 3.12-2.95 (m, 4H), 2.94-2.68 (m, 8H), 2.58-2.52 (m, 2H), 2.39-2.25 (m, 2H), 2.10 (d, 6H,  $J_{\text{HH}} = 11.5$  Hz, A), 1.81 (s, 3H, B)

**<sup>13</sup>C NMR (300 MHz, C<sub>6</sub>D<sub>6</sub>):** δ 171.2, 170.6, 170.5, 170.4, 135.6, 135.0, 134.9, 134.7, 134.5, 133.7, 133.5, 133.1, 129.2, 128.7, 128.4, 128.2, 127.7, 127.5, 127.4, 126.9, 126.8, 126.5, 126.1, 60.7, 60.1, 59.4, 57.2, 44.0, 42.4, 38.0, 36.6, 28.9, 28.8, 28.0, 27.9, 22.6, 22.4, 21.1, 21.0.

**ESI-HRMS:** calculated for  $C_{22}H_{24}N_2O_2Na^+$  ( $M + Na^+$ ) 371.17268; found 371.17300.

***dl* N,N'-diacetyl-1,1',2,2',3,3',4,4'-octahydro-1,1'-biisoquinoline (2.17b)**<sup>29</sup>

**<sup>1</sup>H NMR ( 400 MHz, C<sub>6</sub>D<sub>6</sub>):**  $\delta$  6.96 (t, 2H,  $J_{HH} = 7.3$  Hz), 6.90 (d, 2H,  $J_{HH} = 7.3$  Hz), 6.65 (t, 2H,  $J_{HH} = 7.3$  Hz), 5.99 (d, 2H,  $J_{HH} = 7.3$  Hz), 5.69 (s, 2H), 3.84-3.79 (m, 2H), 3.67-3.59 (m, 2H), 2.81 (dt, 2H,  $^1J_{HH} = 10.6$  Hz,  $^2J_{HH} = 5.9$  Hz), 2.40 (dt, 2H,  $^1J_{HH} = 15.7$  Hz,  $^2J_{HH} = 5.5$  Hz), 1.79 (s, 6H).

**<sup>13</sup>C NMR ( 300 MHz, C<sub>6</sub>D<sub>6</sub>):**  $\delta$  170.8, 135.4, 134.3, 129.7, 127.6, 127.5, 127.4, 125.3, 57.0, 44.2, 28.0, 22.3.

**ESI-HRMS:** calculated for  $C_{22}H_{24}N_2O_2Na^+$  ( $M + Na^+$ ) 371.17273; found 371.17300.

***meso, dl* N,N'-dibenzoyl-1,1',2,2',3,3',4,4'-octahydro-1,1'-biisoquinoline (2.17c,d)**<sup>29b</sup>

**<sup>1</sup>H NMR (500 MHz, CDCl<sub>3</sub>):**  $\delta$  7.47-7.07 (m, 22H, *meso* & *dl*), 7.00 (d, 2H,  $J_{HH} = 6.9$  Hz, *meso*), 6.93 (d,  $J_{HH} = 6.9$  Hz, *meso*), 6.75 (d, 2H,  $J_{HH} = 6.9$  Hz, *dl*), 6.69 (d, 2H,  $J_{HH} = 6.4$  Hz, *dl*), 6.48 (s, 2H, *dl*), 6.41 (d, 2H,  $J_{HH} = 6.0$  Hz, *dl*), 6.08 (d, 2H,  $J_{HH} = 7.8$  Hz, *meso*), 5.25 (d, 2H,  $J_{HH} = 7.3$  Hz, *meso*), 5.07 (s, 2H, *meso*), 4.54-4.37 (m, 2H, *dl*), 3.64-3.55 (m, 4H, *meso* & *dl*), 3.34-3.15 (m, 5H, *meso* & *dl*), 2.93-2.75 (m, 5H, *meso* & *dl*), 2.53-2.35 (m, 2H, *dl*).

**<sup>13</sup>C NMR (500 MHz, CDCl<sub>3</sub>):**  $\delta$  171.6, 171.3, 170.7, 137.1, 136.3, 135.9, 135.4, 134.4, 134.1, 133.6, 133.3, 129.6, 129.5, 129.4, 129.3, 129.0, 128.8, 128.6, 128.5, 128.4, 128.1, 127.9, 127.5, 127.0, 126.9, 126.8, 126.7, 126.5, 126.5, 126.2, 126.0, 61.3, 60.1, 57.5, 55.1, 43.0, 38.5, 38.1, 29.2, 28.7, 27.6, 27.1.

**ESI-HRMS:** calculated for  $C_{32}H_{28}N_2O_2Na^+$  ( $M + Na^+$ ) 495.20430; found 495.20489.

## 2.4 References

- (1) (a) Britovsek, G.J.P.; Gibson, V.C.; Wass, D.F. *Angew. Chem., Int. Ed.* **1999**, *38*, 428. (b) Ittel, S.D.; Johnson, L.K.; Brookhart, M. *Chem. Rev.* **2000**, *100*, 1169. (c) Imanishi, Y.; Naga, N. *Prog. Polym. Sci.* **2001**, *26*, 1147. (d) Michalak, A.; Ziegler, T. *Theoretical Aspects of Transition Metal Catalysts, Topics in Organometallic Chemistry*, Springer Berlin: Heidelberg, 2005. (e) Dong, J.-Y.; Hu, Y. *Coor. Chem. Rev.* **2006**, *250*, 47.
- (2) (a) Heck, R.F. In *Comprehensive Organic Synthesis* Pergamon Press: Oxford, **1991**. (b) Daves, G.D.; Hallberg, A. *Chem. Rev.* **1989**, *89*, 1433. (c) Beletskaya, I.P.; Cheprakov, A.V. *Chem. Rev.* **2000**, *100*, 3009.
- (3) Trost, B.M.; Frederiksen, M.U.; Rudd, M.T. *Angew. Chem. Int. Ed.* **2005**, *44*, 6630.
- (4) Fu, G.C. in *Transition Metals for Organic Synthesis, Vol 2*. 2nd Edition; Wiley-VCH, Weinheim, Germany **2004**.
- (5) Hegedus, L.S. *Transition Metals in the Synthesis of Complex Organic Molecules* University Science Books: Sausalito, **1999**.
- (6) For examples of direct observation of imine insertion: (a) Muller, F.; van Koten, G.; Vrieze, K.; Heijdenrijk, D. *Organometallics* **1989**, *8*, 33. (b) Fryzuk, M.D.; Piers, W.E. *Organometallics* **1990**, *9*, 986. (c) Reduto, A.C.; Hegedus, L.S. *Organometallics* **1995**, *14*, 1586. (d) Debad, J.D.; Legzdins, P.; Lumb S.A.; Batchelor, R.J.; Einstein, F.W.B. *Organometallics* **1995**, *14*, 2543. (e) Obora, Y.; Ohta, T.; Stern, C.L.; Marks, T.J. *J. Am. Chem. Soc.* **1997**, *119*, 3745. (f) Krug, C.; Hartwig, J. F. *J. Am. Chem. Soc.* **2004**, *126*, 2694. (g) Krug, C.; Hartwig, J. F. *Organometallics* **2004**, *23*, 4594.
- (7) (a) Crabtree, R.H. *The Organometallic Chemistry of Transition Metals*, Wiley-Interscience: Hoboken, N.J., **2005**. (b) Collman, J.P.; Hegedus, L.S.; Norton, J.R.; Finke, R.G. *Principles and Application of Organotransition Metal Chemistry*, University Science Books: Sausalito, **1987**. (c) Ittel, S.D.; Johnson, L.K.; Brookhart, M. *Chem. Rev.* **2000**, *100*, 1169.
- (8) Palladium catalyzed: (a) Nakamura, H.; Iwama, H.; Yamamoto, Y. *J. Am. Chem. Soc.* **1996**, *118*, 6641. (b) Nakamura, H.; Aoyagi, K.; Shim, J.G.; Yamamoto, Y. *J. Am.*

- Chem. Soc.* **2001**, *123*, 372. Rhodium catalyzed: (b) Oi, S.; Moro, M.; Fukuhara, H.; Kawanishi, T.; Inoue, Y. *Tetrahedron Lett.* **1999**, *40*, 9259. (c) Ueda, M.; Miyaura, N. *J. Organomet. Chem.* **2000**, *595*, 31. (d) Hayashi, T.; Ishigedani, M. *J. Am. Chem. Soc.* **2000**, *122*, 976. (e) Ueura, K.; Miyamura, S.; Satoh, T.; Miura, M. *J. Organomet. Chem.* **2006**, *691*, 2821. (f) Ueda, M.; Saito, A.; Miyaura, N. *Synlett* **2000**, 1637. (g) Ishiyama, T.; Hartwig, J. *J. Am. Chem. Soc.* **2000**, *122*, 12043. Stoichiometric in rhodium: (h) Krug, C.; Hartwig, J.F. *J. Am. Chem. Soc.* **2004**, *126*, 2694. (i) Krug, C.; Hartwig, J.F. *Organometallics* **2004**, *23*, 4594.
- (9) Dghaym, R.D.; Yaccato, K.J.; Arndtsen, B.A. *Organometallics* **1998**, *17*, 4.
- (10) Kacker, S.; Kim, J.S.; Sen, A. *Angew. Chem., Int. Ed. Engl.* **1998**, *37*, 1251.
- (11) Davis J.L.; Arndtsen, B.A. *Organometallics* **2000**, *19*, 4657.
- (12) (a) Dghaym, R.D.; Dhawan, R.; Arndtsen, B.A. *Angew. Chem., Int. Ed.* **2001**, *40*, 3228. (b) Dhawan, R.; Dghaym, R.D.; Arndtsen, B.A. *J. Am. Chem. Soc.* **2003**, *125*, 1474. (c) Dhawan, R.; Arndtsen, B.A. *J. Am. Chem. Soc.* **2004**, *126*, 468.
- (13) (a) Ittel, S.D.; Johnson, L.K. *Chem. Rev.* **2000**, *100*, 1169. (b) Boffa, L.S.; Novak, B.M. *Chem. Rev.* **2000**, *100*, 1479. (c) Kamigaito, M.; Ando, T.; Sawamoto, M. *Chem. Rev.* **2001**, *101*, 3689. (d) Mecking, S. *Angew. Chem., Int. Ed.* **2001**, *40*, 534. (e) Poli, R. *Angew. Chem. Int. Ed.* **2006**, *45*, 5058.
- (14) Younkin, T.R.; Connor, E.F.; Henderson, J.I.; Friedrich, S.K.; Grubbs, R.H.; Bansleben, D.A. *Science* **2000**, *287*, 460.
- (15) Connor, E.F.; Younkin, T.R.; Henderson, J.I.; Waltman, A.W.; Grubbs, R.H. *Chem. Commun.* **2003**, 2272.
- (16) (a) Bauers, F.M.; Mecking, S. *Macromolecules* **2001**, *34*, 1165. (b) Bauers, F.M.; Mecking, S. *Angew. Chem. Int. Ed.* **2001**, *40*, 3020. (c) Zuideveld, M.A.; Wehrmann, P.; Röhr, C.; Mecking, S. *Angew. Chem. Int. Ed.* **2004**, *43*, 869.
- (17) (a)  $^1\text{H}$  NMR spectrum of **2.11n** (400 MHz,  $\text{C}_6\text{D}_6$ ) (listing distinctive peaks only):  $\delta$  9.80 (d, 2H,  $J_{\text{HH}} = 7.7$  Hz), 7.90 (s, 1H), 7.71 (d, 2H,  $J_{\text{HH}} = 7.7$  Hz), 7.54 (s, 1H), 6.43 (t, 2H,  $J_{\text{HH}} = 7.3$  Hz), 4.20 (sept., 1H,  $J_{\text{HH}} = 6.6$  Hz), 3.83 (sept., 1H,  $J_{\text{HH}} = 6.6$  Hz), 2.03 (s, 3H), 1.42 (d, 3H,  $J_{\text{HH}} = 6.6$  Hz), 1.24 (d, 3H,  $J_{\text{HH}} = 6.6$  Hz), 1.17 (d, 3H,  $J_{\text{HH}} = 6.2$  Hz), 0.90 (d, 3H,  $J_{\text{HH}} = 6.2$  Hz), -1.04 (s, 3H). (b)  $^1\text{H}$  NMR spectrum of **2.11o**



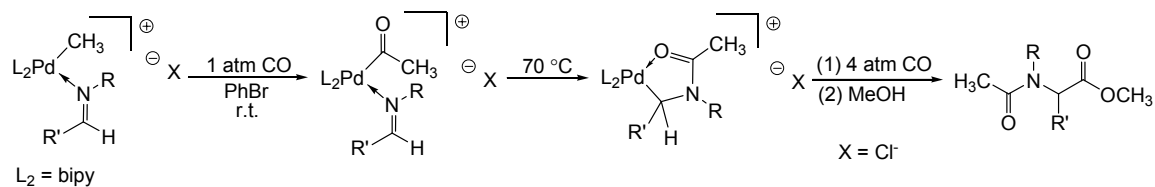
- (400 MHz, C<sub>6</sub>D<sub>6</sub>) (listing distinctive peaks only):  $\delta$  9.77 (d, 2H,  $J_{\text{HH}} = 7.7$  Hz), 8.14 (s, 1H), 7.75 (d, 2H,  $J_{\text{HH}} = 7.7$  Hz), 7.56 (s, 1H), 6.42 (t, 2H,  $J_{\text{HH}} = 7.7$  Hz), 4.35 (sept., 1H,  $J_{\text{HH}} = 6.8$  Hz), 3.87 (sept., 1H,  $J_{\text{HH}} = 6.8$  Hz), 2.02 (s, 3H), 1.42 (d, 3H,  $J_{\text{HH}} = 7.0$  Hz), 1.33 (d, 3H,  $J_{\text{HH}} = 6.2$  Hz), 1.19 (d, 3H,  $J_{\text{HH}} = 6.6$  Hz), 0.94 (d, 3H,  $J_{\text{HH}} = 6.6$  Hz), -0.96 (s, 3H).
- (18) Wang, C.; Friedrich, S.; Younkin, T.R.; Li, R.T.; Grubbs, R.H.; Bansleben, D.A.; Pay, M.W. *Organometallics* **1998**, 17, 3149.
- (19) Liberation of ethane is observed. <sup>1</sup>H NMR (400MHz, C<sub>6</sub>D<sub>6</sub>):  $\delta$  0.77 ppm (6H, s).  
References: Hesse, M.; Meier, H.; Zeeh, B. *Spectroscopic Methods in Organic Chemistry*, G. Thieme, Stuttgart, **1997**.
- (20) CO insertion into Ni-R complexes are observed to occur readily at room temperature. Example with Ni-CH<sub>3</sub>: (a) Shultz, C.S.; DeSimone, J.M.; Brookhart, M. *J. Am. Chem. Soc.* **2001**, 123, 9172. (b) De Angelis, F.; Sgamellotti, A.; Re, N. *Organometallics* **2002**, 21, 2036. Example with Ni-Ph (c) Maruyama, K.; Ito, T.; Yamamoto, A. *J. Organomet. Chem.* **1978**, 157, 463.
- (21) Liberation of methane is observed with an approximate yield ranging from 5 to 15%.  
<sup>1</sup>H NMR (400MHz, C<sub>6</sub>D<sub>6</sub>):  $\delta$  0.16 ppm (4H, s). References: (a) Hesse, M.; Meier, H.; Zeeh, B. *Spectroscopic Methods in Organic Chemistry*, G. Thieme, Stuttgart, **1997**. (b) Kato, T.; Reed, C.A. *Angew. Chem. Int. Ed.* **2004**, 43, 2908. (c) Matsuo, T.; Kawaguchi, H. *J. Am. Chem. Soc.* **2006**, 128, 12362.
- (22) <sup>1</sup>H NMR (400 MHz, C<sub>6</sub>D<sub>6</sub>):  $\delta$  7.61 (s, 1H, HC=N), 5.42 (s, 1H, NiC(H)NCOCH<sub>3</sub>), 4.05 (mult., 2H, CH(CH<sub>3</sub>)<sub>2</sub>), 2.35-2.20 (mult., 2H, NCH<sub>2</sub>CH<sub>2</sub>), 2.10-1.97 (mult., 2H, NCH<sub>2</sub>CH<sub>2</sub>), 1.43 (d, 3H, CH(CH<sub>3</sub>)<sub>2</sub>), 1.28 (d, 3H, CH(CH<sub>3</sub>)<sub>2</sub>), 1.14-1.10 (mult., 6H, CH(CH<sub>3</sub>)<sub>2</sub>), 0.65 (s, 3H, NiC(H)NCOCH<sub>3</sub>).
- (23) Montgomery, J. *Angew. Chem. Int. Ed.* **2004**, 43, 3890.
- (24) Norman, R.O.C.; Waters, W.A. *J. Chem. Soc.* **1958**, 167.
- (25) Layer, R.W. *Chem. Rev.* **1963**, 63, 489.
- (26) Pelletier, J.C.; Cava, M.P. *J. Org. Chem.* **1987**, 52, 616.
- (27) Kaschbe, W.; Porschke, K.R.; Wilke, G. *J. Organomet. Chem.* **1988**, 355, 525.

- (28) Wang, C.; Friedrich, S.; Younkin, T.R.; Li, R.T.; Grubbs, R.H.; Bansleben, D.A.; Pay, M.W. *Organometallics* **1998**, *17*, 3149.
- (29) (a) Nielsen, A.T. *J. Org. Chem.* **1970**, *35*, 2498. (b) Elliott, M.C.; Williams, E. *Org. Biomol. Chem.* **2003**, *1*, 3038.

**Mechanistic Studies on the Insertion of Imines into Palladium-Carbon  $\sigma$ -Bonds:  
How Similar are Imines to Olefins as Insertion Monomers?**

**3.0 Introduction**

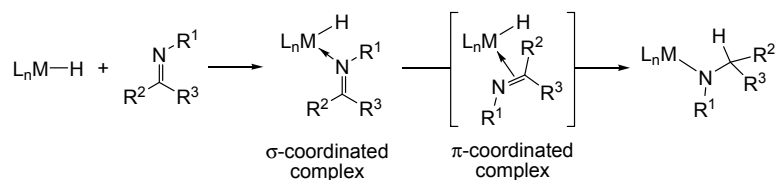
Olefins and imines are isoelectronic species. While the insertion of olefins into metal-carbon  $\sigma$ -bonds has been extensively studied in polymer synthesis (*e.g.* polyolefins,<sup>1</sup> olefin/CO copolymerization<sup>2</sup>) and organic synthesis (*e.g.* Heck reaction,<sup>3</sup> alkene-alkyne coupling reactions,<sup>4</sup> etc.), imines are much less well-explored as insertion substrates. Substituting imines for olefins would incorporate nitrogen-containing functionality into many of these catalyzed processes. Because imines are easy to synthesize and can be readily diversified, they would add interesting scope to the aforementioned reactions. Imines have been exploited in rhodium-catalyzed Heck-type reactions,<sup>5</sup> as well as with cross-coupling type reactions with organometallic reagents.<sup>6</sup> In addition, we<sup>7</sup> have demonstrated the potential use of carbon monoxide and imine sequential insertion as a route to synthesize  $\alpha$ -amino acid derivatives [Scheme 3.1].<sup>8</sup>



**Scheme 3.1:** The sequential insertion of carbon monoxide and imines into palladium-methyl complexes towards  $\alpha$ -amino acid derivatives.

Using imines as insertion substrates in what are often olefin-based processes raises the question of how imine insertion occurs, *i.e.* whether the insertion mechanism for imines proceeds in a similar manner to olefins. Imines are known to undergo 1,2-insertion into transition metal-hydride bonds in both catalytic hydrogenation and

hydrosilation reactions.<sup>9</sup> In most cases, the catalyst employed also mediates the corresponding reduction of olefins, and the mechanism is postulated to proceed in an analogous fashion. This involves the insertion of a  $\pi$ -coordinated imine into the metal-hydride bond [Scheme 3.2].<sup>10</sup>



**Scheme 3.2:** The postulated 1,2-insertion of imine into transition metal-hydride bonds.

However, imines typically coordinate to transition metal complexes in an  $\eta^1$ -fashion through their more basic lone pair, rather than via  $\eta^2$ -coordination of the  $\pi$ -system.<sup>11</sup> This additional coordination mode of imines adds a degree of complexity to the insertion mechanism and implies imine insertion may be significantly more hindered than olefins because the imine must first rearrange to a higher energy  $\pi$ -complex. Direct mechanistic evidence of this rearrangement is limited.<sup>12</sup>

Our group recently reported that  $\sigma$ -coordinated imine palladium complexes can undergo 2,1-migratory insertion into the Pd-acyl bond in  $[(\text{bipy})\text{Pd}(\text{COCH}_3)(\text{RN}=\text{C}(\text{H})\text{R}') ]^+$  to form a well-defined metallacycle.<sup>7</sup> A simplified representation of this reaction was the subject of a density functional study by Cavallo.<sup>13</sup> The results suggest that the  $\pi$ -coordination of imine to palladium is significantly less stable than  $\sigma$ -coordination (by ca. 18-20 kcal/mol) and does not represent an energy minimum (*i.e.* not a reaction intermediate). In addition, the reaction pathway for imine insertion shows no evidence for coordination of the imine  $\pi$ -system to palladium except in the last stages of the approach towards the reaction transition state.

In our laboratory, kinetic and thermodynamic studies on the coordination and 2,1-migratory insertion of imines into palladium-carbon  $\sigma$ -bonds were the focus of former student Rania Dghaym, Ph.D.<sup>7,14</sup> We will summarize and discuss those results, as well as my contributions to this work. Together these results will show that: (i)  $\sigma$ -coordination of the imine is a productive intermediate for the reaction, and (ii) in contrast to olefins,

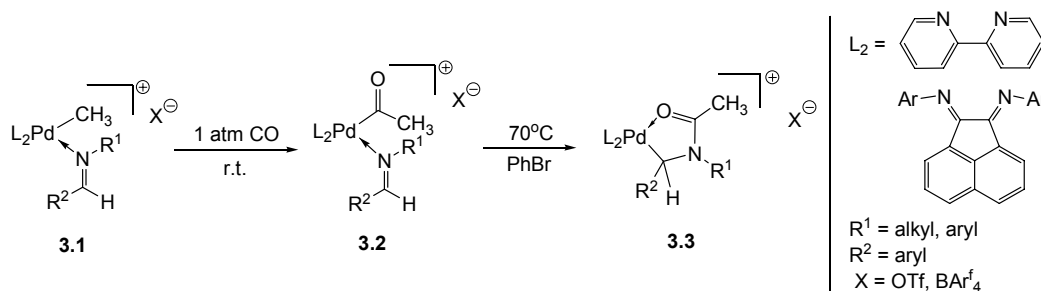
the polar nature of the imine C=N bond, rather than  $\pi$ -coordination, is more important for achieving insertion into the Pd-C bond. Considering that these palladium complexes are also known to mediate olefin insertion,<sup>2d,15</sup> this study allows for direct comparison of imine and olefin insertion mechanisms, and to determine the features that facilitate each process.

### 3.1 Results and Discussion

#### 3.1.1 Results Obtained From Previous Work by Rania Dghaym, Ph.D.

##### 3.1.1.1 Characteristics of the Sequential Insertion of Carbon Monoxide and Imine with $[L_2Pd(CH_3)(R^1N=C(H)R^2)]^+X^-$

The addition of 1 atm CO to a *d*<sub>5</sub>-bromobenzene (*d*<sub>5</sub>-PhBr) solution of **3.1**<sup>16</sup> results in rapid insertion of CO into the palladium-methyl bond to form the analogous palladium-acyl complexes **3.2**. Heating the palladium-acyl complexes **3.2** to 70°C causes these to disappear and new palladium complexes **3.3** to form [Scheme 3.3].

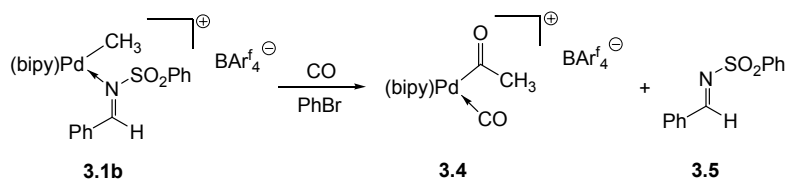


**Scheme 3.3:** The sequential insertion of carbon monoxide and imine to generate an amide-palladacycle.

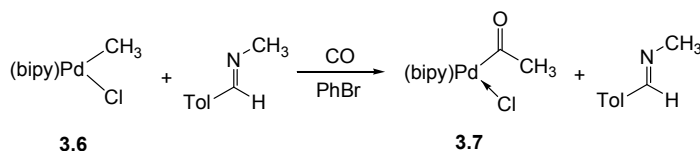
The sequential insertion of carbon monoxide and imine into a palladium-methyl bond was demonstrated to be a general reaction, and proceeds in high yield with a variety of ligands (bipy, BIAN), counteranions ( $OTf^-$  and  $BAr_4^-$ ), and imine substituents ( $R^1$  = alkyl, aryl and  $R^2$  = aryl). The generation of a 5-membered chelate provides a strong thermodynamic driving force for this reaction, due to the combination of amide bond formation and the coordination of the amide oxygen to the cationic palladium center.

In the presence of poorly  $\sigma$ -donating imines, such as *N*-sulfonyl substituted imines **3.5**, or coordinating counteranions, such as chloride, no imine insertion is observed. For example, insertion studies with complex **3.1b** under 1 atm CO yielded uncoordinated imine and the palladium-acyl complex **3.4** [Scheme 3.4]. No evidence of

interaction between **3.4** and this imine is noted, and heating the reaction simply lead to decomposition. In the case of neutral palladium complex (bipy)Pd(CH<sub>3</sub>)Cl **3.6**, the addition of *N*-methyl tolualdimine and 1 atm CO immediately generates palladium-acyl complex **3.7** [Scheme 3.5]. No conditions afforded imine coordination or insertion. The lack of coordination is likely due to strong binding by the chloride counteranion. Both of these results show the importance of imine  $\sigma$ -coordination for insertion into the palladium-acyl bond.



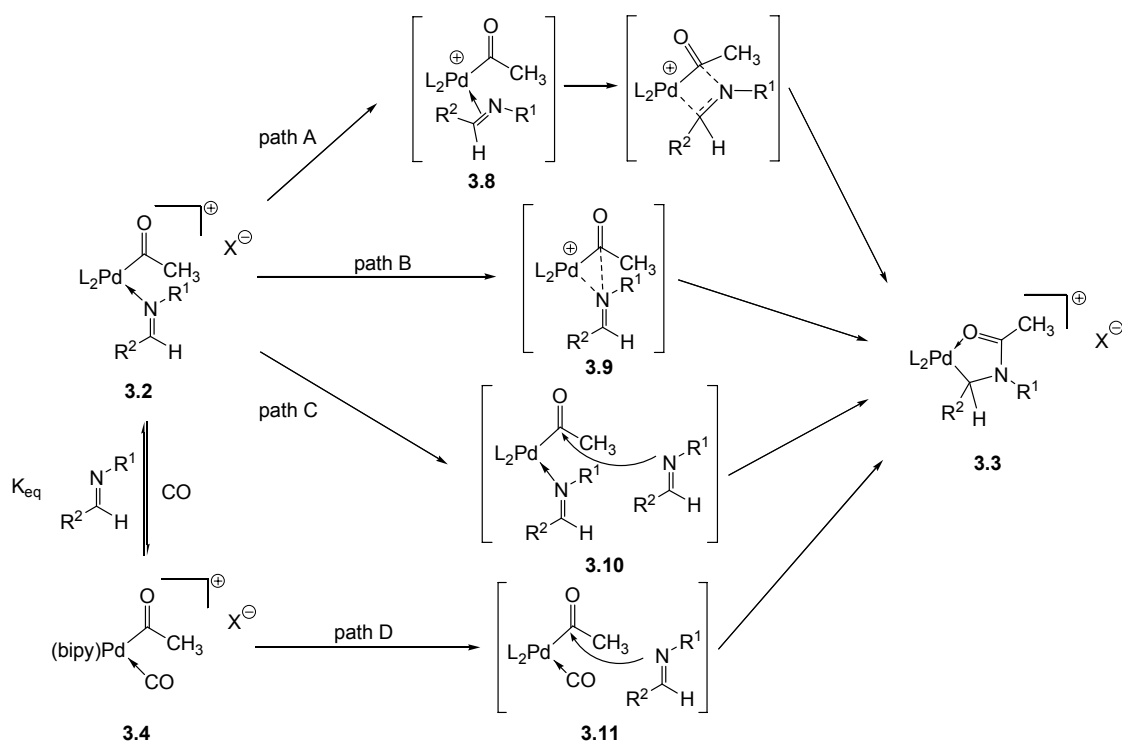
**Scheme 3.4:** The reaction of *N*-sulfonyl substituted imine palladium-methyl complex and carbon monoxide.



**Scheme 3.5:** The reaction of *N*-methyl tolualdimine and (bipy)Pd(CH<sub>3</sub>)Cl under 1 atm of CO.

### 3.1.1.2 Mechanistic Investigation of Imine Insertion into the Palladium-Acyl Bond

Several mechanistic possibilities can be proposed to account for the transformation of the palladium-acyl complexes **3.2** into **3.3** [Scheme 3.6]. One plausible mechanism involves forming the  $\pi$ -imine complex **3.8** prior to the migratory insertion of imine into the palladium-acyl bond (path A). This mechanism is similar to that previously proposed for imine migratory insertions,<sup>9a,17</sup> and is directly analogous to the established mechanism of insertion for the isoelectronic olefins.<sup>2</sup>



**Scheme 3.6:** Four proposed mechanisms for the imine insertion into palladium-acyl complexes.

However, unlike olefins, imines bind through the nitrogen lone pair in  $\eta^1$ -coordination mode and  $\pi$ -coordinated mononuclear imine complexes have not been previously detected with late metal complexes. The  $\eta^1$ -coordination mode of the imine suggests that the nitrogen lone pair may be involved in imine insertion and other mechanistic possibilities are envisioned [Scheme 3.6]. The lone pair on the imine nitrogen, which olefins lack, can act as a nucleophile. Intermolecular nucleophilic attack of a free imine molecule on the acyl ligand could generate 3.3. This nucleophilic attack could occur on either 3.2 (path C) or its CO-coordinated analogue 3.4 (path D). Alternatively, a concerted intramolecular nucleophilic attack directly from  $\sigma$ -imine complex 3.9 would generate the imine insertion product (path B).

Of the mechanisms outlined in Scheme 3.6, two are intermolecular reactions (paths C and D) and two are intramolecular rearrangements (paths A and B). These pathways should display distinct features affecting the rate of formation of complex 3.3. Dynamic equilibrium of imine coordination to 3.2 exists; the equilibrium between 3.2 and



**3.4** is rapidly established prior to the migratory insertion step. Therefore, a pre-equilibrium kinetic analysis of all pathways is required to obtain the rate expression.<sup>18</sup> Analysis of this mechanism provides distinctive rate expressions for the bimolecular paths C ( $k_C$ ) and D ( $k_D$ ). On the other hand, paths A and B will display identical kinetic behavior. Because both paths involve the intramolecular rearrangement of the imine ligand in **3.2** to generate the insertion product, they have the same rate expression  $k_{A/B}$ .

**Table 3.1:** Rate expressions for the mechanisms of imine insertion.

Pathways	Rate Equations <sup>a</sup>	Imine Saturation Condition <sup>b</sup>	CO Saturation Condition <sup>c</sup>
A and B	$k_{obs} = \frac{k_{A/B} K_{eq} [\text{imine}]}{[\text{CO}] + K_{eq} [\text{imine}]}$	$k_{obs} = k_{A/B}$	$k_{obs} = \frac{k_{A/B} K_{eq} [\text{imine}]}{[\text{CO}]}$
C	$k_{obs} = \frac{k_C [\text{imine}]^2}{[\text{CO}] + K_{eq} [\text{imine}]}$	$k_{obs} = \frac{k_C [\text{imine}]}{K_{eq}}$	$k_{obs} = \frac{k_C [\text{imine}]^2}{[\text{CO}]}$
D	$k_{obs} = \frac{k_D [\text{imine}] [\text{CO}]}{[\text{CO}] + K_{eq} [\text{imine}]}$	$k_{obs} = \frac{k_D [\text{CO}]}{K_{eq}}$	$k_{obs} = k_D [\text{imine}]$

**a** Rate equation for the first order formation of complex **3.3** from an equilibrium of complexes **3.2** and **3.4**; **b** Equilibrium between **3.2** and **3.4** saturated towards complex **3.2**; **c** Equilibrium between **3.2** and **3.4** saturated towards complex **3.4**.

These equations greatly simplify under imine saturation conditions (*i.e.* the equilibrium between **3.2** and **3.4** is saturated towards the imine complex **3.2**, or CO-coordinated complex **3.4**). As shown in **Table 3.1**, paths A, B, and D all yield rates independent of imine concentration under imine saturation conditions, while path C is still expected to show linear rate dependence on imine concentration. Alternatively, the expressions reveal that paths A, B and C should be inhibited by CO pressure, while a mechanism following path D should be facilitated by CO concentration until saturation is reached.

During her Ph.D. studies, Rania Dghaym demonstrated several important aspects critical to discern the mechanistic pathway involved in the 2,1-migratory insertion of imines into metal-acyl  $\sigma$ -bonds, based on both kinetic analysis and other observations. From kinetic studies, with complexes **3.2**, it was found that imine insertion shows a zero-

Interestingly, in the cases involving weakly coordinating imines (*e.g.* complex **3.2c**), a surprising decrease in rate was observed with the increase of imine concentration [Table 3.2, entries 1 and 2]. At low imine concentration, analysis of the reaction products revealed a competitive formation of the protonated iminium salt **3.12** in addition to the amide palladacycle **3.3**. The formation of **3.12** in this case suggests that de-coordination of imine to form  $[(\text{bipy})\text{Pd}(\text{COCH}_3)\text{CO}]^+\text{OTf}^-$  **3.4** leads to by-product formation, while imine insertion occurs directly from **3.2**. Consistent with this observation, increasing imine concentration reduces the presence of **3.4**, inhibits the formation of iminium salt **3.12**, and favours insertion. The precise mechanism to form the protonated iminium salt **3.13** from **3.4** remains unclear. However, its generation is also accompanied by the precipitation of palladium black, suggesting that as **3.4** decomposes,  $\text{H}^+$  is liberated from the acidic acyl ligand.

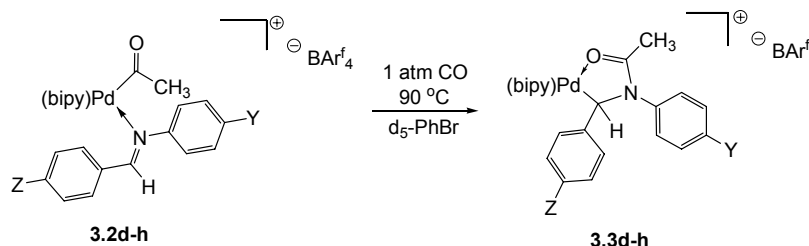
**3.2c** X = OTf  
**3.2d** X = BARf<sub>4</sub>

**a** Determined by  $^1\text{H}$  NMR analysis of formation of **3.3c,d** under 1 atm CO at  $90^\circ\text{C}$  in  $d_5$ -PhBr with 0.067M **3.2c,d**; **b**  $^1\text{H}$  NMR yields; **c** Could not be detected; **d**  $\text{X} = \text{BAr}_4^-$ .

- 68 -

amounts of iminium salt **3.12**, a plausible rationale for the accelerated rate of insertion at lower imine concentrations is that the iminium salt produced subsequently catalyzes the insertion process. In order to confirm this hypothesis, the effect of iminium salt on insertion rate in complex **3.2d** was examined. As predicted, the rate of insertion is accelerated in the presence of  $[\text{Ph}(\text{H})\text{N}=\text{C}(\text{H})\text{ToI}]^+ \text{BAr}_4^-$  [Table 3.2, entry 4]. The effect of acid catalysis in imine migratory insertion is further investigated in the following text.

**Table 3.3:** Influence of imine substituents on insertion rate.



Entry	Compound	Y	Z	$k_{\text{obs}} (\times 10^{-4} \text{ s}^{-1})^a$
1	<b>3.2d</b>	H	CH <sub>3</sub>	8.2 (0.5)
2	<b>3.2e</b>	OCH <sub>3</sub>	CH <sub>3</sub>	8.4 (0.5)
3	<b>3.2f</b>	NO <sub>2</sub>	CH <sub>3</sub>	8.8 (0.3)
4	<b>3.2g</b>	H	OCH <sub>3</sub>	7.9 (0.6)
5	<b>3.2h</b>	H	NO <sub>2</sub>	8.1 (0.7)

<sup>a</sup> Determined by <sup>1</sup>H NMR analysis of formation of **3.3d-h** under 1 atm CO at 90°C in *d*<sub>5</sub>-PhBr and 10-fold excess imine.

Discerning between paths A and B requires investigation into the nature of the transition state, since both of these have identical kinetic behaviour. By probing the electronic influences on insertion [Table 3.3], similar rates of imine insertion were found by Rania Dghaym for all complexes with either electron donating or withdrawing substituents.<sup>14</sup> This leads us to conclude that the rate is independent of the electronic properties of the imine, and suggests that the transition state has an almost identical charge distribution on the imine ligand to that in the ground state; *i.e.* the polar features of the imine in the  $\sigma$ -coordinated imine palladium complex **3.3** are also present in the transition state of insertion. In considering pathways A and B, this would be consistent

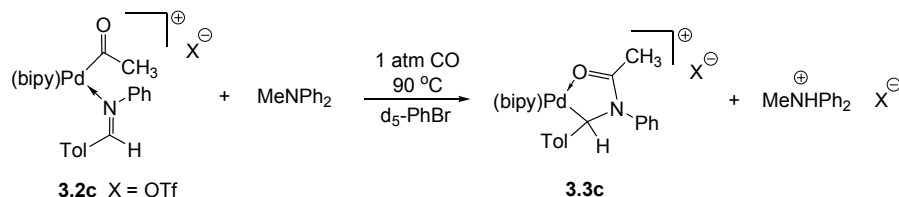
with pathway B, where there is no change in the  $\sigma$ -coordination mode of the imine (and thus charge distribution).

This data leaves pathways B and D as the most plausible for imine insertion, both of which involve a nucleophilic attack on the acyl ligand. However, as previously mentioned, imine  $\sigma$ -coordination to the palladium complex is required for insertion, as manifested, for example, by the non-reactivity of the neutral palladium complex (bipy)Pd(COCH<sub>3</sub>)Cl **3.7** towards insertion. This observation indirectly suggests that insertion proceeds through an imine coordinated intermediate (*e.g.* complex **3.2**) rather than a CO coordinated intermediate (*e.g.* complex **3.4**). However, to confidently eliminate the possibility of path D as a mechanism a kinetic study varying the pressure of carbon monoxide is critical. Thus, it will be presented further in the text.

### 3.1.2 My Results and Mechanistic Data Analysis

#### 3.1.2.1 Base Additive Effect with Weakly Coordinating Imines

To further investigate the influence of acid on the rate of insertion for complex **3.2c**, the rate of imine insertion was determined in the presence of methyldiphenylamine [Scheme 3.7]. The base traps any acid generated during the reaction, and does not interfere with imine coordination to the metal center. As shown in Table 3.4, the rate of imine insertion in the presence of 1 equivalent of base is inhibited, and similar to that observed at high imine concentration (where acid is not generated). This is consistent with the postulate that acid can accelerate imine insertion in complex **3.2c**, and thus we can confidently eliminate any dependence of imine concentration on the rate of insertion. Collectively, the kinetic observations rule out the possibility of path C.



**Scheme 3.7:** The effect of amine base on the rate of insertion for **3.2c**.

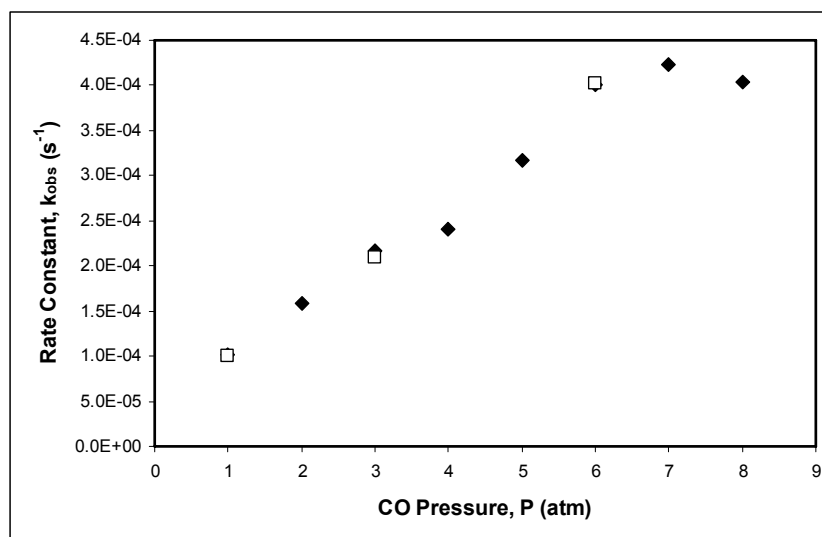
**Table 3.4:** Insertion chemistry of **3.2c** with various ligands.

Entry	Compound	L (M)	$k_{\text{obs}}$ ( $\times 10^{-4} \text{ s}^{-1}$ ) <sup>a</sup>	Yield <b>3.3</b> <sup>b</sup>	Yield <b>3.11</b> <sup>b</sup>
1	<b>3.2c</b>	-	6.2 (0.5)	74 %	23 %
2	<b>3.2c</b>	0.58 M PhN=C(H)Tol	2.0 (0.1)	94 %	n/a <sup>c</sup>
3	<b>3.2c</b>	0.07 M MeNPh <sub>2</sub>	2.4 (0.1)	90 %	n/a <sup>c</sup>

**a** Determined by <sup>1</sup>H NMR analysis of formation of **3.3c** under 1 atm CO at 90°C in *d*<sub>5</sub>-PhBr with 0.067M **3.2c**; **b** <sup>1</sup>H NMR yields; **c** Could not be detected.

### 3.1.2.2 Effect of Carbon Monoxide Pressure on the Insertion Rate

The effect of CO pressure on the imine insertion rate was probed by monitoring the kinetics of **3.3a** formation by <sup>1</sup>H NMR spectroscopy [Figure 3.1]. The data shows that at low CO pressures the rate of **3.3a** formation is accelerated with increasing CO concentration until a maximum rate is achieved at approximately 6 atm of CO. At pressures of 6 atm of CO and greater, the insertion rate saturates.

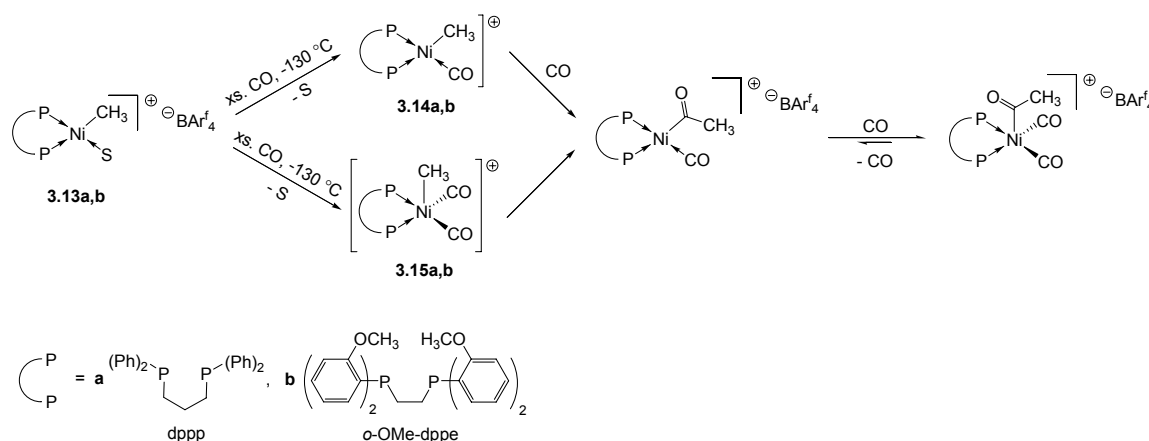


**Figure 3.1:** Plot of  $k_{\text{obs}}$  vs. [CO] for the reaction of **3.2a** to form **3.3a** in the presence of 0.2 M (□) and 0.4 M (◆) of MeN=C(H)Tol.

The increase observed in the rate of imine insertion with increasing CO pressures would appear to be most consistent with pathway D, *i.e.* increasing the concentration of CO pushes the equilibrium towards **3.4**, the active species for insertion in path D. The acceleration by CO pressure would saturate when the equilibrium is saturated. However the imine employed in this study, *N*-methyl tolualdimine, is strongly coordinated to the palladium in **3.2a**, and monitoring the reaction at all CO pressures reveals no evidence of **3.4**. This suggests CO pressure is not significantly perturbing the equilibrium between **3.2** and **3.4** with complex **3.2a** and saturation is not the result of saturating this equilibrium. Consistent with this hypothesis, the rates of insertion for the various pressures of CO were probed at two concentrations of imines and both sets of data demonstrate similar rates [Figure 3.1]. These data suggest the concentration of **3.4** does not influence the rate of imine insertion, and are inconsistent with path D.

This implies that insertion occurs most likely via path B, but raises the question of what underlying role does CO pressure have in affecting the rate of insertion, especially since CO pressure should not influence the rate of insertion step? In the case of ethylene and carbon monoxide copolymerization catalyzed by nickel (II) complexes **3.13a,b** mechanistic studies revealed that five-coordinate species **3.15a,b** have a lower barrier towards insertion [Scheme 3.8].<sup>19</sup> Insertion is observed to occur from both four- and five-coordinate complexes **3.14** and **3.15** respectively, with the five-coordinate pathway dominating at high pressures of carbon monoxide. Considering the similarity of this system to ours for imine insertion it seems plausible that the increased rate of imine insertion may be a result of CO coordinating to the apical site of the palladium complex **3.2** to generate a transient five-coordinate species.<sup>20</sup> Examining the <sup>13</sup>C NMR spectra of complex **3.2a** under various <sup>13</sup>CO pressures (1, 4, 6 and 8 atm), two <sup>13</sup>C carbonyl resonances are observed; the acyl resonance at  $\delta$  225.7 and a broadened resonance at  $\delta$  184.1 (25 °C).<sup>21</sup> This latter signal is in a similar position to free carbon monoxide ( $\delta$  184.5), as well as that in related CO coordinated complexes (*e.g.* (phen)Pd(COCH<sub>3</sub>)CO<sup>+</sup>  $\delta$  174.1),<sup>2d</sup> suggesting the broadening may result from a rapid exchange between uncoordinated and coordinated CO. Attempts to slow this exchange at low temperature (-20 °C) were unfortunately unsuccessful, implying a low barrier to this exchange process. This broadened <sup>13</sup>C NMR signal, together with the observed rate increase with CO

pressure, implies that transient coordination of CO at the apical site of the palladium is occurring. The latter would create a more electron deficient palladium metal center through backbonding influences, which could aid insertion at high CO pressures. A similar rate increase in imine insertion was observed when the electron withdrawing groups are introduced of the ligand framework.<sup>14,22</sup>



**Scheme 3.8:** Mechanism of carbon monoxide insertion for Ni (II) complexes of 1,3-bis-(diphenylphosphino)propane (dppp) **3.13a** and 1,2-bis(bis(2-methoxyphenyl)phosphino)ethane (o-OMe-dppe) **3.13b**.

### 3.1.3 Mechanistic Picture of Imine Insertion into Palladium-Acyl $\sigma$ -Bond

Previous studies by Rania Dghaym, Ph.D. showed through kinetic studies that imine insertion does not involve the intermolecular nucleophilic attack of an uncoordinated imine on the palladium-acyl imine complex (path C). In addition, indirect evidence suggests the importance of imine coordination for insertion [Schemes 3.4 and 3.5], arguing against path D. The CO pressure effects on insertion rates presented here confirm these deductions. Instead, imine insertion appears to occur via an intramolecular reaction directly from complex **3.2**. This leaves paths A and B as plausible mechanisms for insertion.

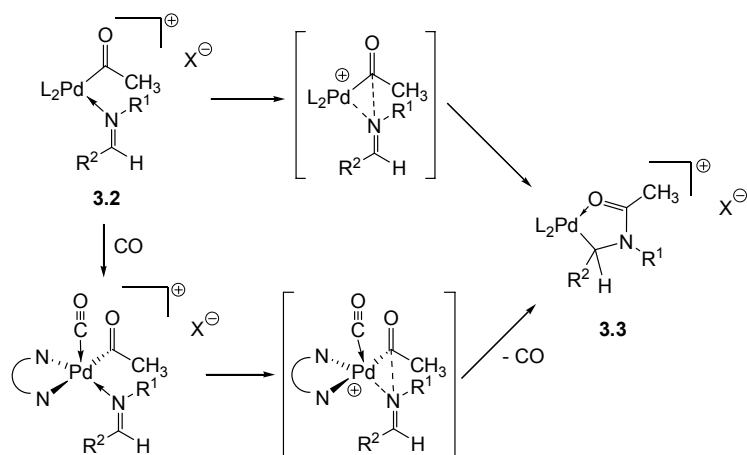
While pathways A and B are kinetically indistinguishable, conceptually these processes are quite different. Path A requires the nitrogen lone pair to dissociate from the palladium center, allowing the orthogonal C=N  $\pi$ -bond to coordinate to the palladium

center prior to insertion. In path B,  $\sigma$ -coordination of the nitrogen lone pair represents an active intermediate that allows concerted nucleophilic attack on the acyl carbon. In principle, these two mechanisms would be expected to have different electronic influences on the reaction rate. The results by Rania Dghaym suggest path A is less likely. In path A, the dissociation of the imine lone pair, and the  $\pi$ -coordination of the C=N bond, is expected to be facilitated by substituents which decrease the imine's  $\sigma$ -basicity and increase its backbonding ability (*i.e.* its electron acceptor ability).<sup>11a</sup> However, the fact that all the rate data for imine insertion are within the experimental error of one another strongly implies a dramatic change in the imine coordination environment is not occurring. Accordingly, this argues against a significant de-coordination of the nitrogen lone pair in the transition-state for imine insertion.

This intramolecular nucleophilic attack mechanism (path B) provides a reasonable rationale for the effect of CO pressure on the reaction, where the rate of imine insertion is enhanced with CO pressure without influencing imine binding. A transient five-coordinate palladium complex with carbon monoxide at its apical site is a plausible intermediate. Increasing the electrophilicity by the coordination of CO to complex **3.2** stabilizes the transition state for insertion.

Overall, our data suggests a concerted mechanism for imine insertion from complex **3.2** [Scheme 3.9]. Here, the  $\sigma$ -coordination of the imine is a vital intermediate for an intramolecular nucleophilic attack on the acyl ligand.<sup>23</sup> This concerted mechanism uses the polar features of the imine C=N bond to achieve insertion and is enhanced by features that accentuate the electrophilicity of the palladium-acyl bond. This is consistent with our observation that imine insertion into the palladium-carbon bond only occurs after CO insertion to generate the acyl ligand.

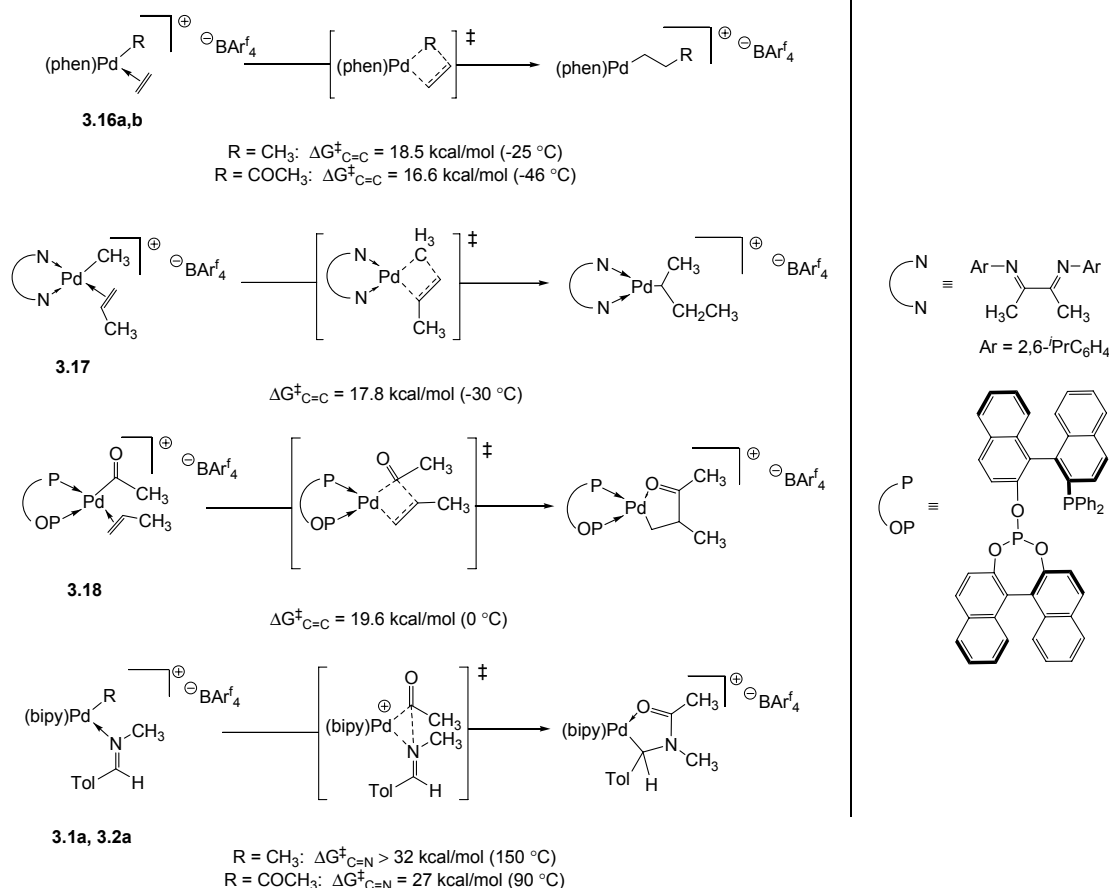




**Scheme 3.9:** Two proposed pathways involved in path B for the imine insertion palladium-acyl bond: concerted intramolecular nucleophilic attack of imine on acyl ligand.

### 3.1.4 Comparison of Imine to Olefin Insertion Mechanisms into Palladium-Carbon Bonds

The intramolecular migratory insertion of alkenes into the palladium-methyl and -acyl bonds of  $[(L_2)Pd(R)(alkene)]^+BAR_4^{f-}$  **3.16a,b**, **3.17** and **3.18** (defined in **Figure 3.2**) have been the subject of thorough mechanistic studies.<sup>15,24</sup> The similarity between these complexes, and palladium-imine complexes **3.1a**, and **3.2b** allows for a direct comparison of the factors influencing imine and olefin insertion in analogous palladium complexes. The calculated free energy barriers<sup>25</sup> for migratory insertion in these literature systems, and imine complexes **3.1a** and **3.2a** are shown in **Figure 3.2**. Assuming a minimal entropic contribution to  $\Delta G^\ddagger$  in the intramolecular insertion reaction, the free energy barriers can be directly compared. These show that ethylene and propene insertion into palladium-carbon bonds are significantly lower barrier processes than the analogous insertion of the imine  $CH_3N=C(H)Tol$ , by approximately 10 kcal/mol.

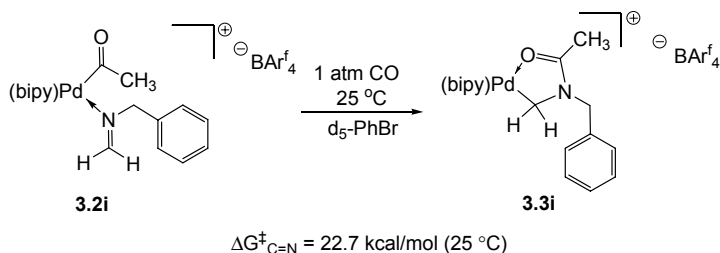


**Figure 3.2:** Mechanism and kinetic barriers for ethylene, propene and imine insertion into cationic palladium-carbon bonds. Value of  $\Delta G^\ddagger_{\text{C}=\text{N}} > 32 \text{ kcal/mol}$  for  $R = \text{CH}_3$  estimated from decomposition of **3.2a** upon warming to  $150^\circ\text{C}$ .

While this data suggests that imine insertion occurs with a significantly higher barrier than alkene insertion, it is important to note that the imine in **3.2a** is a *trans*-disubstituted substrate, while the alkenes are sterically unencumbered ethylene and propene. Indeed, to our knowledge, *trans*-aryl substituted alkenes have not been found to be viable insertion polymerization monomers.

To gain a better comparison to alkenes, the rate of insertion with the simple formaldimine  $\text{H}_2\text{C}=\text{NBn}$  palladium complex **3.1i** was examined [Scheme 3.10]. As shown in Scheme 3.10, this imine inserts at a much lower temperature than that of **3.2a**. The conversion of **3.2i** to **3.3i** was monitored by  $^1\text{H}$  NMR spectroscopy at  $25^\circ\text{C}$  and the observed rate of insertion  $k_{\text{obs}}$  was  $1.46 \pm 0.09 \times 10^{-4} \text{ s}^{-1}$  ( $\Delta G^\ddagger = 22.7 \text{ kcal/mol}$ ). Thus,

alkene insertion into a palladium-carbon bond has a similar yet approximately 3-5 kcal/mol lower barrier than the analogous insertion of the formaldimine  $\text{BnN}=\text{CH}_2$ .



**Scheme 3.10:** The 2,1-migratory insertion of formaldimine  $\text{H}_2\text{C}=\text{NBn}$  in complex **3.2i**.

In addition to the rate differences, comparing the data for alkene and imine insertion shows the latter is much more dependent on the type of Pd-carbon bond into which it inserts. The barriers of insertion for olefins into analogous palladium-methyl and -acyl ligands are roughly similar, whereas there is a dramatic difference in free energy barriers for imine insertion.<sup>26</sup> This is likely a direct consequence of the *distinct mechanisms by which imines and olefins undergo insertion in these systems*. For the concerted migratory insertion of alkenes into the Pd-R bond, the  $\pi$ -bound olefin does not rely on the electrophilicity of the Pd-C bond to provide a low barrier route to insertion. Consequently, alkenes have similar barriers of migratory insertion into both the palladium-methyl and -acyl bonds ( $\Delta G^\ddagger_{\text{C=C}} = \sim 18 \text{ kcal/mol}$ ). Conversely, the mechanistic studies above suggest that imine insertion occurs directly from the  $\sigma$ -coordinated complex, and involves interaction of the nucleophilic imine nitrogen with the electrophilic palladium-acyl bond. Thus, in contrast to olefins, the complementarity between the electrophilic Pd-C bond and nucleophilic  $\text{C}=\text{N}$  is of paramount importance to imine insertion. The importance of this apparent mechanistic distinction between olefin and imine insertion with cationic palladium complexes is illustrated in our attempts to facilitate the formation of complex **3.3** by favoring imine  $\pi$ -coordination (*i.e.* increased palladium backbonding, weakened imine  $\sigma$ -donor ability, occupation of the nitrogen lone pair). This not only fails to accelerate insertion, but often blocks the reaction. Therefore, while imines can undergo migratory insertions into palladium-carbon bonds to generate products analogous to those with olefins, the polarization of the  $\text{C}=\text{N}$  and Pd-C bonds,

rather than involvement of  $\pi$ -coordination, appears to be the key factor to carrying out this process with low kinetic barriers.

### 3.2 Conclusion

These studies demonstrate that the migratory insertion of imines into palladium-carbon bond is uniquely facilitated by the presence of an acyl ligand, which can be generated *in-situ* upon initial insertion of carbon monoxide into the palladium-methyl bond of **3.1**. Our mechanistic data suggest that imine insertion is distinct from olefin insertion and involves the concerted migratory attack of the  $\sigma$ -coordinated imine to the electrophilic acyl ligand. This mechanistic picture is consistent with previous theoretical studies of this reaction and provide a reasonable rationale for the lack of examples of imine 2,1-insertion into late metal-alkyl bonds that are less electrophilic. Considering that carbon monoxide insertion to generate metal-acyl ligands is a relatively general reaction for a wide variety of metal-alkyl complexes and that imine  $\sigma$ -coordination is also easily achieved, this low barrier mechanism for imine insertion could extend to a wide variety of metal complexes. Indeed, we already observed that sequential CO/imine insertion can also be achieved with cationic nickel complexes,<sup>27</sup> neutral nickel complexes (**Chapter 2**) and neutral manganese carbonyl complexes.<sup>28</sup> The sequential insertion of CO and imine could also enable using imines as olefin analogues in metal catalyzed processes. Studies directed towards the latter are currently the subject of research in our laboratory.

### 3.3 Experimental Section

Unless otherwise noted, all manipulations were carried out under an inert atmosphere in a Vacuum Atmosphere 553-2 drybox or by using standard Schlenk or vacuum line techniques. NMR spectra were collected using a JEOL 270MHz spectrometer. Unless otherwise specified all reagents were used without further purification: silver triflate (Aldrich, 99 %), carbon monoxide (Matheson, 99.98 %), diphenylmethylamine (Aldrich, 96 %) and benzylbenzoate (Aldrich,  $\geq 99.0$  %) were dried over 4Å molecular sieves before use. All solvents were freshly distilled and degassed before use and stored under nitrogen over molecular sieves. Diethyl ether was distilled from sodium benzophenone. Pentane, methylene chloride and bromobenzene were distilled from CaH<sub>2</sub>. Deuterated solvents were dried as their protonated analogues, but vacuum transferred from the drying agent. Aldimines were prepared using standard literature procedures.<sup>29</sup> (bipy)Pd(CH<sub>3</sub>)Cl<sup>30</sup> and NaBAr<sub>4</sub><sup>f,31</sup> were prepared according to literature procedures. Complexes **3.1a-i**, **3.2a-i** and **3.3a-i** were prepared according to the procedure in Rania Dghaym's thesis.<sup>14</sup>

#### 3.3.1 Synthesis of [(bipy)Pd(CH<sub>3</sub>)(BnN=CH<sub>2</sub>)]<sup>+</sup>BAr<sub>4</sub><sup>f-</sup> (**3.1i**)<sup>14</sup>

(bipy)PdMeCl (100.0 mg, 0.32 mmol) and BnN=CH<sub>2</sub> (76.3 mg, 0.64 mmol) were dissolved in dichloromethane (*ca.* 10 mL). To this yellow solution, a slurry of NaBAr<sub>4</sub><sup>f</sup> (283.0 mg, 0.32 mmol) in dichloromethane (*ca.* 5 mL) was added. The resulting mixture was stirred for 90 min at ambient temperature providing a brown solution with a white precipitate. The mixture was then filtered through a Celite plug. The filtrate was concentrated down to approximately 3 mL in volume under vacuo and layered with diethyl ether (*ca.* 5 mL) before cooling to -40°C for crystallization. Crystals were collected by filtration and washed with pentane (*ca.* 3 x 3 mL).

**Yield:** 71%

**<sup>1</sup>H NMR (500 MHz, CD<sub>2</sub>Cl<sub>2</sub>):**  $\delta$  8.57 (d, 1H,  $J_{\text{HH}} = 5.0$  Hz), 8.13-7.98 (m, 6H), 7.74-7.57 (m, 15H), 7.43 (d, 1H,  $J_{\text{HH}} = 4.6$  Hz), 7.34-7.30 (m, 3H), 4.95 (s, 2H), 0.86 (s, 3H).

**<sup>13</sup>C NMR (500 MHz, CD<sub>2</sub>Cl<sub>2</sub>):** δ 164.3, 162.6, 162.2, 161.8, 161.4, 156.8, 152.8, 149.4, 147.4, 140.4, 139.9, 135.0, 133.4, 130.3, 129.7, 129.4, 129.2, 129.0, 128.7, 128.0, 127.2, 127.1, 125.9, 123.7, 123.2, 122.4, 121.5, 117.7, 70.8, 31.9.

**ESI-HRMS:** calculated for C<sub>19</sub>H<sub>20</sub>N<sub>3</sub>Pd<sup>+</sup> (M<sup>+</sup>) 396.06947; found 396.06866.

### 3.3.2 Synthesis of [(bipy)Pd(η<sup>2</sup>-CH<sub>2</sub>N(Bn)COCH<sub>3</sub>)]<sup>+</sup>BAr<sup>f</sup><sub>4</sub><sup>-</sup> (**3.3i**)<sup>14</sup>

[(bipy)Pd(CH<sub>3</sub>)(BnN=CH<sub>2</sub>)]<sup>+</sup>BAr<sup>f</sup><sub>4</sub><sup>-</sup> **3.1i** (189.0 mg, 0.15 mmol) was dissolved in CH<sub>2</sub>Cl<sub>2</sub> (*ca.* 5 mL) in 50 mL reaction bomb. The solution was placed under 1 atm of CO (15 psi) and stirred at ambient temperature for 1 hour. The reaction was then heated at 50 °C for 3 hrs. The solution was filtered through a Celite plug, filtrate was layered with *ca.* 5 mL of diethyl ether, and cooled to -40 °C overnight. The crystalline solids were collected by filtration, washed with pentane (3 x *ca.* 5 mL) and dried under vacuo overnight to yield a beige powder.

**Yield:** 93%

**<sup>1</sup>H NMR (500 MHz, CD<sub>2</sub>Cl<sub>2</sub>):** δ 8.70 (d, 1H, *J*<sub>HH</sub> = 4.4 Hz), 8.17-8.12 (m, 5H), 7.99 (d, 2H, *J*<sub>HH</sub> = 6.6 Hz), 7.74 (s, 7H), 7.57 (s, 5H), 7.47-7.41 (m, 4H), 7.27 (s, 2H), 4.57 (s, 2H), 4.18 (s, 2H), 2.37 (s, 3H).

**<sup>13</sup>C NMR (500 MHz, C<sub>6</sub>D<sub>5</sub>Br):** δ 181.0, 162.9, 162.5, 162.1, 161.7, 155.8, 151.9, 150.1, 148.1, 139.6, 139.3, 135.1, 133.4, 130.7, 130.3, 130.0, 128.8, 128.3, 128.0, 126.9, 126.8, 125.9, 123.7, 122.8, 122.1, 121.5, 117.7, 55.5, 49.9, 19.6.

**ESI-HRMS:** calculated for C<sub>20</sub>H<sub>20</sub>N<sub>3</sub>PdO<sup>+</sup> (M<sup>+</sup>) 424.06418; found 424.06357.

### 3.3.3 Kinetic Experimental

Imine insertion rate constants were measured by integrating the <sup>1</sup>H NMR spectroscopy product peaks of **3.3** relative to the internal standard benzyloxybenzoate. A general protocol follows. Complex **3.1a** (38.2 mg, 0.030 mmol) and a 10-fold excess of CH<sub>3</sub>N=C(H)Tol (40.0 mg, 0.30 mmol) were dissolved in *d*<sub>5</sub>-bromobenzene (1.10 g, 6.79 mmol, 0.04 M) and transferred to a J-Young capped NMR tube. 1 atm of CO (14.70 psi) was added to the NMR tube, resulting in the formation of a bright yellow solution. The

solution was left to stand at ambient temperature for 30 min to ensure the palladium-acyl complex was fully formed. The NMR tube was then placed in a thermostat NMR probe and the spectra were collected periodically. The rate data collected for the formation of **3.3** was fitted to a first order plot to calculate the observed rate constant ( $k_{\text{obs}}$ ).

### **3.3.4 Influence of CO Pressure on Imine Insertion**

Modifications to the general protocol involve varying the carbon monoxide pressures. For pressures from 1 to 4 atm (14.70 to 58.80 psi) J-Young capped NMR tubes were used, however for pressures from 5 to 8 atm (73.50 to 117.60 psi) Parr high-pressure NMR tubes were used.

### **3.3.5 Influence of Base Additive on the Imine Insertion in 3.2c**

The general procedure was applied with the following modifications. The concentration of the experiment was modified to 0.07M. Complex **3.1c** (29.7 mg, 0.048 mmol) and MeNPh<sub>2</sub> (8.8 mg, 0.048 mmol) were dissolved in *d*<sub>5</sub>-bromobenzene (1.10 g, 6.79 mmol, 0.07M) and transferred to a J-Young capped NMR tube. The remaining protocol is as described in the general procedure.



### 3.4 References

- (1) (a) Britovsek, G.J.P.; Gibson, V.C.; Wass, D.F. *Angew. Chem., Int. Ed.* **1999**, *38*, 428. (b) Imanishi, Y.; Naga, N. *Prog. Polym. Sci.* **2001**, *26*, 1147. (c) Michalak, A.; Ziegler, T. *Theoretical Aspects of Transition Metal Catalysts, Topics in Organometallic Chemistry*, Springer Berlin: Heidelberg, 2005. (d) Dong, J.-Y.; Hu, Y. *Coord. Chem. Rev.* **2006**, *250*, 47.
- (2) (a) Drent, E.; Budzelaar, P.H.M. *Chem. Rev.* **1996**, *96*, 663. (b) Abu-Surrah, A.S.; Reiger, B. *Angew. Chem. Int. Ed. Engl.* **1996**, *357*, 2475. (c) Sen, A. *Acc. Chem. Res.* **1993**, *26*, 303. (d) Rix, F.C.; Brookhart, M.; White, P.S. *J. Am. Chem. Soc.*, **1996**, *118*, 4746 and references therein.
- (3) (a) Heck, R.F. In *Comprehensive Organic Synthesis*; Trost, B. M.; Fleming, I., Eds.; Pergamon Press: Oxford, 1991; Vol. 4. (b) Daves, G.D.; Hallberg, A. *Chem. Rev.* **1989**, *89*, 1433. (c) Beletskaya, I.P.; Cheprakov, A.V. *Chem. Rev.* **2000**, *100*, 3009.
- (4) Trost, B.M.; Frederiksen, M.U.; Rudd, M.T. *Angew. Chem. Int. Ed.* **2005**, *44*, 6630.
- (5) Ishiyama, T.; Hartwig J. *J. Am. Chem. Soc.* **2000**, *122*, 12043.
- (6) With arystannanes: (a) Oi, S.; Moro, M.; Fukuhara, H.; Kawanishi, T.; Inoue, Y. *Tetrahedron Lett.* **1999**, *40*, 9259. (b) Ueda, M.; Miyaura, N. *J. Organomet. Chem.* **2000**, *595*, 31. (c) Hayashi, T.; Ishigedani, M. *J. Am. Chem. Soc.* **2000**, *122*, 976. (d) Davis, J.L.; Dhawan, R.; Arndtsen, B.A. *Angew. Chem. Int. Ed.* **2004**, *43*, 590. With arylborates: (e) Ueura, K.; Miyamura, S.; Satoh, T.; Miura, M. *J. Organomet. Chem.* **2006**, *691*, 2821. With arylboronic acids: (f) Ueda, M.; Saito, A.; Miyaura, N. *Synlett* **2000**, 1637.
- (7) Dghaym, R.D.; Yaccato, K.J.; Arndtsen, B.A. *Organometallics* **1998**, *17*, 4.
- (8) (a) Dhawan, R.; Dghaym, R.D.; Arndtsen, B.A. *J. Am. Chem. Soc.* **2003**, *125*, 1474. (b) Dhawan, R.; Dghaym, R.D.; St. Cyr, D.J.; Arndtsen, B.A. *Org. Lett.* **2006**, *8*, 3927.
- (9) For reviews: (a) James, B. R. *Cat. Today* **1997**, *37*, 209. (b) Sanchez-Delgado, R. A.; Rosales, M. *Coord. Chem. Rev.* **2000**, *196*, 249. (c) Martens, J. In *Stereoselective Synthesis* Helmchen, G.; Hofmann, R. W.; Mulzer, J.; Schaumann, E.; Eds., Theime,

- Stuttgart, 1996. Vol. 7, 4194. (d) Kobayashi, S.; Ishitani, H. *Chem. Rev.* **1999**, *99*, 1069.
- (10) (a) Baranyai, A.; Ungváry, F.; Markó, L. *J. Mol. Catal.* **1985**, *32*, 343. (b) Longley, C.J.; Goodwin, T.J.; Wilkinson, G. *Polyhedron* **1986**, *5*, 1625. (c) Brune, H.A.; Unsin, J.; Hemmer, R.; Reichhardt, M. *J. Organomet. Chem.* **1989**, *369*, 335. (d) Becalski, A.G.; Cullen, W.R.; Fryzuk, M.D.; James, B.R.; Kang, G.J.; Rettig, S.J. *Inorg. Chem.* **1991**, *30*, 5002. e) Baralt, E.; Smith, S.J.; Hurwitz, J.; Horváth, I.T.; Fish, R.H. *J. Am. Chem. Soc.* **1992**, *114*, 5187.
- (11) (a) Stark, G.A.; Gladysz, J.A. *Inorg. Chem.* **1996**, *35*, 5509. (b) Lenges, C.P.; Brookhart, M.; White, P.S. *Angew. Chem. Int. Ed. Engl.* **1999**, *38*, 552. (c) Knight, D.A.; Dewey, M.A.; Stark, G.A.; Bennet, B.K.; Arif, A.M.; Gladysz, J.A. *Organometallics*, **1993**, *12*, 4523.
- (12) Transfer hydrogenation of imines has been suggested to occur via the concerted addition of imine across H-M-L-H: (a) Noyori, R.; Hashiguchi, S. *Acc. Chem. Res.* **1997**, *30*, 97. (b) Uematsu, N.; Fujii, A.; Hashiguchi, S.; Ikariya, T.; Noyori, R. *J. Am. Chem. Soc.* **1996**, *118*, 4916. (c) Zassinovich, G.; Mestroni, G.; Gladiali, S. *Chem. Rev.* **1992**, *92*, 1051. (d) Yamakawa, M.; Ito, H.; Noyori, R. *J. Am. Chem. Soc.* **2000**, *122*, 1466. (e) Alosio, D.A.; Brandt, P.; Nordin, S.J.M.; Andersson, P.G. *J. Am. Chem. Soc.* **1999**, *121*, 9580.
- (13) Cavallo, L. *J. Am. Chem. Soc.* **1999**, *121*, 4238.
- (14) Dghaym, R. “*The Novel Sequential Insertion of Carbon Monoxide and Imines into Palladium-Carbon  $\sigma$ -Bonds: Synthesis, Mechanism and Reactivity*” Ph.D. Thesis, McGill University, **2000**.
- (15) (a) Johnson, L.K.; Killian, C.M.; Brookhart, M. *J. Am. Chem. Soc.* **1995**, *117*, 6414.
- (16) Palladium complex studied in this text:  $[(bipy)Pd(CH_3)(CH_3N=C(H)Tol)]^+BAr_4^{f-}$  **3.1a**;  $[(bipy)Pd(CH_3)(PhSO_2N=C(H)Ph)]^+BAr_4^{f-}$  **3.1b**;  $[(bipy)Pd(CH_3)(PhN=C(H)Tol)]^+OTf^-$  **3.1c**;  $[(bipy)Pd(CH_3)(PhN=C(H)Tol)]^+BAr_4^{f-}$  **3.1d**;  $[(bipy)Pd(CH_3)(p-OMeC_6H_4N=C(H)Tol)]^+BAr_4^{f-}$  **3.1e**;  $[(bipy)Pd(CH_3)(p-NO_2C_6H_4N=C(H)Tol)]^+BAr_4^{f-}$  **3.1f**;  $[(bipy)Pd(CH_3)(PhN=C(H)C_6H_4p-OMe)]^+BAr_4^{f-}$

**3.1g;**  $[(\text{bipy})\text{Pd}(\text{CH}_3)(\text{PhN}=\text{C}(\text{H})\text{C}_6\text{H}_4\text{p-NO}_2)]^+\text{BAr}^{\text{f}-}$  **3.1h** and  $[(\text{bipy})\text{Pd}(\text{CH}_3)(\text{BnN}=\text{CH}_2)]^+\text{BAr}^{\text{f}-}$  **3.1i.**

- (17) Imine insertions into M-H are known, and have been postulated in catalytic hydrogenations: (a) Palmer, M.J.; Wils, M. *Tetrahedron: Asymmetry* **1999**, *10*, 2045. (b) James, B.R. *Chem. Ind. (Dekker)* **1995**, *62*, 167. (c) Debad, J.D.; Legzdins, P.; Lumb, S.A.; Batchelor, R.J.; Einstein, F.W.B. *Organometallics* **1995**, *14*, 2543. (d) Willoughby, C.A.; Buchwald, S.L. *J. Am. Chem. Soc.* **1994**, *116*, 11703 and references therein. (e) Fryzuk, M.O.; Piers, W.E. *Organometallics* **1990**, *9*, 986.
- (18) (a) Lowry, T.H.; Richardson, K.S. *Mechanism and Theory in Organic Chemistry*, Harper: New York, **1987**. (b) Maskill, H. *The Physical Basis of Organic Chemistry*, Oxford University Press: Oxford, **1985**.
- (19) (a) Bernardi, F.; Bottoni, A.; Nicastro, M.; Rossi, I.; Novoa, J.; Prat, X. *Organometallics* **2000**, *19*, 2170. (b) Shultz, C.S.; DeSimone, J.M.; Brookhart, M. *Organometallics* **2001**, *20*, 16. (c) Shultz, C.S.; DeSimone, J.M.; Brookhart, M. *J. Am. Chem. Soc.* **2001**, *123*, 9172.
- (20) (a) Fernández, D.; García-Seijo, M.I.; Kégl, T.; Petőcz, G.; Kollár, L.; García-Fernández, M.E. *Inorg. Chem.* **2002**, *41*, 4435. (b) Bröring, M.; Brandt, C.D; *Chem. Commun.* **2003**, 2156. (d) Fernández, D.; García-Seijo, M.I.; Castiñeiras, A.; García-Fernández M.E. *Dalton Trans.* **2004**, 2526 (c) Bedford, R.B.; Betham, M.; Butts, C.P.; Coles, S.J.; Cutajar, M.; Gelbrich, T.; Hursthouse, M.B.; Scully, P.N.; Wimperis, S. *Dalton Trans.*, **2007**, 459.
- (21)  $^{13}\text{C}$  NMR of  $^{13}\text{CO}$  (500 MHz,  $d_5$ -bromobenzene, 25 °C):  $\delta$  184.5.
- (22) Rates of imine insertion for  $[(\text{BIAN})\text{Pd}(\text{COCH}_3)(\text{CH}_3\text{N}=\text{C}(\text{H})\text{Tol})]^+\text{BAr}^{\text{f}-}$   $k_{\text{obs}} = 1.65 (0.02) \times 10^{-4} \text{ s}^{-1}$ ,  $[(p\text{-OMe-BIAN})\text{Pd}(\text{COCH}_3)(\text{CH}_3\text{N}=\text{C}(\text{H})\text{Tol})]^+\text{BAr}^{\text{f}-}$   $k_{\text{obs}} = 1.28 (0.02) \times 10^{-4} \text{ s}^{-1}$ ,  $[(p\text{-Cl-BIAN})\text{Pd}(\text{COCH}_3)(\text{CH}_3\text{N}=\text{C}(\text{H})\text{Tol})]^+\text{BAr}^{\text{f}-}$   $k_{\text{obs}} = 3.06 (0.01) \times 10^{-4} \text{ s}^{-1}$ , measured by  $^1\text{H}$  NMR at 60 °C in  $d_5$ -bromobenzene under 1 atm CO.
- (23) The intermolecular attack of nucleophiles on metal-acyl ligands is a well-known process for cleavage of the M-C bond: Collman, J. P.; Hegedus, L. S.; Norton, J. R.; Finke R. G. *Principles and Applications of Organotransition Metal Chemistry* University Science Books, Mill Valley, CA 1987.

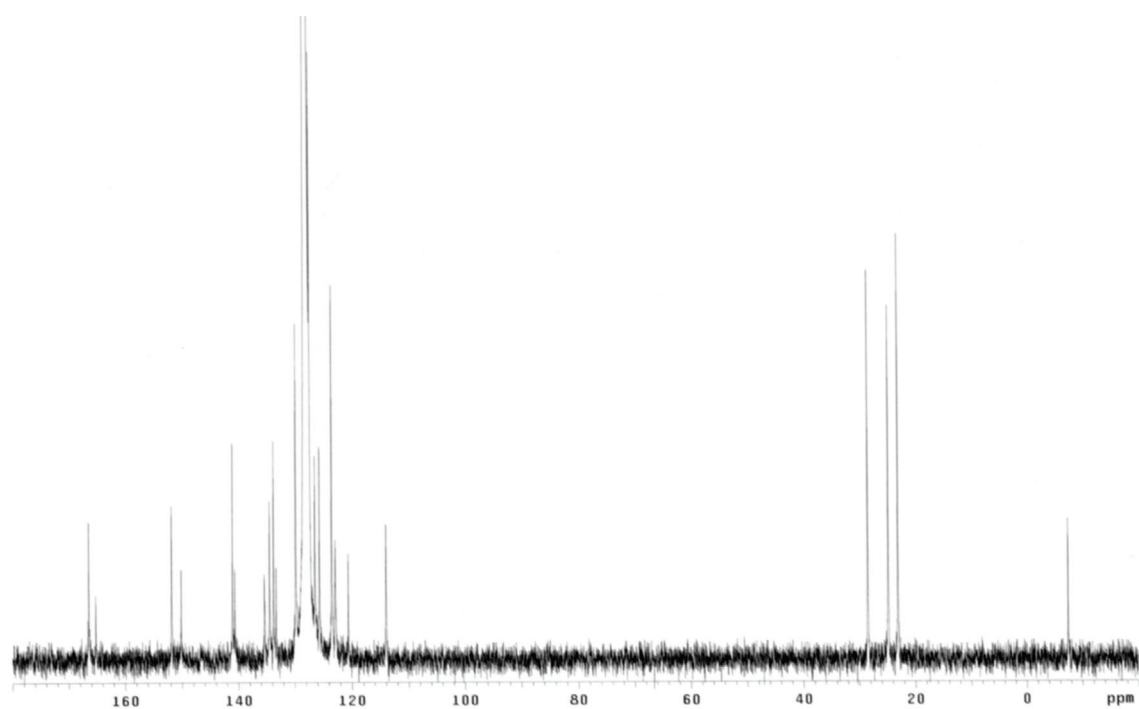
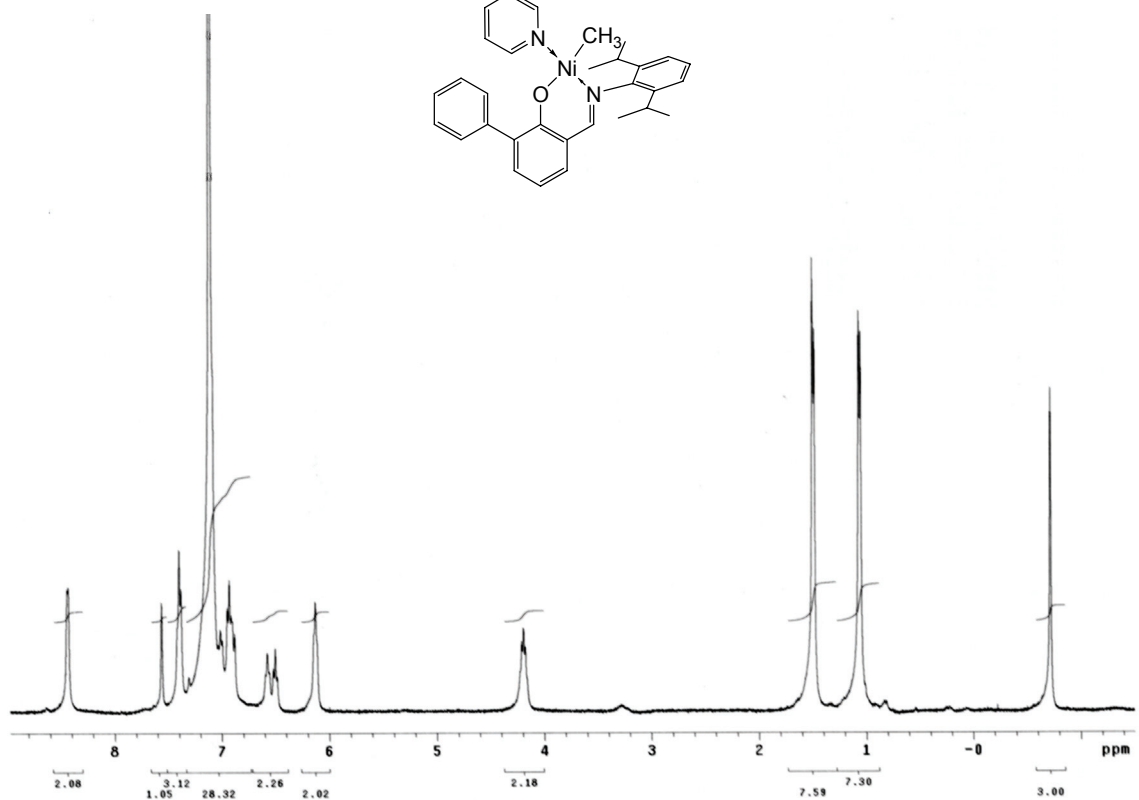
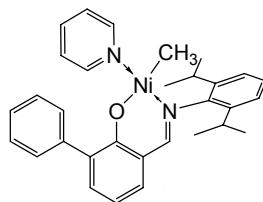
- (24) Nozaki, K.; Sato, N.; Tonomura, Y.; Yasutomi, M.; Takaya, H.; Hiyama, T.; Matsubara, T.; Koga, N. *J. Am. Chem. Soc.* **1997**, *119*, 12779. (b) Nozaki, K.; Kawashima, Y.; Nakamoto, K.; Hiyama, T. *Macromolecules* **1999**, *32*, 5168.
- (25) The free energy barrier of activation is derived from the Eyring equation  $k = \frac{k_B T}{h} e^{-\Delta G^\ddagger / RT}$ , where  $k$  is the rate of reaction,  $k_B$  is the Boltzman constant,  $T$  is the temperature,  $h$  is the Planck constant and  $R$  is the Gas constant.
- (26) Aldimine (e.g.  $\text{CH}_3\text{N}=\text{C}(\text{H})\text{Tol}$ ) insertion into Pd- $\text{CH}_3$  bond was not observed; value of  $\Delta G^\ddagger_{\text{C}=\text{N}} > 32$  kcal/mol estimated from decomposition of **3.2a** warming to 150 °C.
- (27) Davis J.L.; Arndtsen, B.A. *Organometallics*, **2000**, *19*, 4657.
- (28) Lafrance, D.; Davis, J.L.; Dhawan, R.; Arndtsen, B.A. *Organometallics*, **2001**, *20*, 1128.
- (29) Layer, R.W. *Chem. Rev.* **1963**, *63*, 489.
- (30) van Asselt, R.; Gielens, E.E.C.G.; Rülke, R.E.; Vrieze, K.; Elsevier, C.J. *J. Am. Chem. Soc.* **1994**, *116*, 977.
- (31) (a) Brookhart, M.; Grant, B.; Volpe, A.F. Jr *Organometallics* **1992**, *11*, 3920. (b) Yakelis, N.A.; Bergman, R.G. *Organometallics* **2005**, *24*, 3579.

## ∞ APPENDIX A ∞

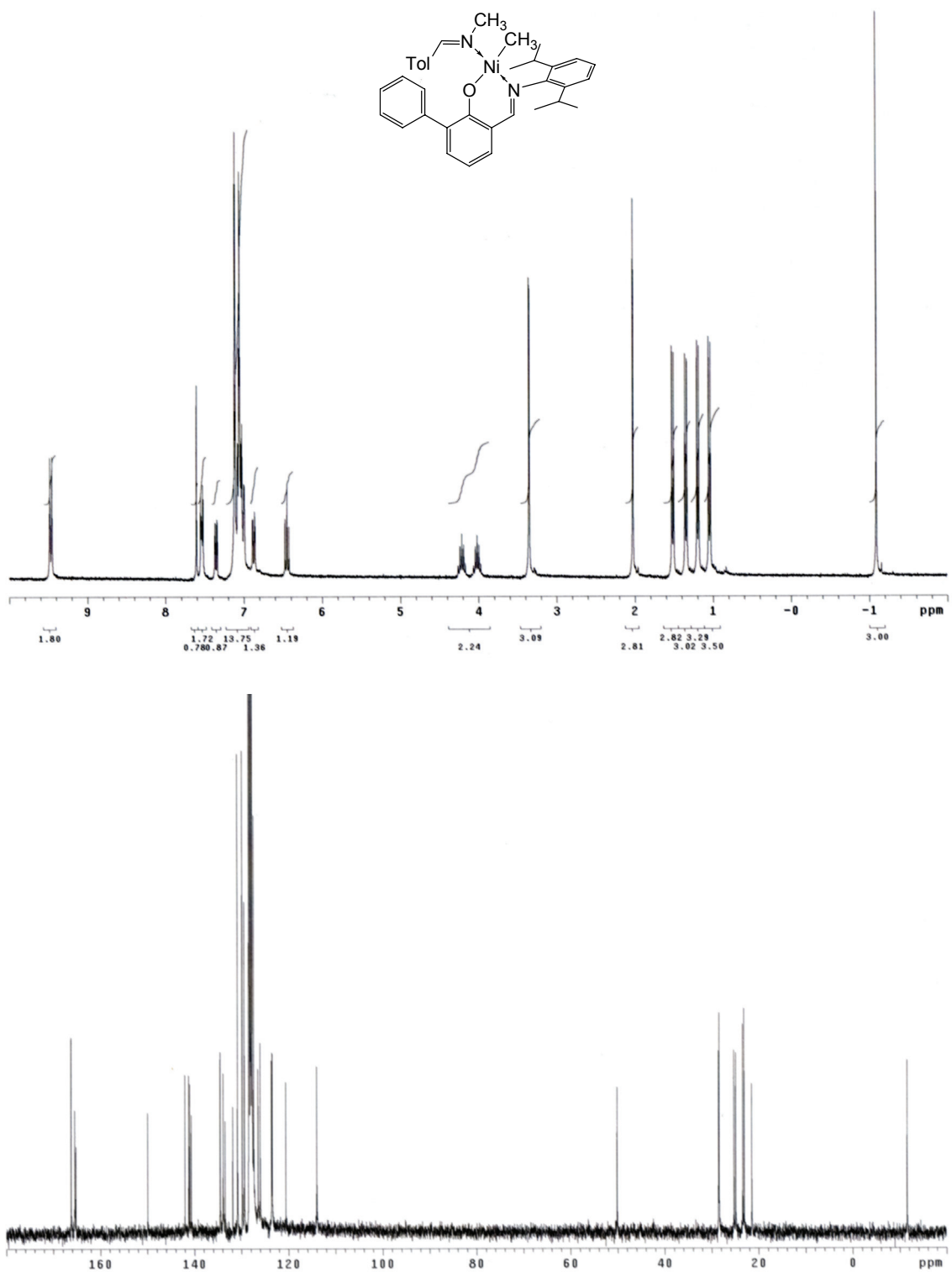
**$^1\text{H}$  and  $^{13}\text{C}$  NMR spectra for Chapter 2**  
**Compounds 2.11a-m,p, 2.12a-d, 2.15a-d and 2.17a-d**

**$^1\text{H}$  and  $^{13}\text{C}$  NMR of (2.11a)**

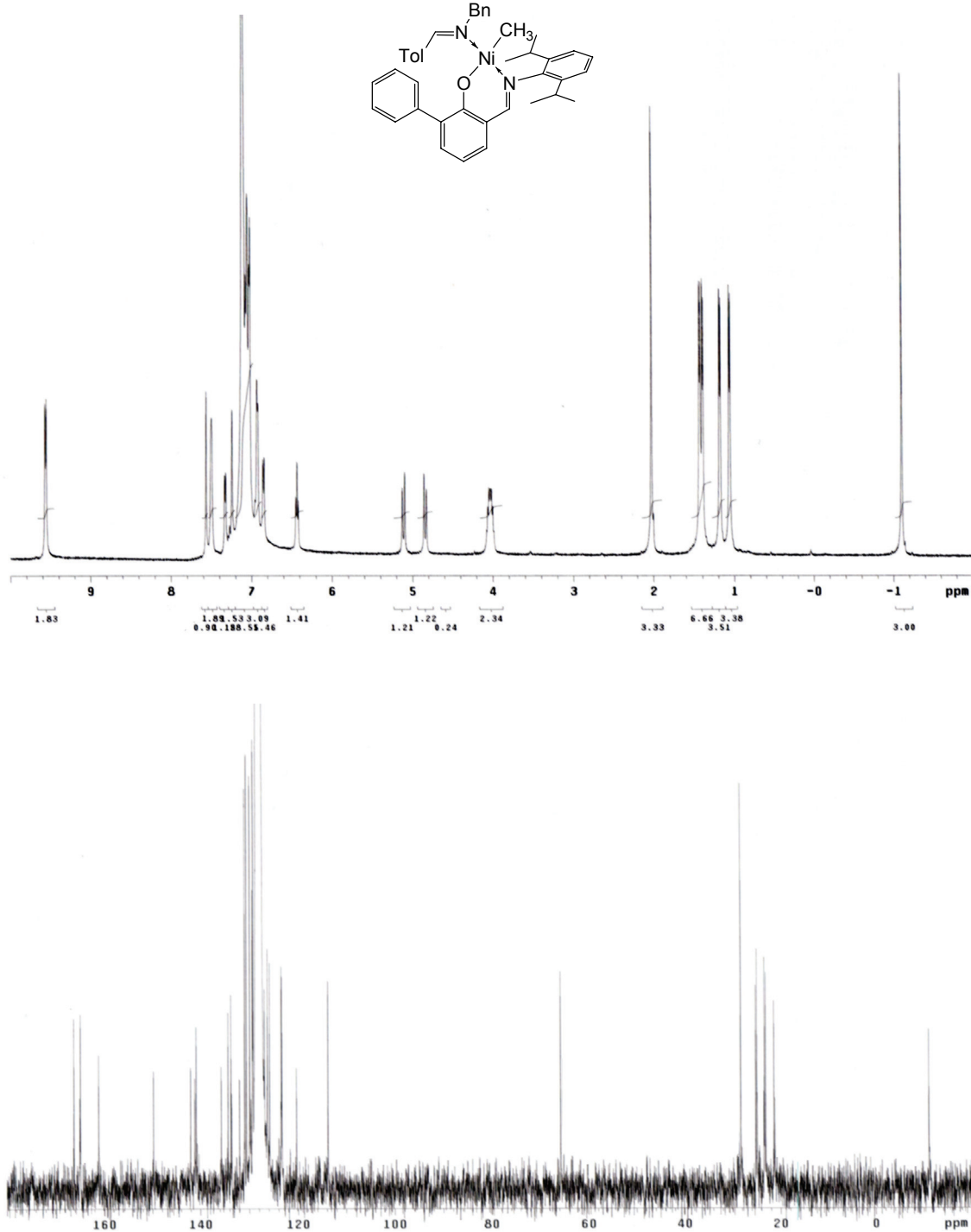
**(6-phenyl-2-((2,6-diisopropylphenyl)iminomethyl)phenoxy)Ni(CH<sub>3</sub>)(pyridine)**



**$^1\text{H}$  and  $^{13}\text{C}$  NMR of (2.11b)**  
**(6-phenyl-2-((2,6-diisopropylphenyl)iminomethyl)phenoxy)Ni(CH<sub>3</sub>)(N-methyl**  
**tolualdimine)**

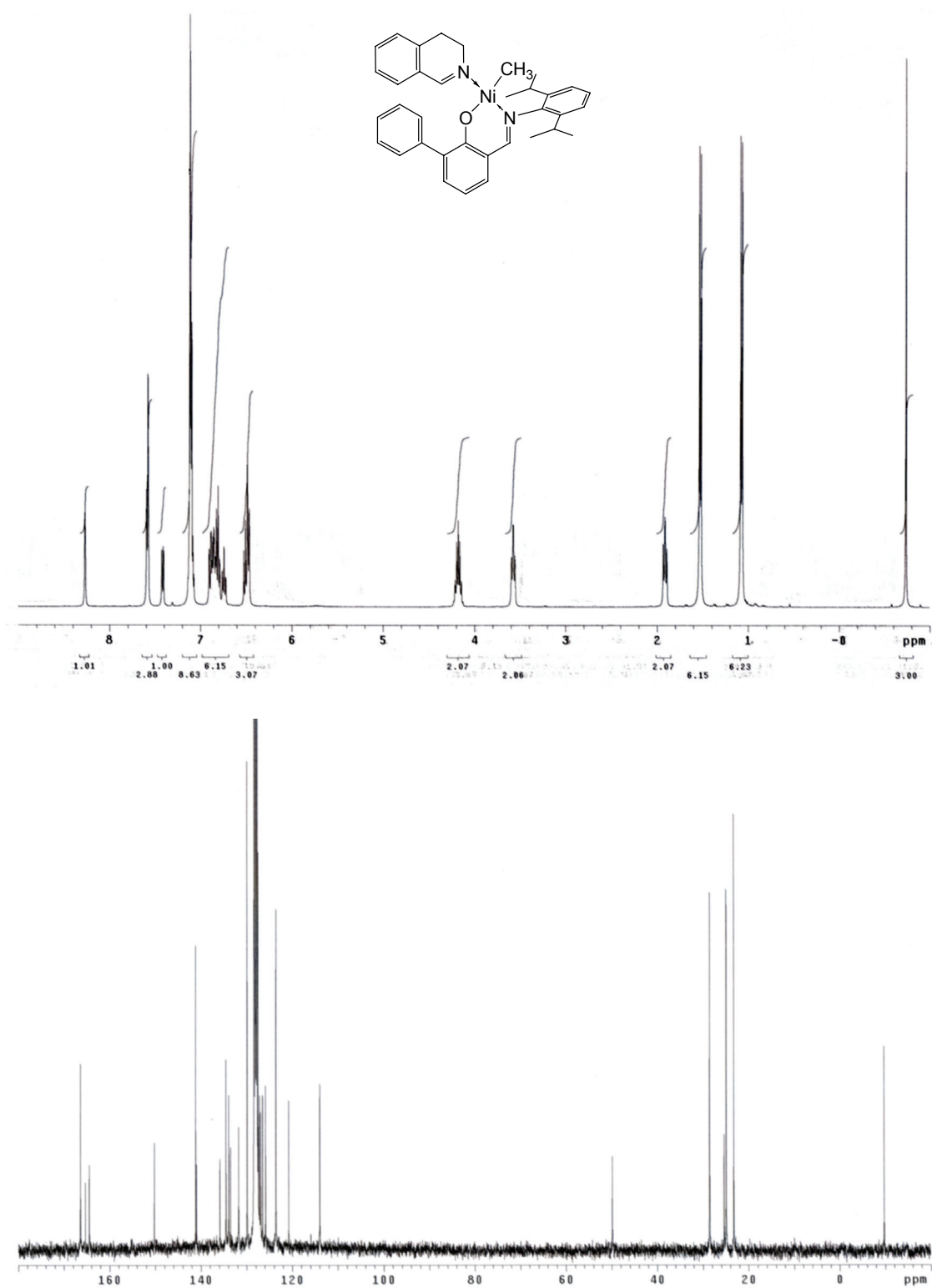


**$^1\text{H}$  and  $^{13}\text{C}$  NMR of (2.11c)**  
**(6-phenyl-2-((2,6-diisopropylphenyl)iminomethyl)phenoxy)Ni(CH<sub>3</sub>)(N-benzyl**  
**tolualdimine)**

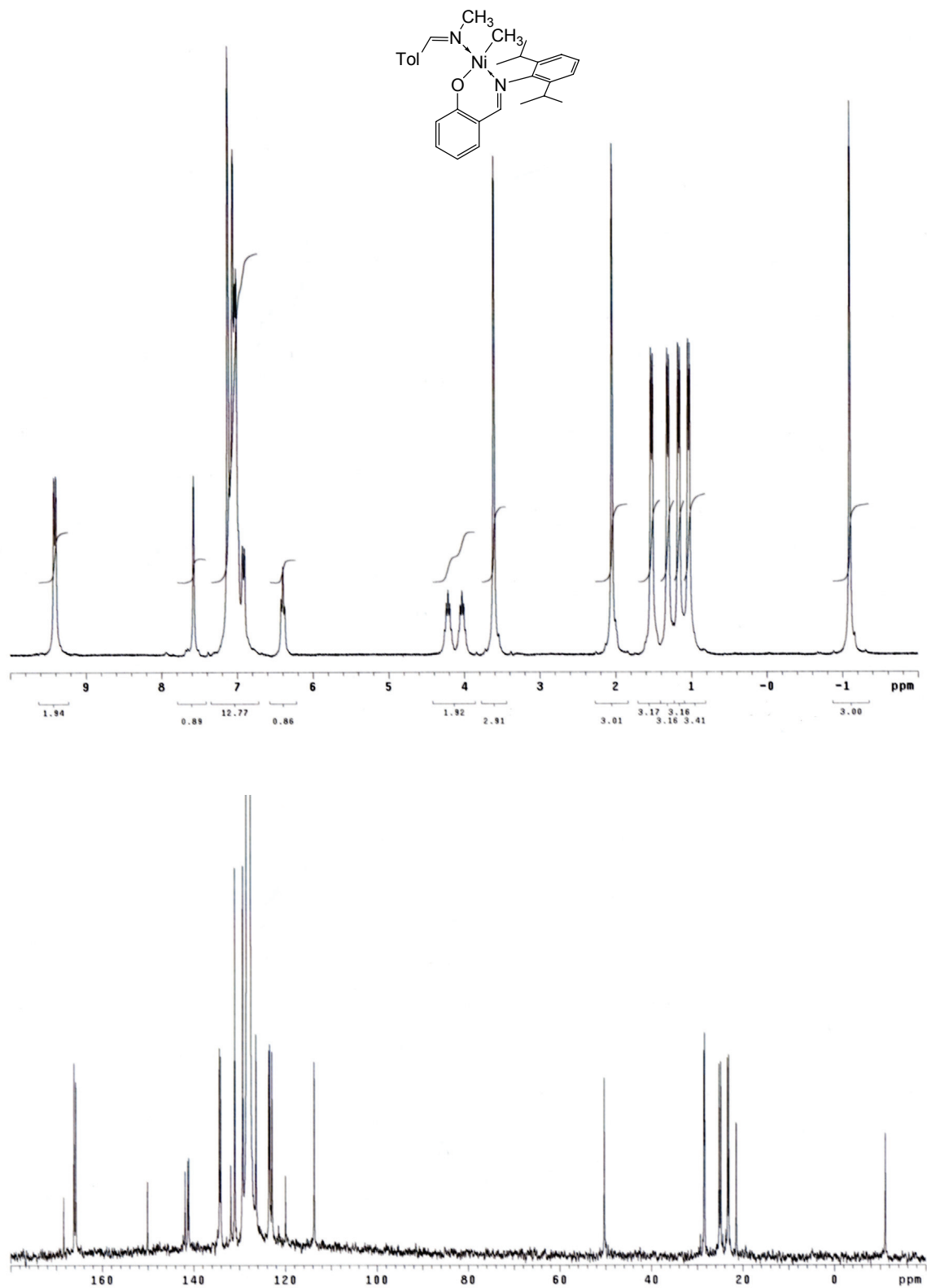




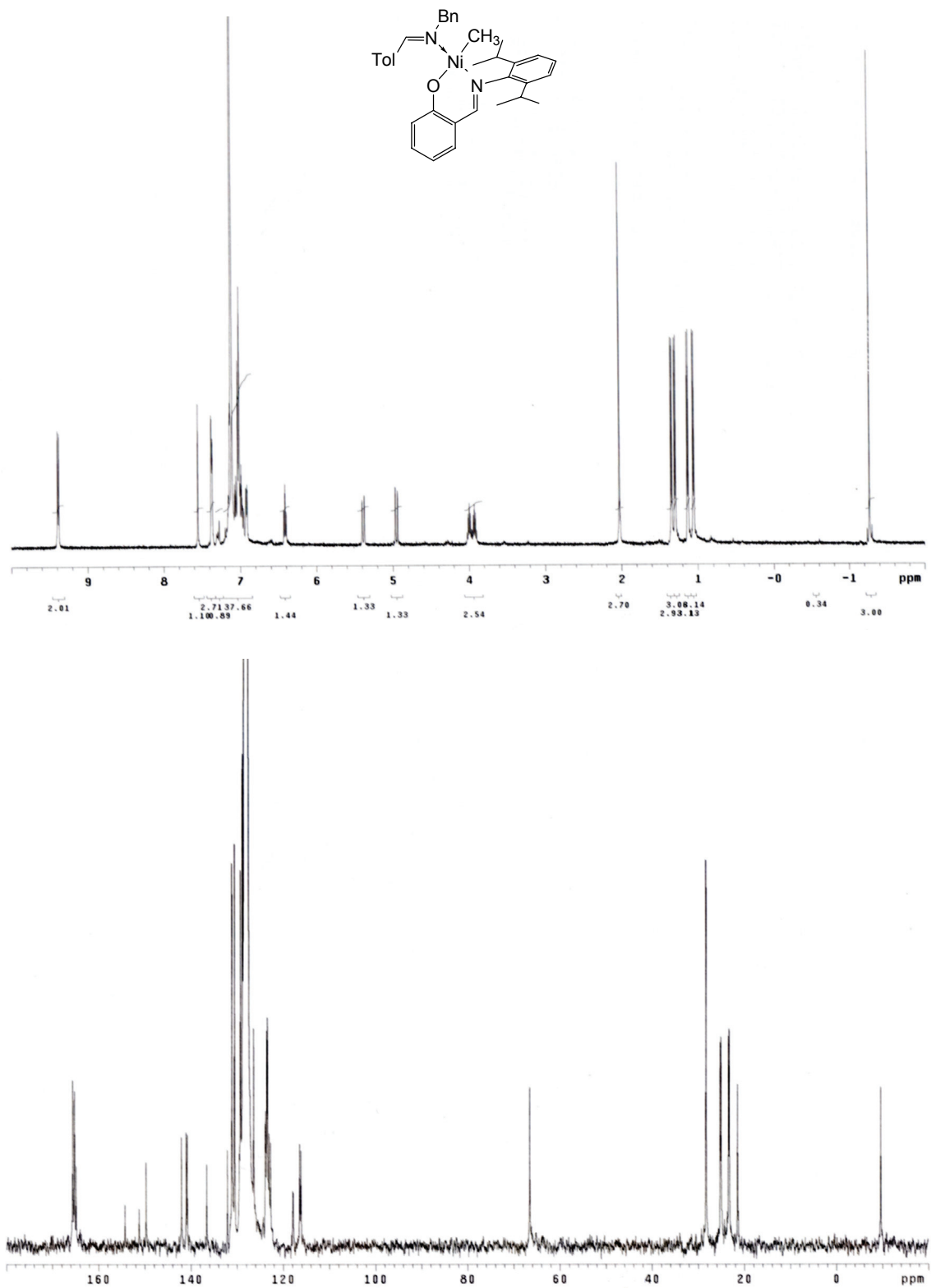
**$^1\text{H}$  and  $^{13}\text{C}$  NMR of (2.11d)**  
**(6-phenyl-2-((2,6-diisopropylphenyl)iminomethyl)phenoxy)Ni(CH<sub>3</sub>)(3,4-**  
**dihydroisoquinoline)**



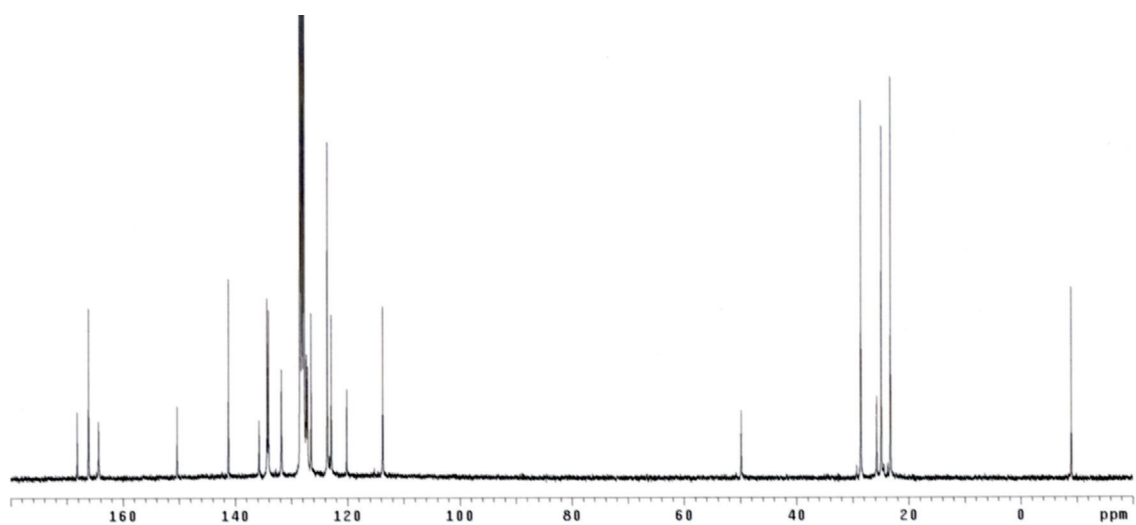
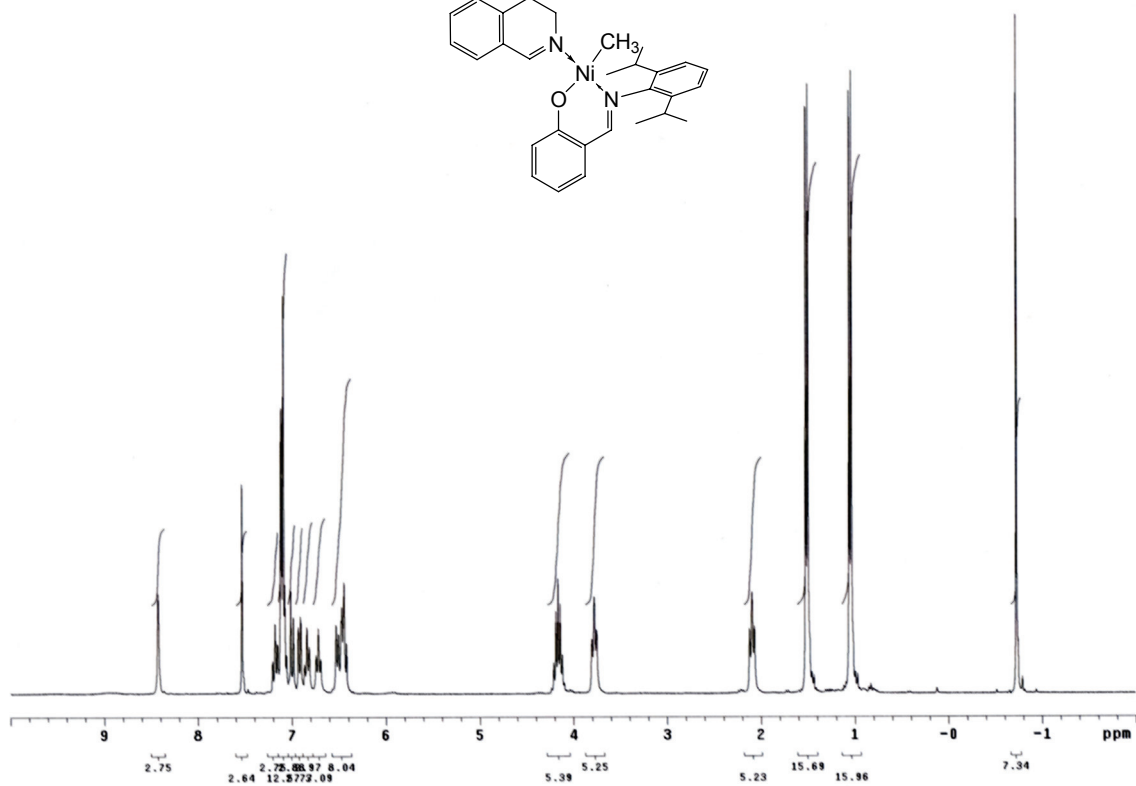
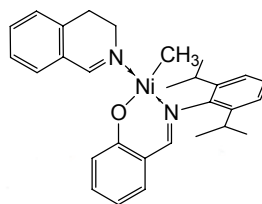
**$^1\text{H}$  and  $^{13}\text{C}$  NMR of (2.11e)**  
**(2-((2,6-diisopropylphenyl)iminomethyl)phenoxy)Ni(CH<sub>3</sub>)(*N*-methyl tolualdimine)**



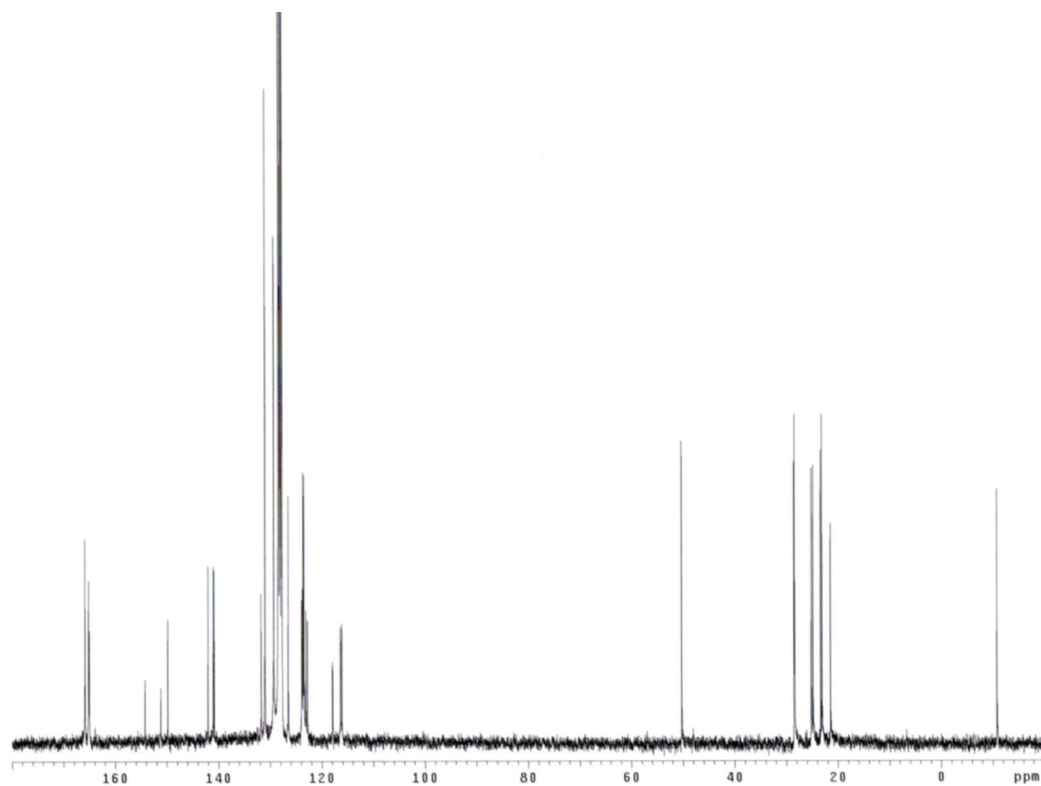
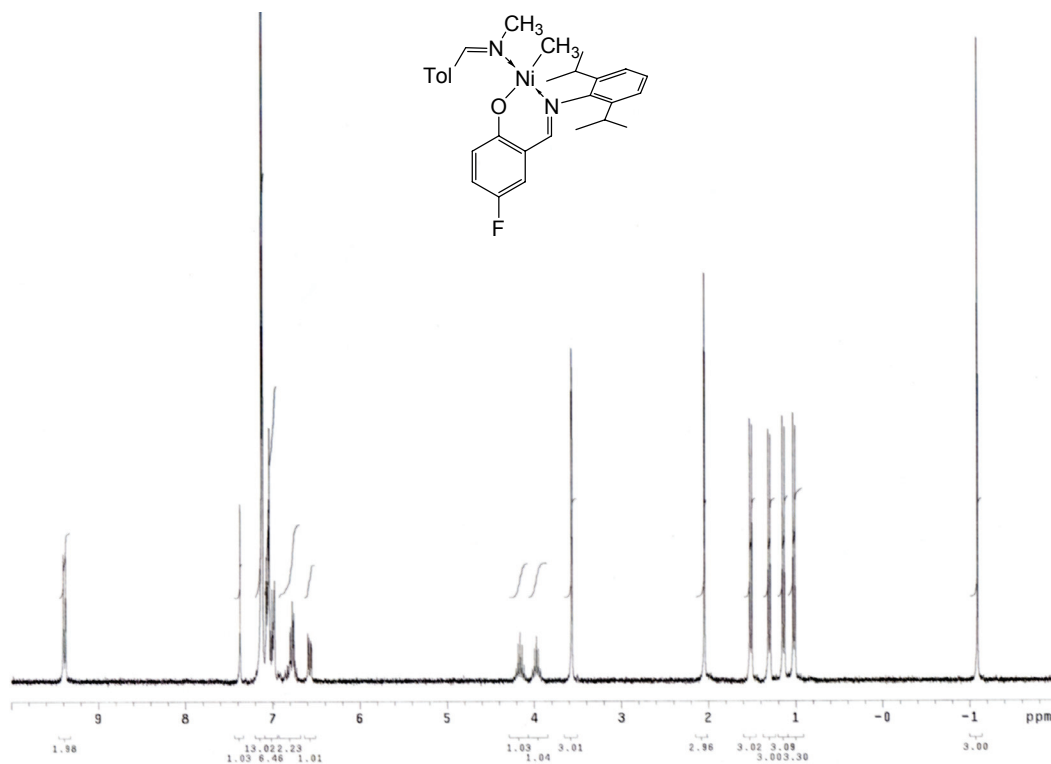
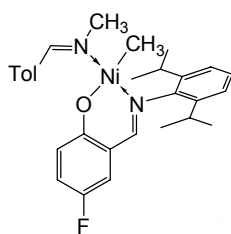
**$^1\text{H}$  and  $^{13}\text{C}$  NMR of (2.11f)**  
**(2-((2,6-diisopropylphenyl)iminomethyl)phenoxy)Ni(CH<sub>3</sub>)(N-benzyl tolualdimine)**



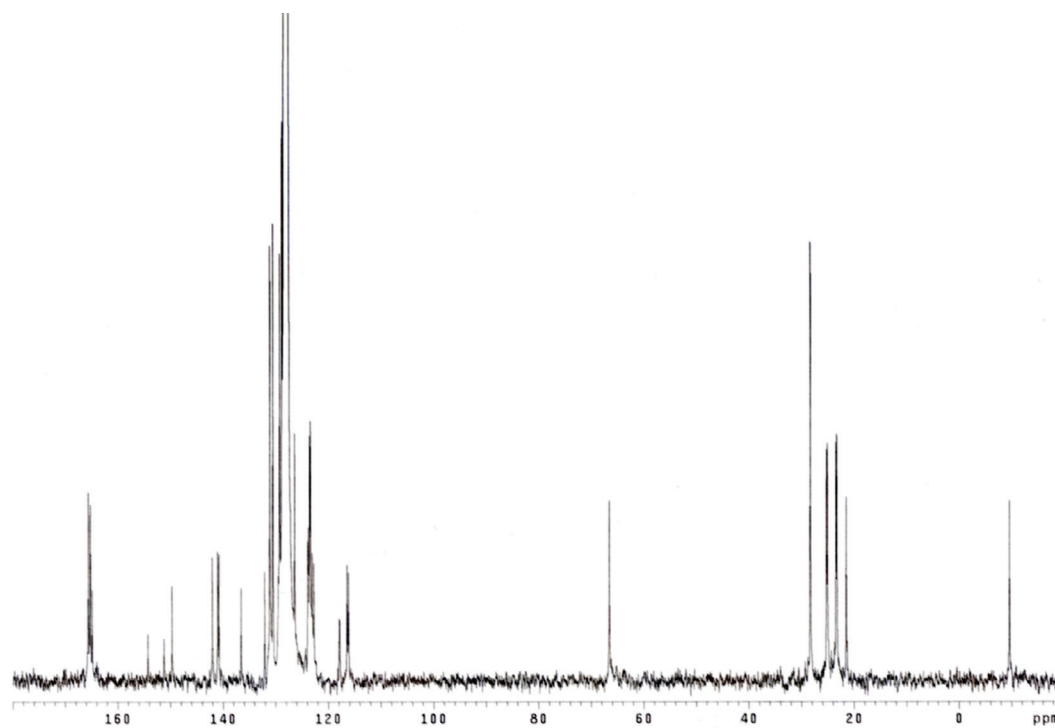
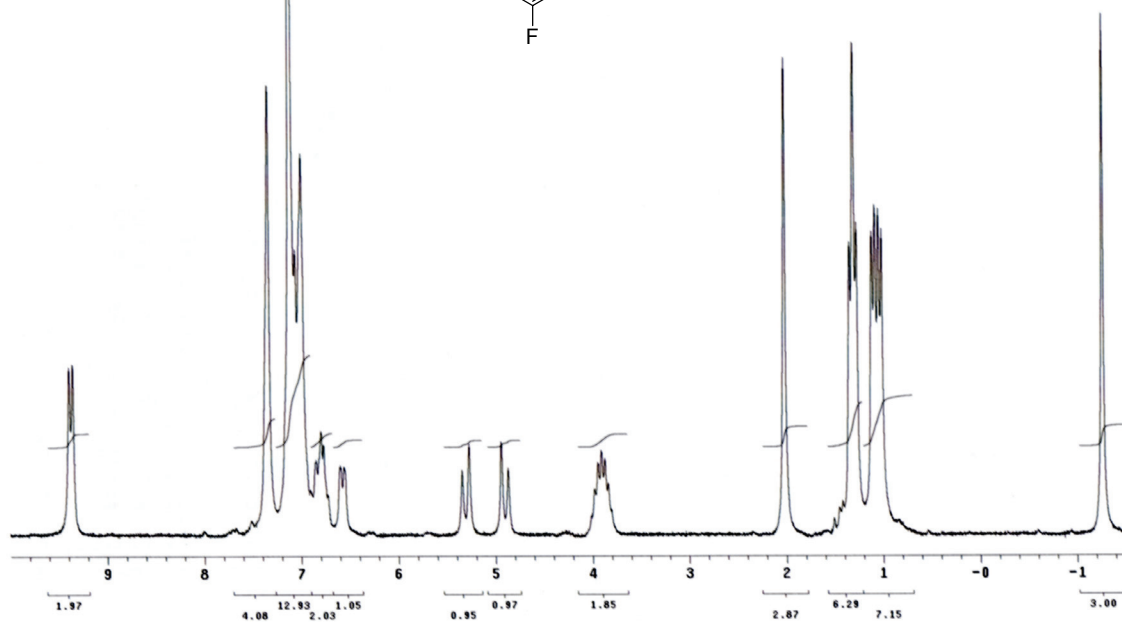
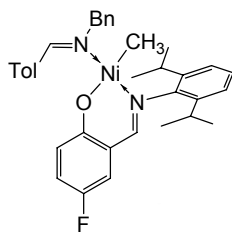
**$^1\text{H}$  and  $^{13}\text{C}$  NMR of (2.11g)**  
**(2-((2,6-diisopropylphenyl)iminomethyl)phenoxy)Ni(CH<sub>3</sub>)(3,4-**  
**dihydroisoquinoline)**



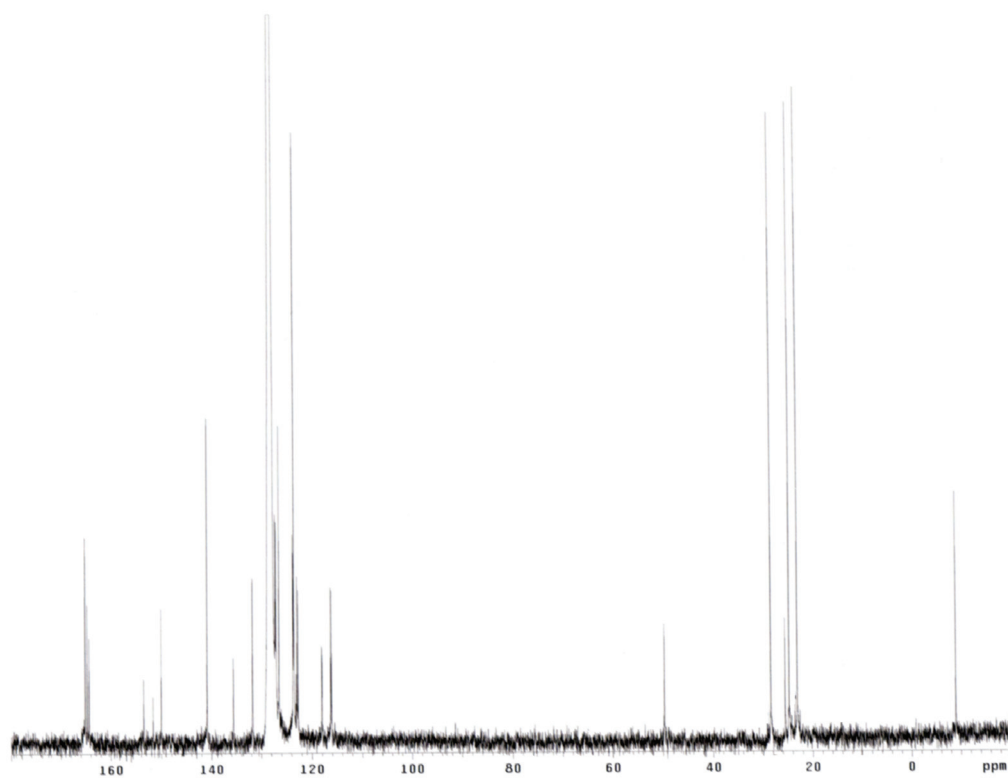
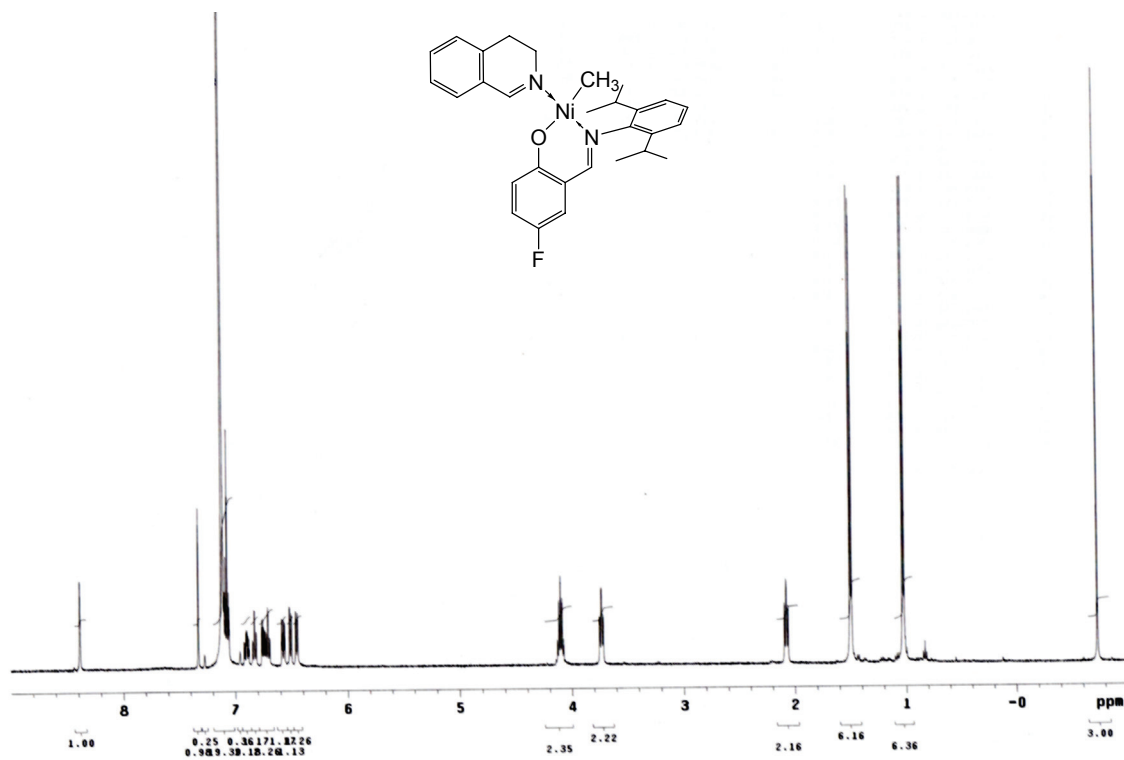
**$^1\text{H}$  and  $^{13}\text{C}$  NMR of (2.11h)**  
**(4-fluoro-2-((2,6-diisopropylphenyl)iminomethyl)phenoxy)Ni(CH<sub>3</sub>)(N-methyl**  
**tolualdimine)**



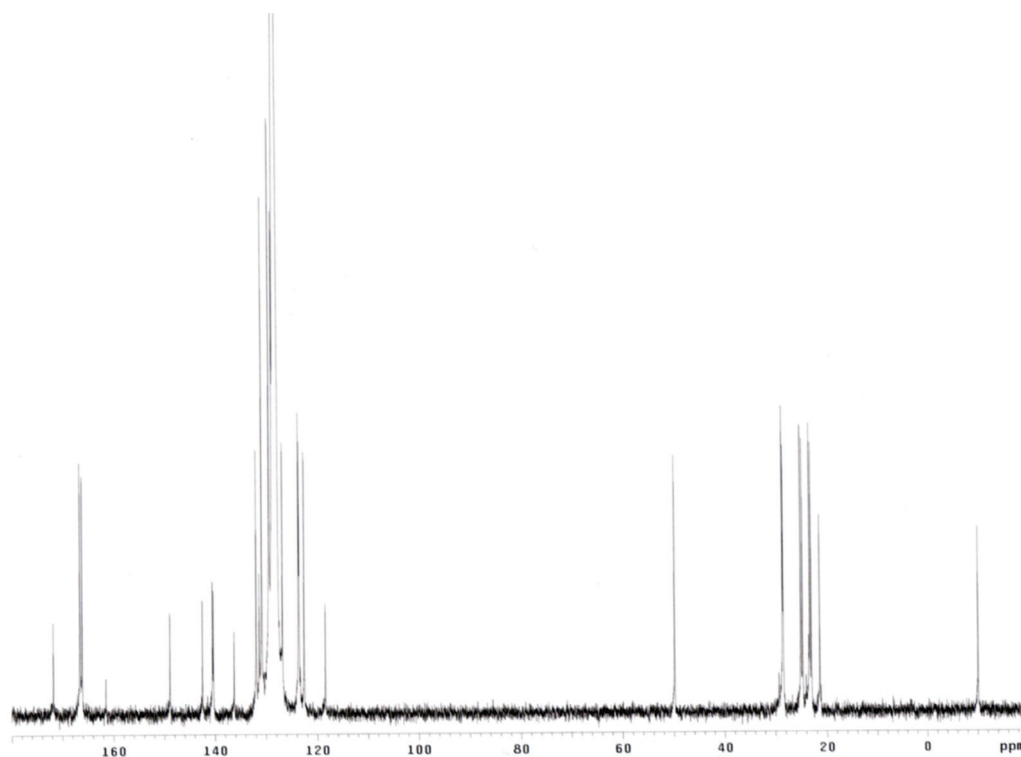
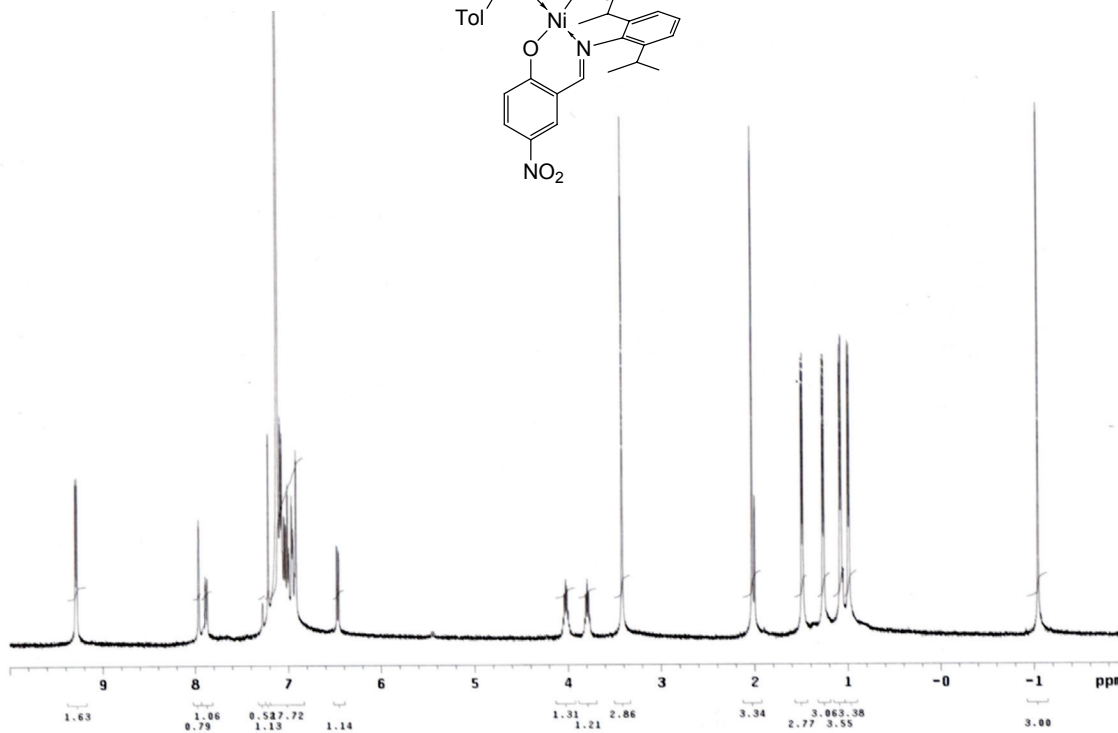
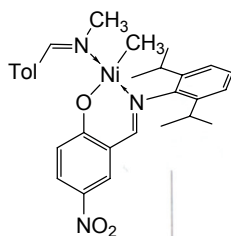
**$^1\text{H}$  and  $^{13}\text{C}$  NMR of (2.11i)**  
**(4-fluoro-2-((2,6-diisopropylphenyl)iminomethyl)phenoxy)Ni(CH<sub>3</sub>)(N-benzyl**  
**tolualdimine)**



**<sup>1</sup>H and <sup>13</sup>C NMR of (2.11j)**  
**(4-fluoro-2-((2,6-diisopropylphenyl)iminomethyl)phenoxy)Ni(CH<sub>3</sub>)(3,4-**  
**dihydroisoquinoline)**

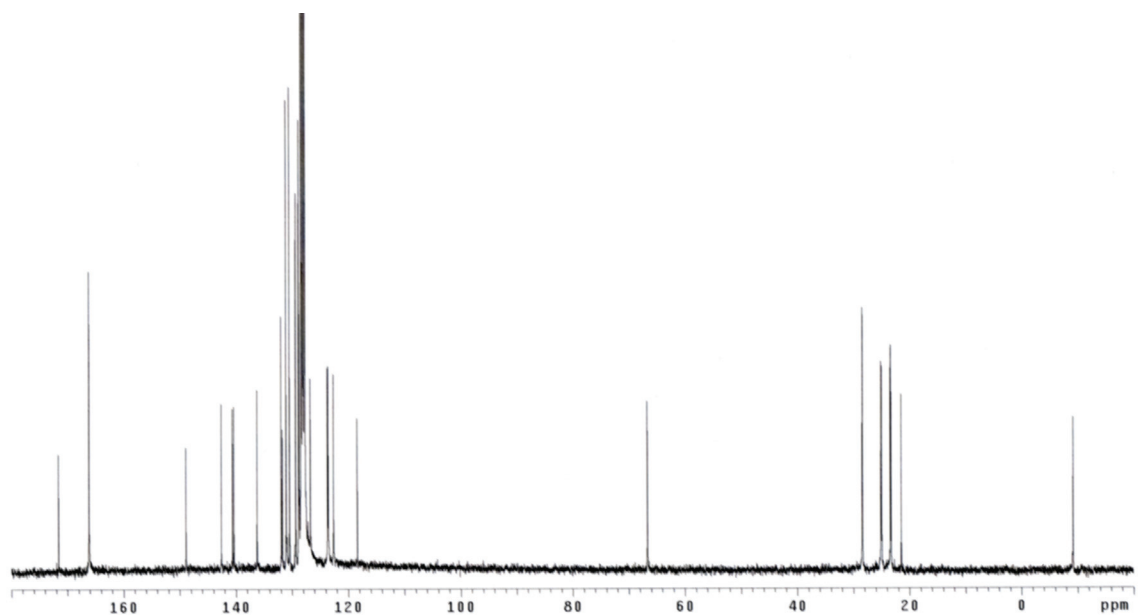
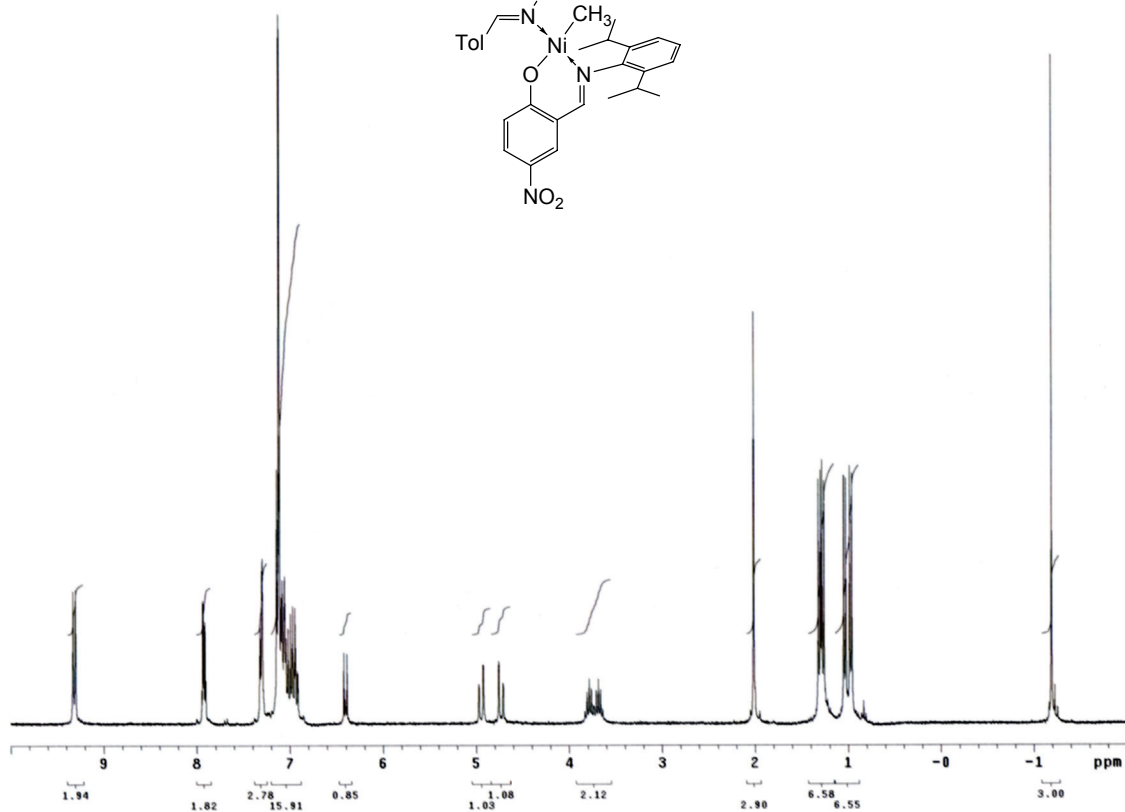
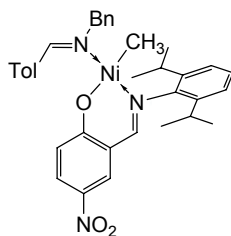


**$^1\text{H}$  and  $^{13}\text{C}$  NMR of (2.11k)**  
**(4-nitro-2-((2,6-diisopropylphenyl)iminomethyl)phenoxy)Ni(CH<sub>3</sub>)(N-methyl**  
**tolualdimine)**

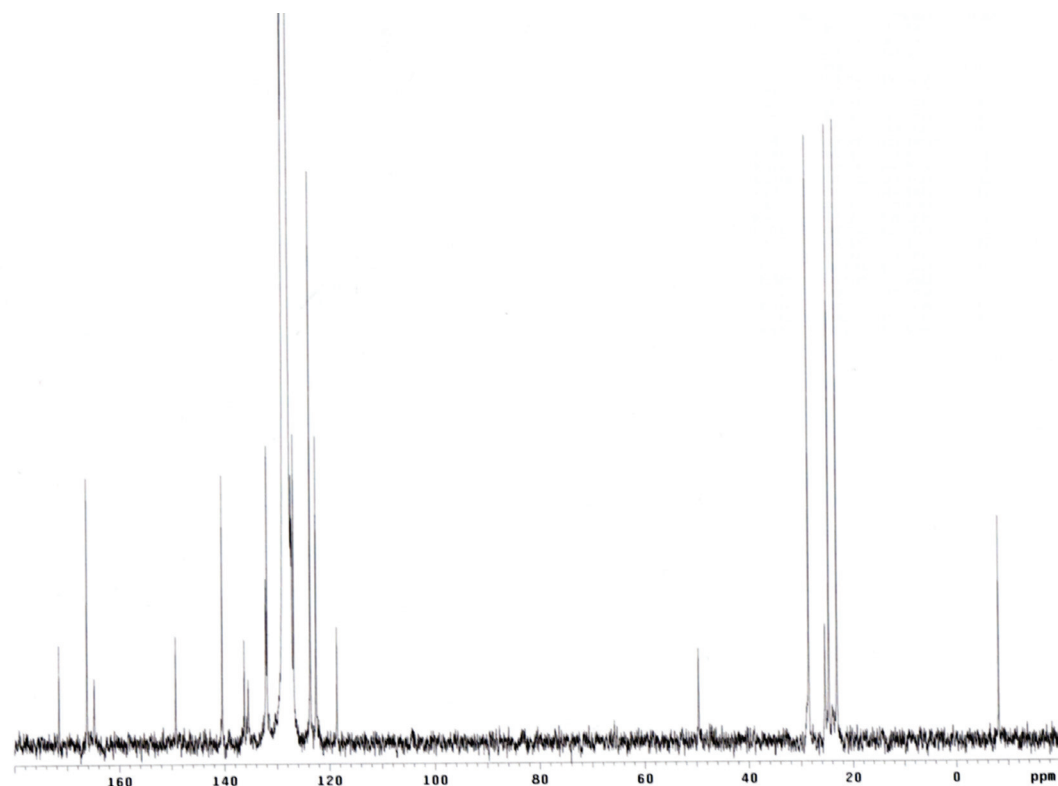
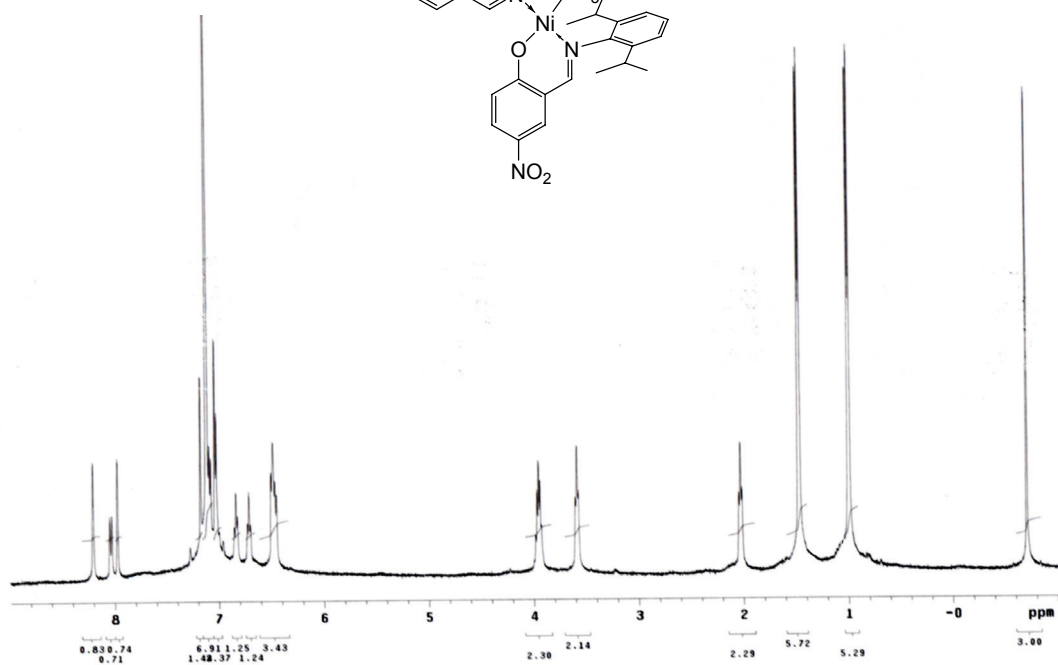
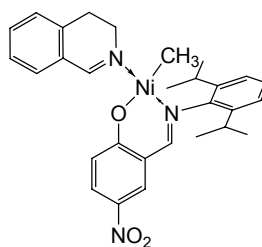




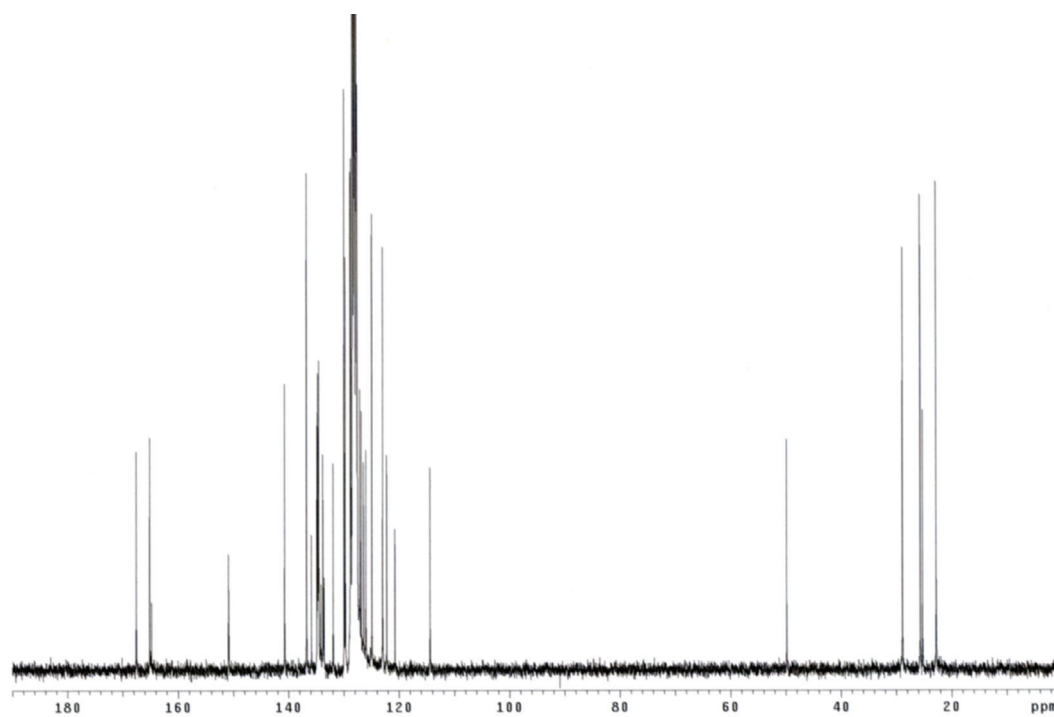
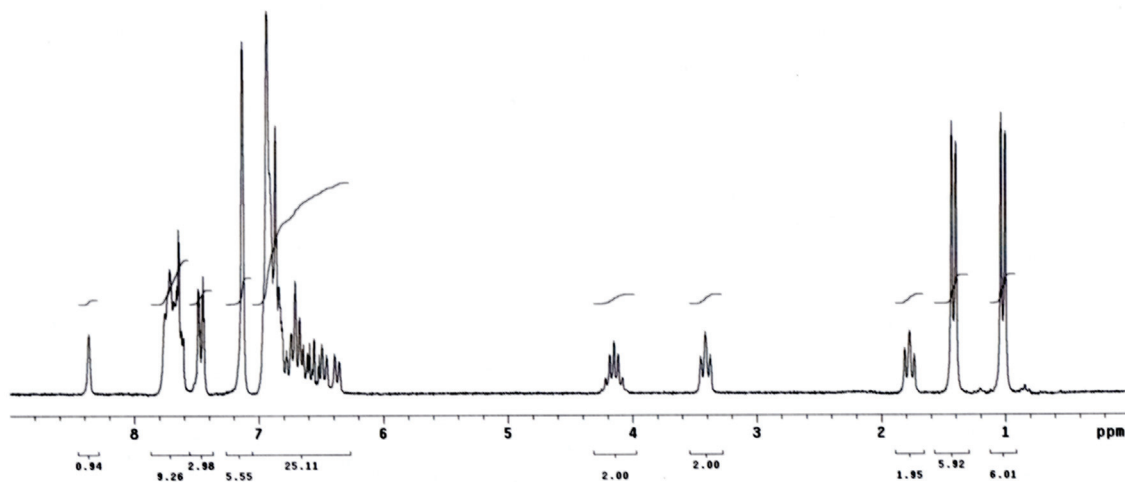
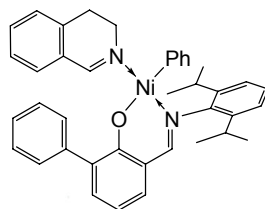
**$^1\text{H}$  and  $^{13}\text{C}$  NMR of (2.11l)**  
**(4-nitro-2-((2,6-diisopropylphenyl)iminomethyl)phenoxy)Ni(CH<sub>3</sub>)(N-benzyl**  
**tolualdimine)**



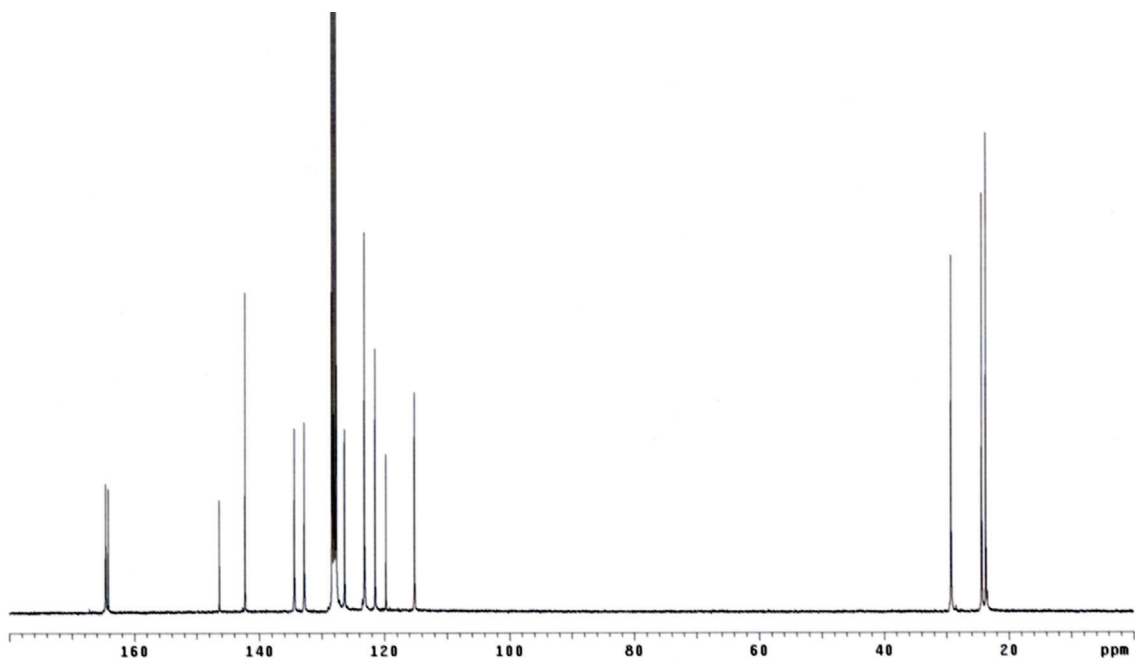
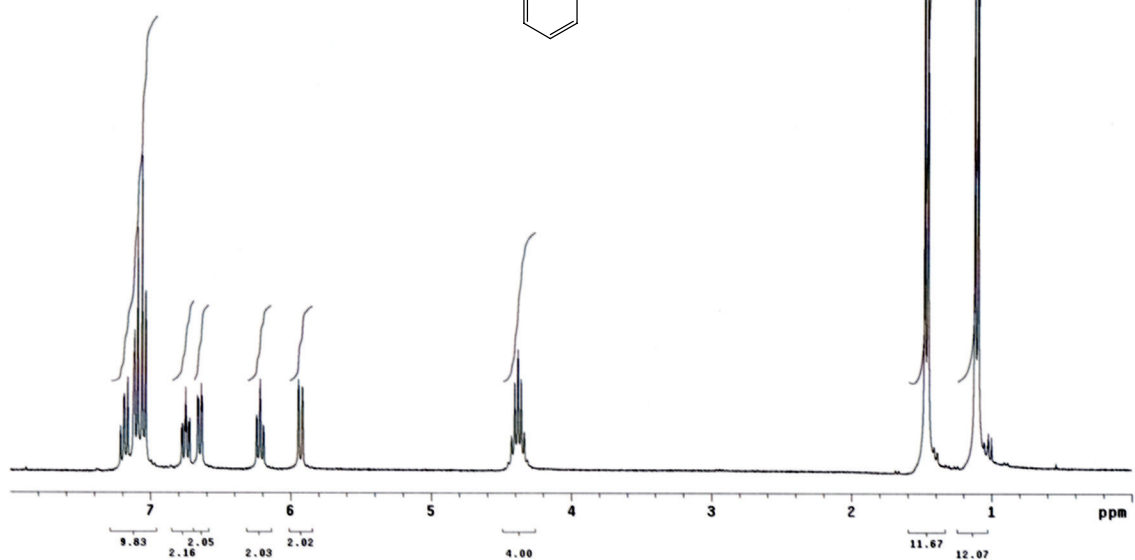
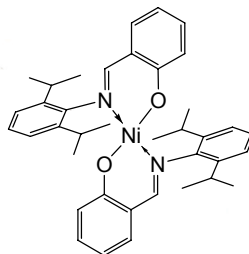
**$^1\text{H}$  and  $^{13}\text{C}$  NMR of (2.11m)**  
**(4-nitro-2-((2,6-diisopropylphenyl)iminomethyl)phenoxy)Ni(CH<sub>3</sub>)(3,4-**  
**dihydroisoquinoline)**



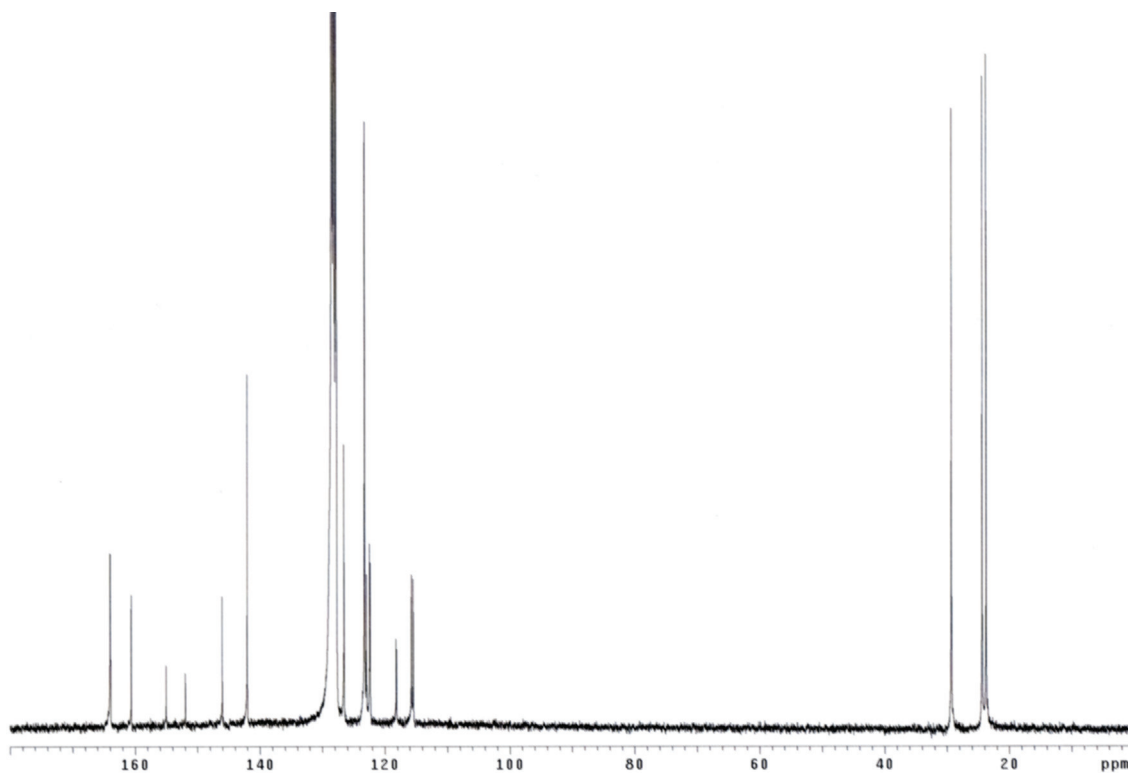
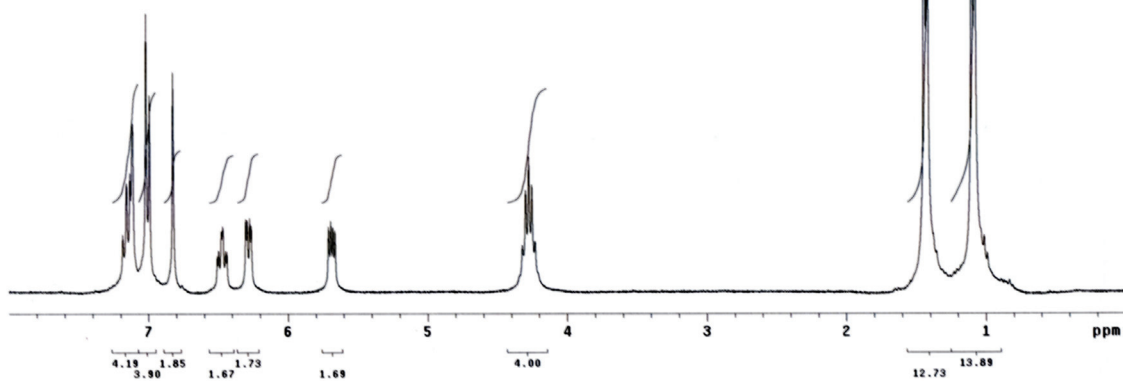
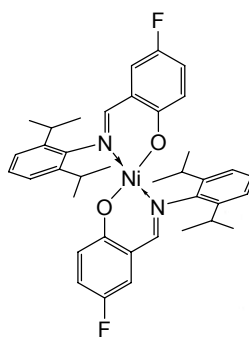
**$^1\text{H}$  and  $^{13}\text{C}$  NMR of (2.11p)**  
**(6-phenyl-2-((2,6-diisopropylphenyl)iminomethyl)phenoxy)Ni(Ph)(3,4-**  
**dihydroisoquinoline)**



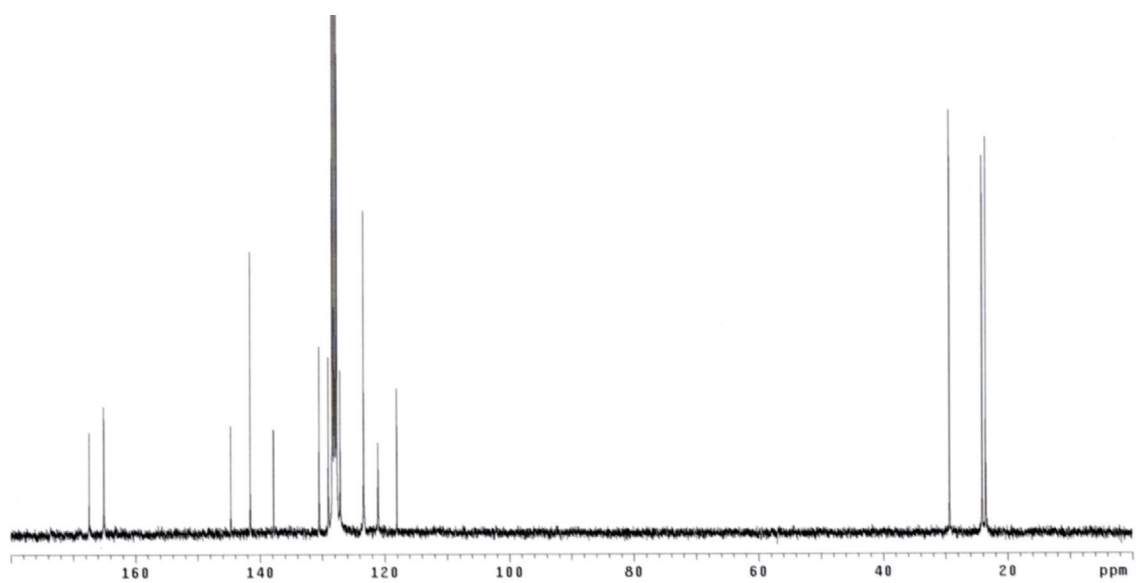
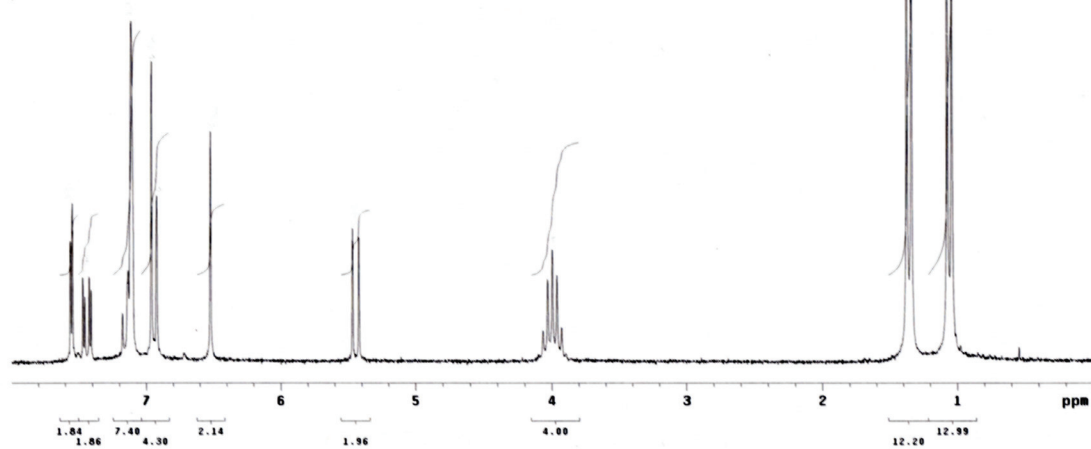
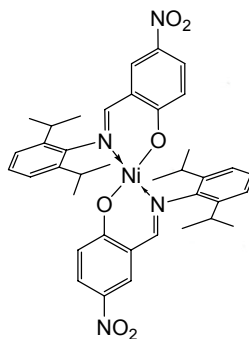
**$^1\text{H}$  and  $^{13}\text{C}$  NMR of (2.12b)**  
**bis(2-((2,6-diisopropylphenyl)iminomethyl)phenoxy)Ni**



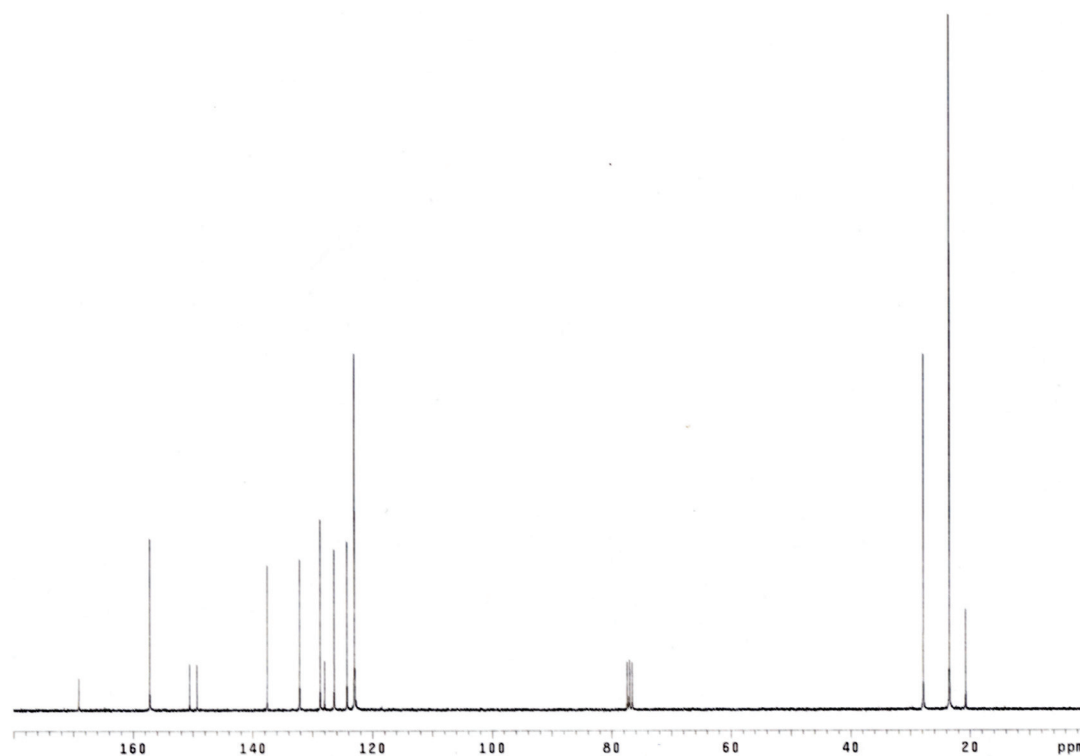
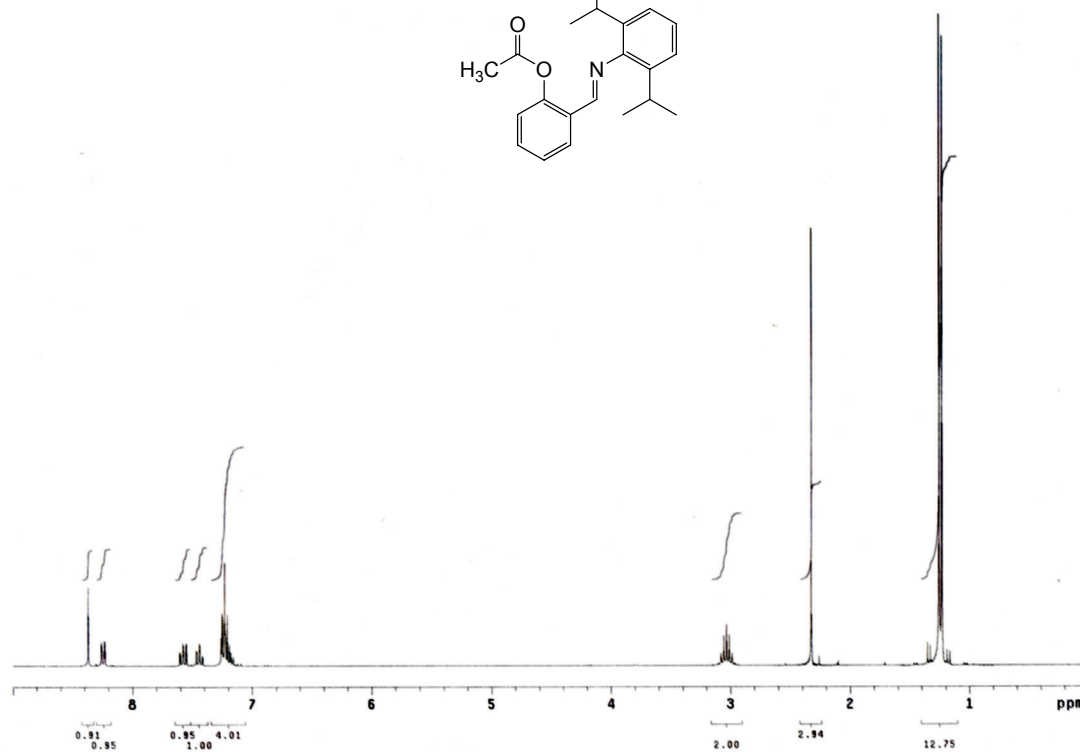
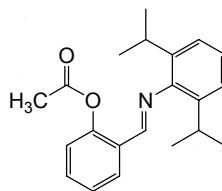
**$^1\text{H}$  and  $^{13}\text{C}$  NMR of (2.12c)**  
**bis(4-fluoro-2-((2,6-diisopropylphenyl)iminomethyl)phenoxy)Ni**



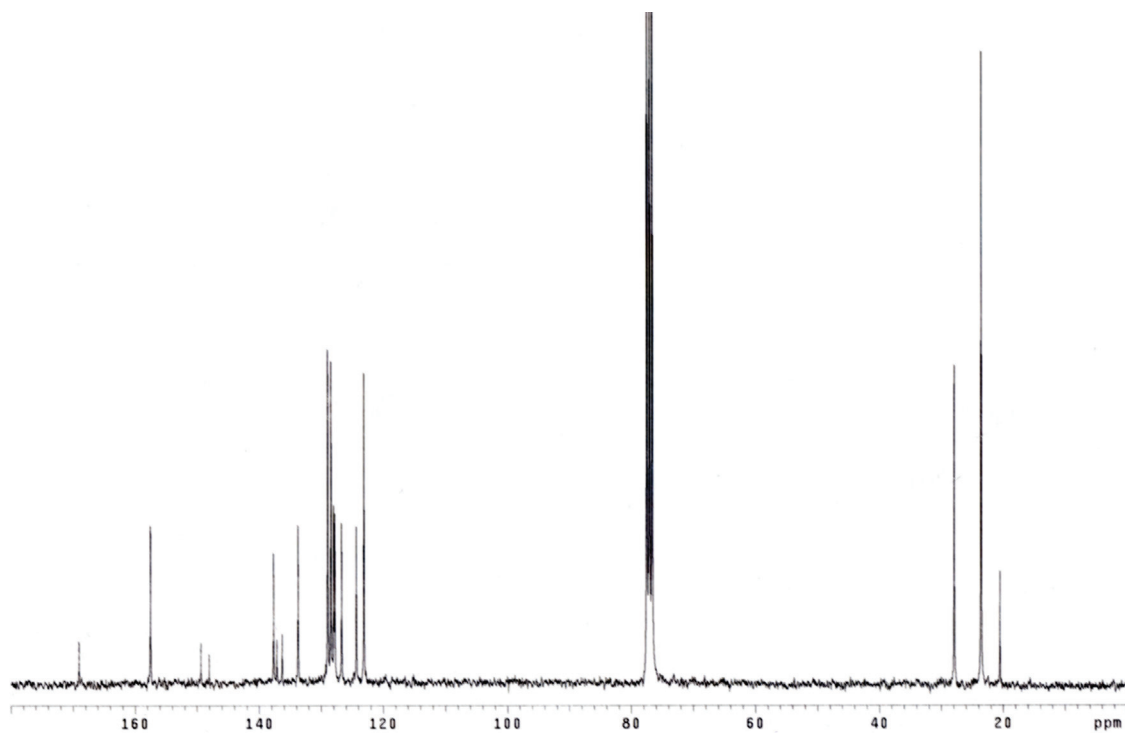
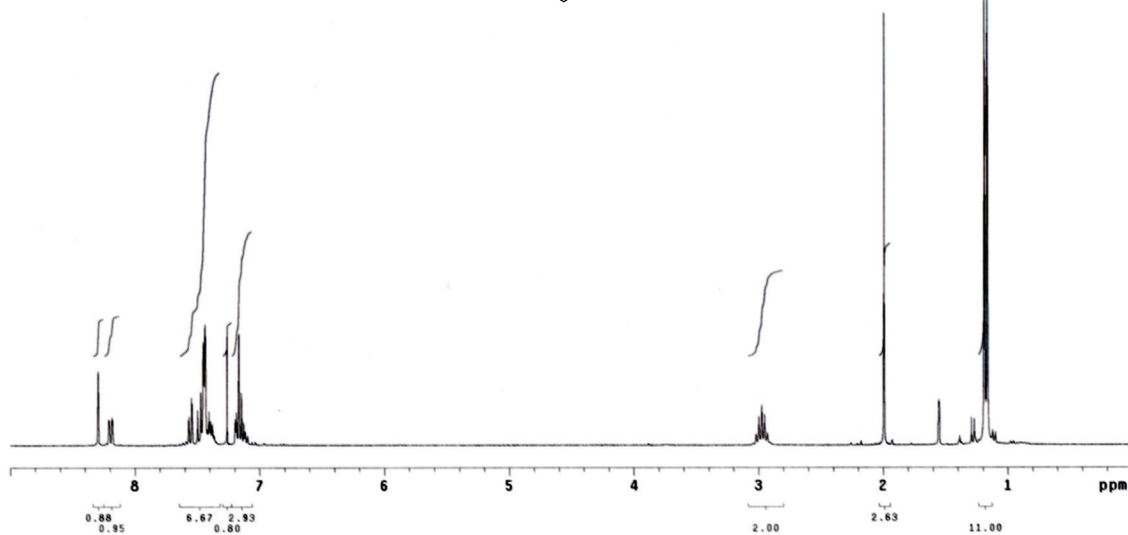
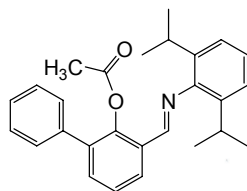
**$^1\text{H}$  and  $^{13}\text{C}$  NMR of (2.12d)**  
**bis(4-nitro-2-((2,6-diisopropylphenyl)iminomethyl)phenoxy)Ni**



**$^1\text{H}$  and  $^{13}\text{C}$  NMR of (2.15a)**  
**Acetic acid 3-((2,6-diisopropylphenyl)iminomethyl)-biphenyl-2-yl ester**

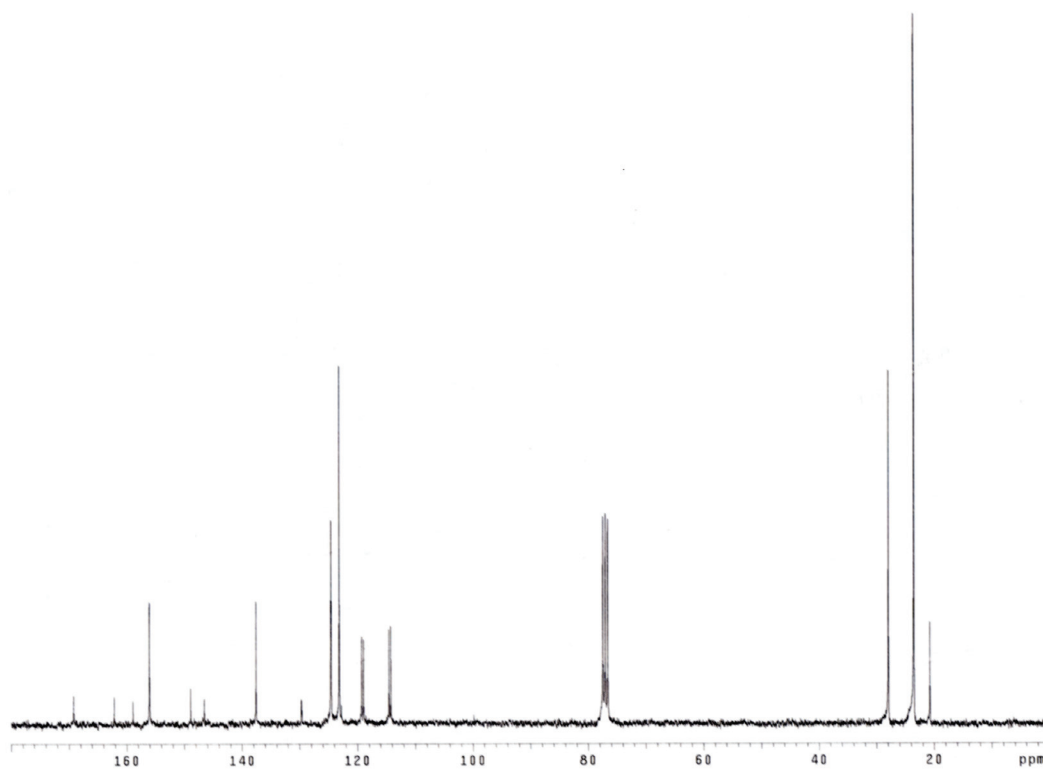
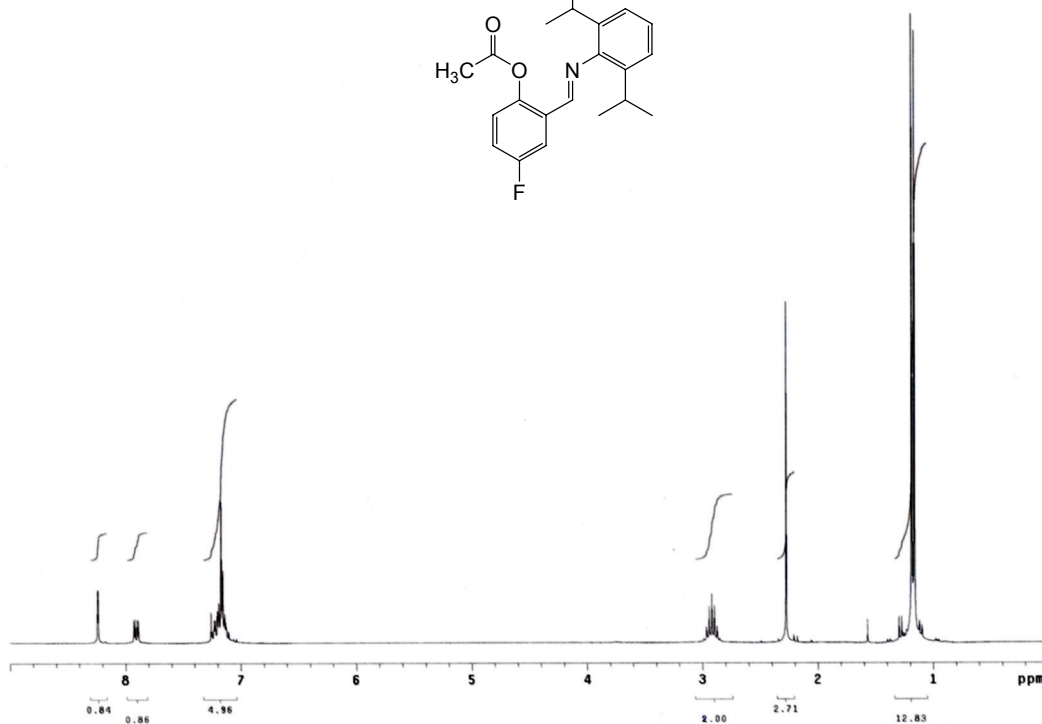
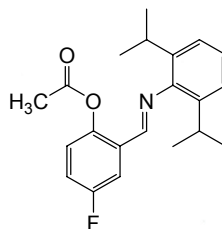


**<sup>1</sup>H and <sup>13</sup>C NMR of (2.15b)**  
**Acetic acid 2-((2,6-diisopropylphenyl)iminomethyl)-phenyl ester**

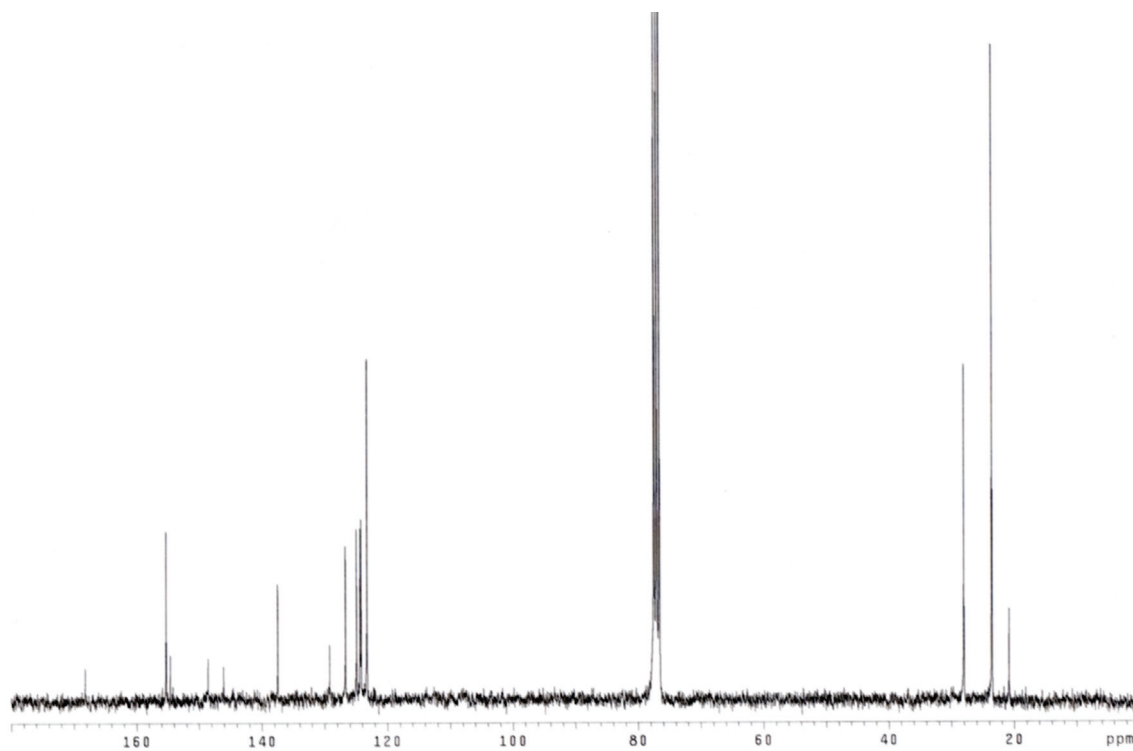
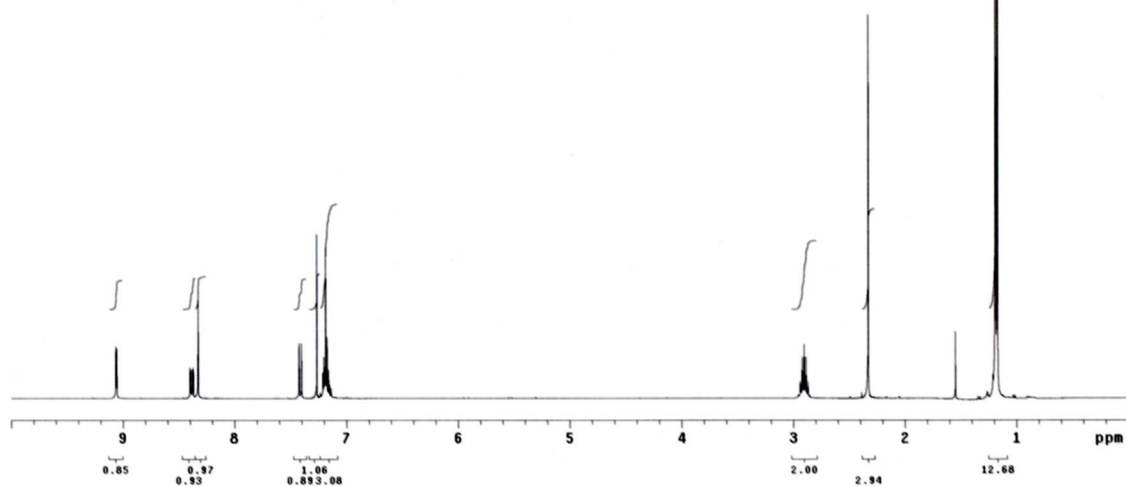
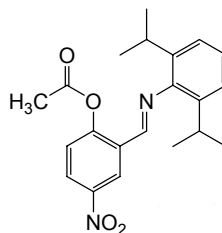




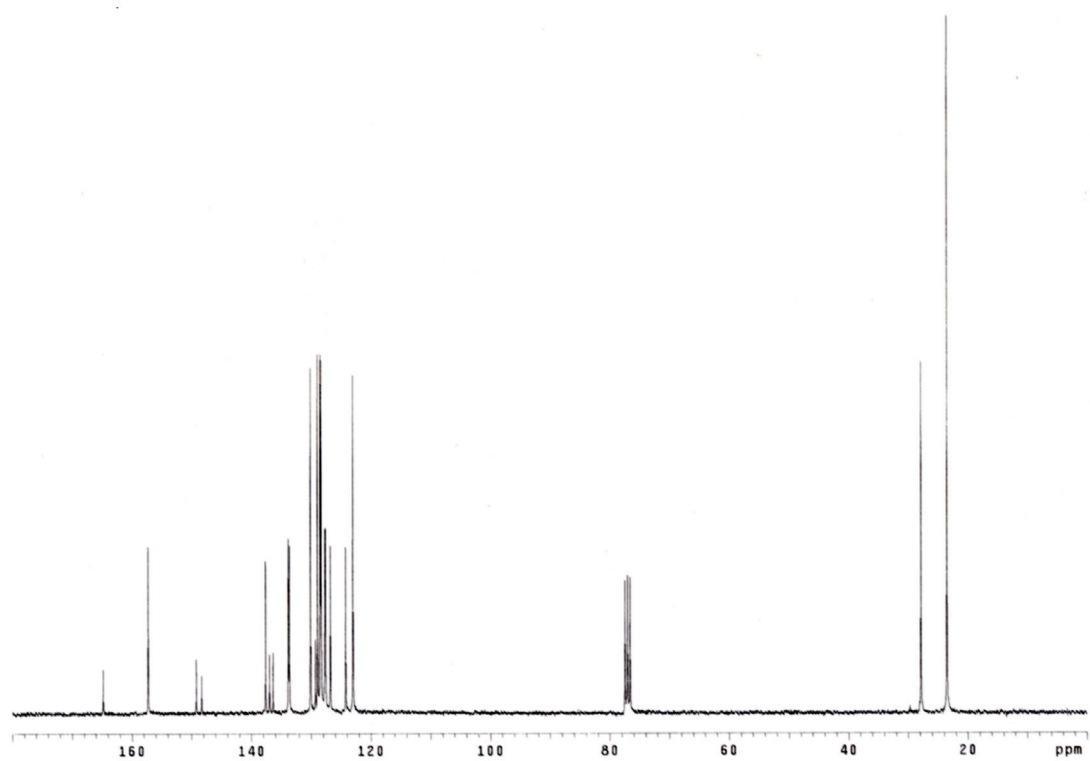
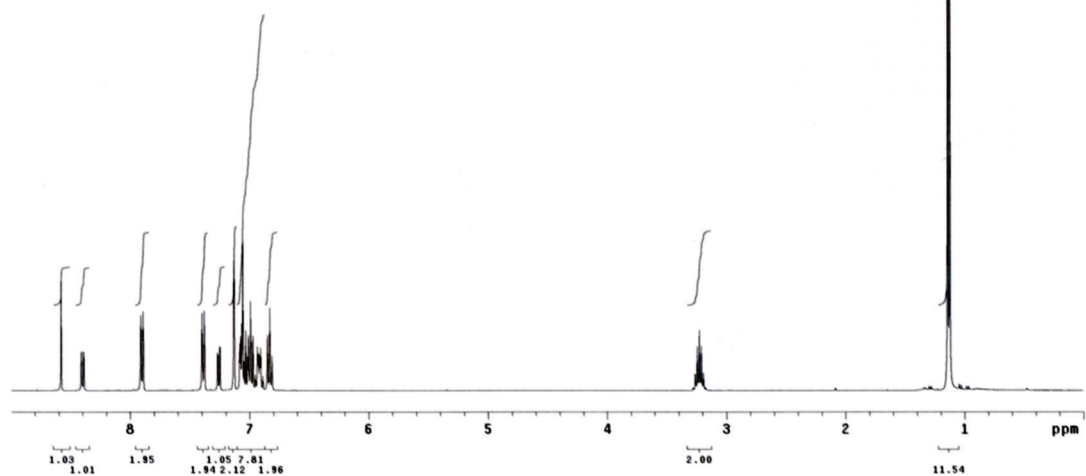
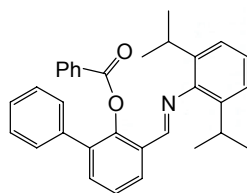
**<sup>1</sup>H and <sup>13</sup>C NMR of (2.15c)**  
**Acetic acid 2-((2,6-diisopropylphenyl)iminomethyl)-4-fluoro-phenyl ester**



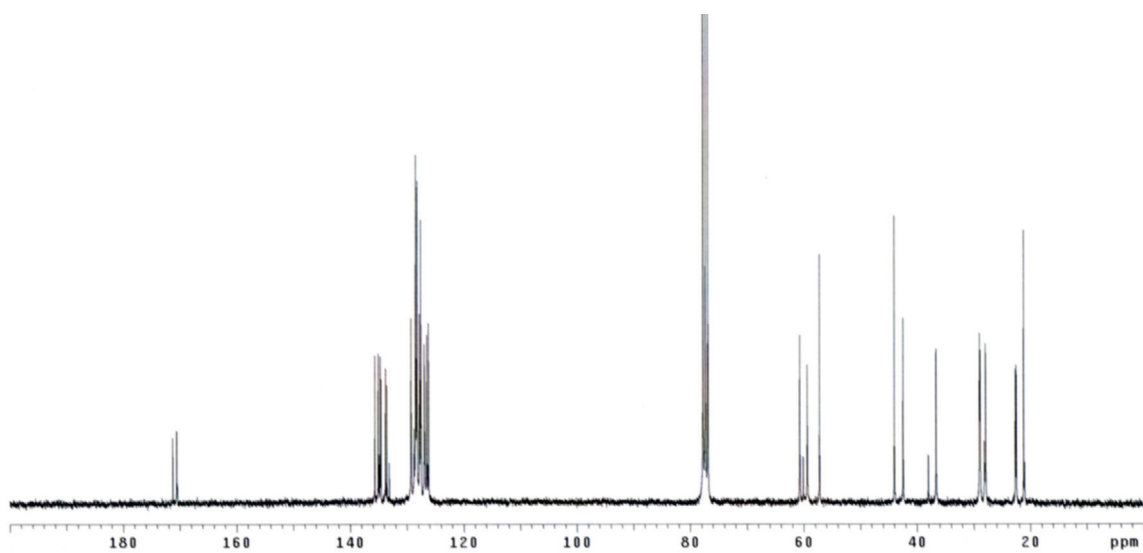
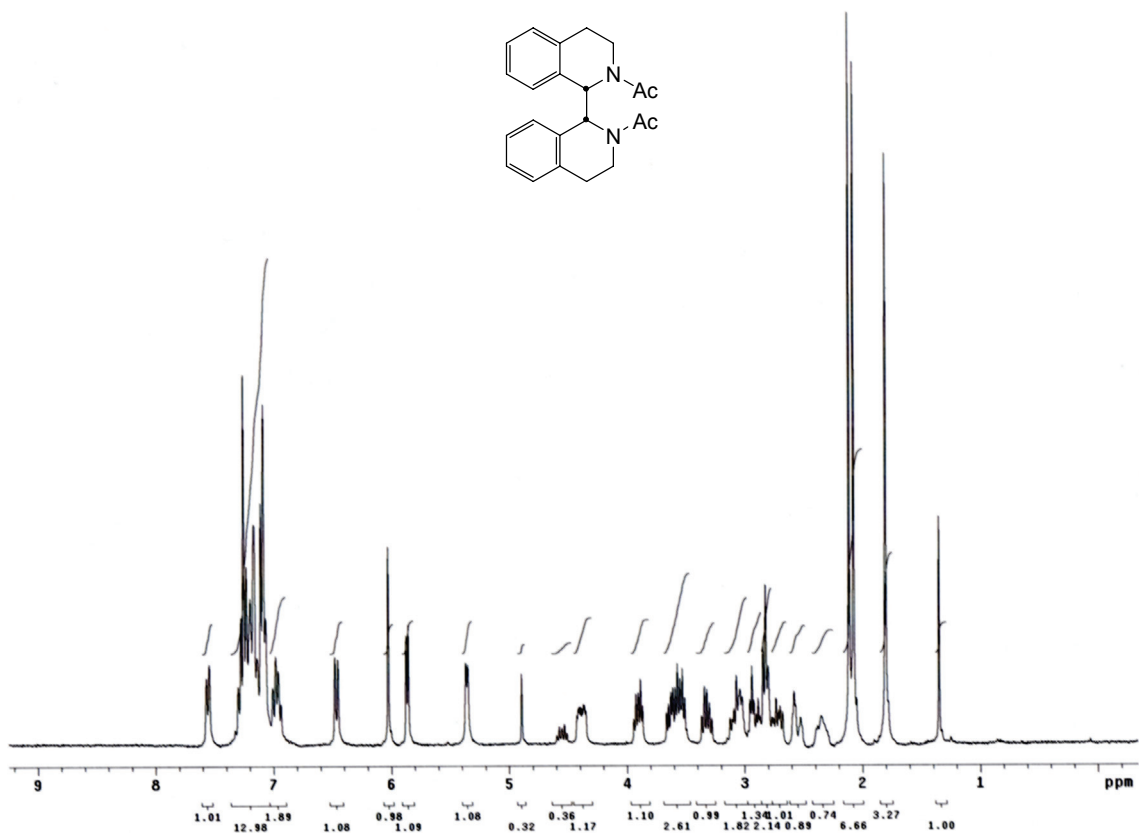
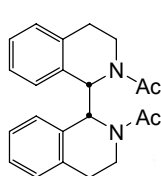
**$^1\text{H}$  and  $^{13}\text{C}$  NMR of (2.15d)**  
**Acetic acid 2-((2,6-diisopropylphenyl)iminomethyl)-4-nitro-phenyl ester**



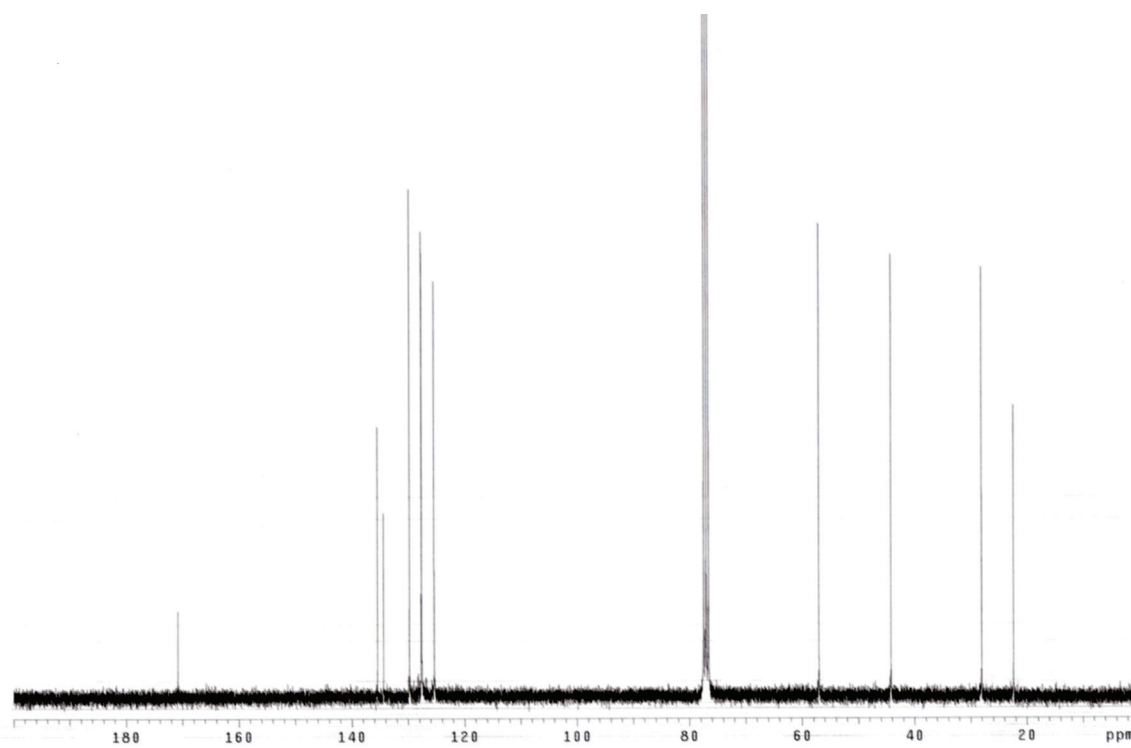
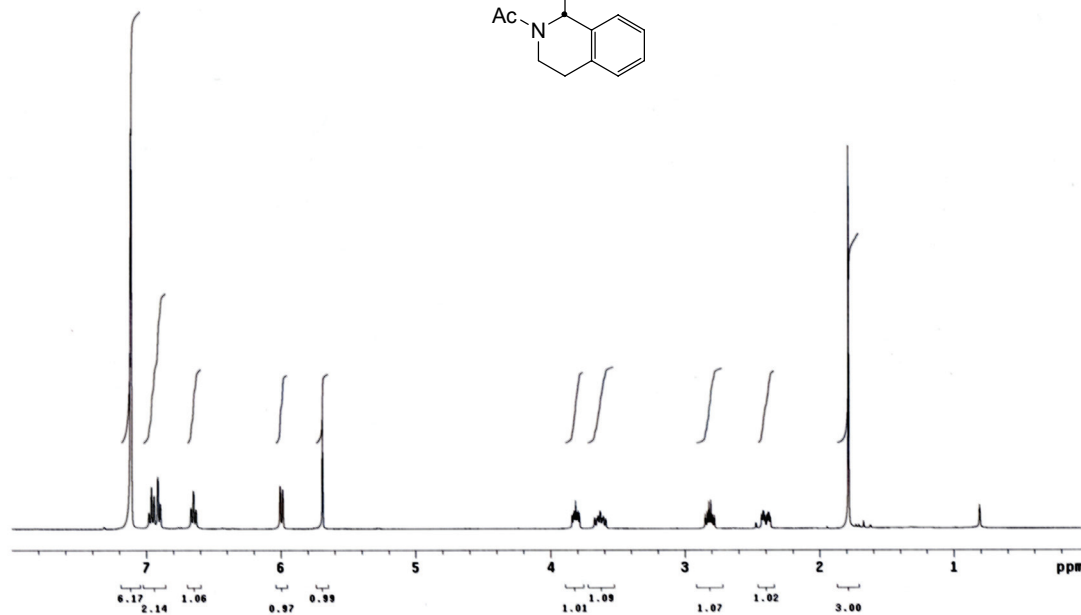
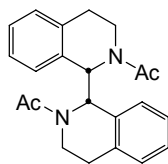
**$^1\text{H}$  and  $^{13}\text{C}$  NMR of (2.15e)**  
**Benzoic acid 3-((2,6-diisopropylphenyl)iminomethyl)-biphenyl-2-yl ester**



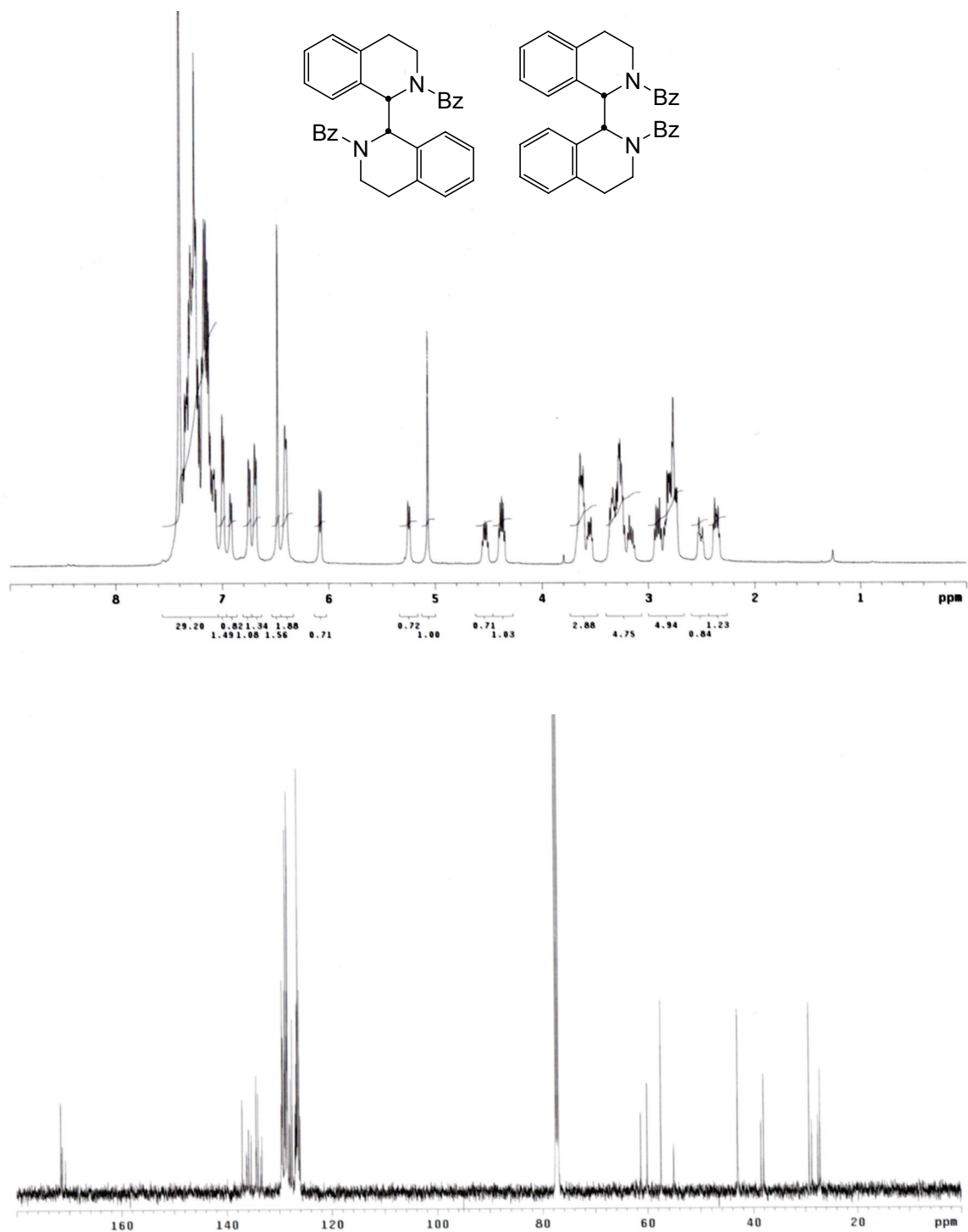
**$^1\text{H}$  and  $^{13}\text{C}$  NMR of (2.17a)**  
**meso N,N'-diacetyl-1,1',2,2',3,3',4,4'-octahydro-1,1'-biisoquinoline**



**$^1\text{H}$  and  $^{13}\text{C}$  NMR of (2.17b)**  
***dl* N,N'-diacetyl-1,1',2,2',3,3',4,4'-octahydro-1,1'-biisoquinoline**



<sup>1</sup>H and <sup>13</sup>C NMR of (2.17c,d)  
*meso, dl N,N'*-dibenzoyl-1,1',2,2',3,3',4,4'-octahydro-1,1'-biisoquinoline

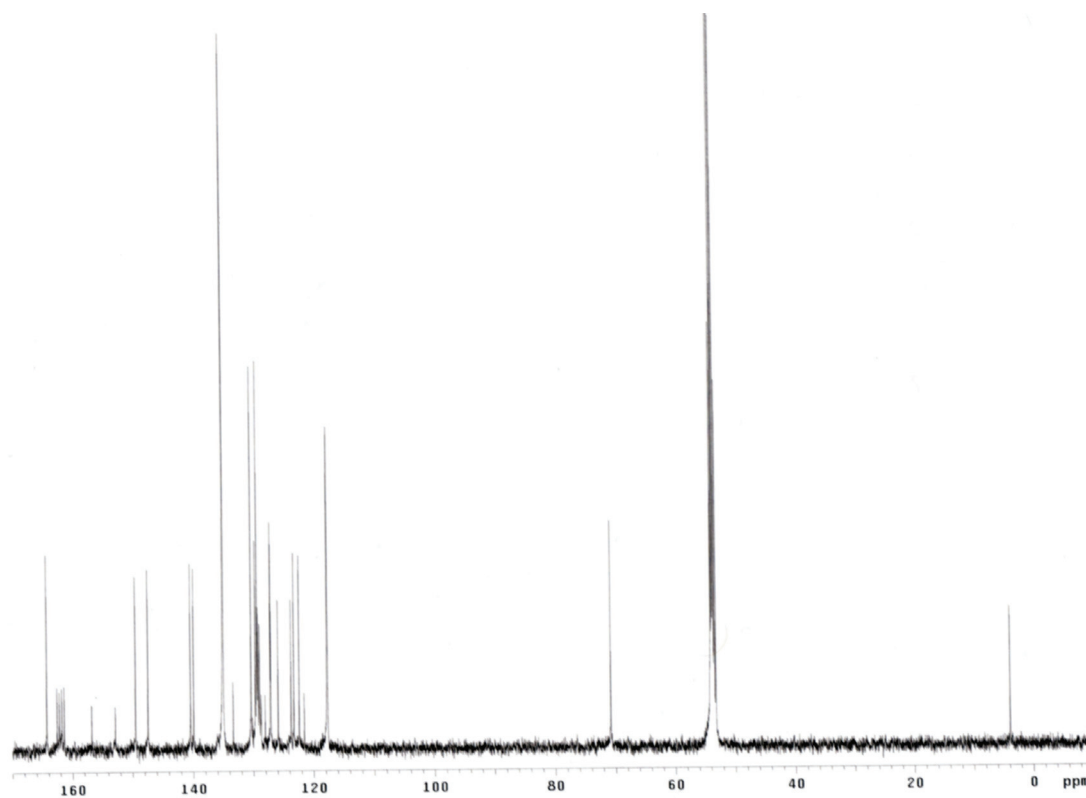
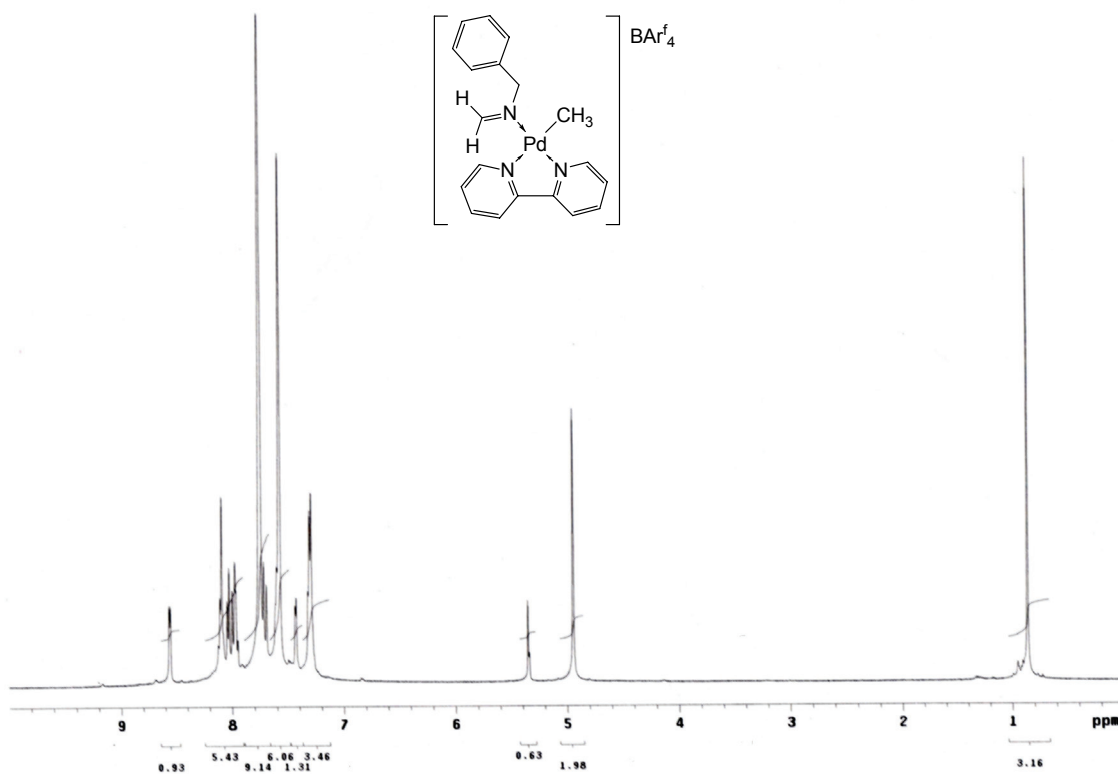
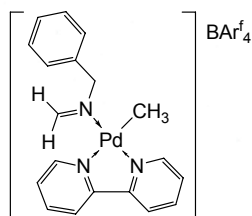


## ≈ APPENDIX B ≈

**$^1\text{H}$  and  $^{13}\text{C}$  NMR spectra for Chapter 3**

**Compounds 3.1i and 3.3i**

**$^1\text{H}$  and  $^{13}\text{C}$  NMR of (3.1i)**





**$^1\text{H}$  and  $^{13}\text{C}$  NMR of (3.3i)**  
 **$[(\text{bipy})\text{Pd}(\eta^2\text{-CH}_2\text{N}(\text{Bn})\text{COCH}_3)]^+\text{BAr}^{\text{f}}_4^-$**

